

AMPLIFICATION
USING TUNNEL DIODES
IN
A REGENERATIVE MODE

A THESIS presented by AVTAR S. OBERAI
for the degree of
DOCTOR OF PHILOSOPHY
of the
UNIVERSITY OF LONDON

Department of Electrical Engineering,
Imperial College of Science and Technology,
July, 1964.

ABSTRACT

This thesis presents a study of a new type of regenerative amplifier using tunnel diodes. From the general study and simplification of a tunnel diode equivalent circuit a method for small signal analysis is arrived at. This regenerative mode of amplification is then studied for a generalized conductance function. The expressions for the gain and the frequency response are derived and studied for optimum results.

The particular conductance functions, due to the tunnel diode and associated circuit elements under the action of different pump amplitude, frequency and waveform, are considered. The dependence of the gain, the frequency response, the sensitivity of the amplifier to the input signal and the shape of the output pulse on the circuit parameters is studied.

A study of such regenerative amplifiers in cascade is presented and practical systems are suggested.

An approximate expression for noise in such amplifiers is proposed and shown to be in good accord with measurements.

The thesis concludes with suggestions for further study.

ACKNOWLEDGMENTS

The author wishes to express his grateful appreciation for the support, guidance and encouragement given by his supervisor DR. A. R. BOOTHROYD of Imperial College.

The author is indebted to Mr. R. A. King for his guidance and helpful discussions during the concluding stages of this work.

Thanks are also extended to the past and the present research students of the Transistor Electronics Laboratory for useful discussions. In particular, the author is grateful to Anek Singhakowinta for stimulating discussions and his interest in the Author's work.

The author wishes to thank the Signal Research and Development Establishment of the Ministry of Aviation, U.K., for the financial assistance and support of his research programme. Earlier financial assistance from the Department of Scientific and Industrial Research, U.K., is also gratefully acknowledged.

Finally, the author wishes to pay a tribute to Joan, his wife, for her encouraging and affectionate support.

TABLE OF CONTENTS

Abstract		2
Acknowledgments		3
Table of Contents		4
Location of Figures		8
Location of Tables		8
List of Principal Symbols		9
<u>CHAPTER ONE</u>	Introduction	
1.1	Introductory Background	12
1.2	Definitions	12
	1.2.1 The Regenerative Principle	13
	1.2.2 The Regenerative Amplifier	13
1.3	Early Experimental Work	14
1.4	Problem to be Investigated	18
1.5	Original Contributions in this Thesis	19
<u>CHAPTER TWO</u>	Tunnel Diode as a Circuit Element	
2.1	Introduction	20
2.2	Tunnel Diode Voltage-Current Characteristics	22
2.3	Small Signal Operation of Tunnel Diodes	25
2.4	Large Signal Operation	28
2.5	Conditions for Regeneration	30
2.6	Modes of Operation	32
	2.6.1 Bistable Operation	32
	2.6.2 Monostable Operation	35
	2.6.3 Negative-Resistance Amplifiers and Oscillators	35
2.7	Requirements of a Regenerative Amplifier	36
<u>CHAPTER THREE</u>	General Theory of Regenerative Amplifier	
3.1	Introduction	37
3.2	Qualitative Description of Regenerative Cycle	40

		5.
3.3	Sampling Process	42
3.4	Analysis of the Linear Regenerative Amplifier	42
3.5	Sensitivity of the Amplifier to Signal Input	45
3.6	Expression for Signal Voltage	47
3.7	Signal Output Waveshape	49
3.8	Frequency Response	52
3.9	Regenerative Amplifier Gain	54
3.10	The Damping Period	56
3.11	Conclusions	56

CHAPTER FOUR

	Regenerative Amplifier with Square Wave Pump	
4.1	Introduction	58
4.2	Type of Conductance Cycles	59
4.3	Amplifier Output	61
4.4	Large Signal Operation of Tunnel Diodes	62
4.5	Effect of the Series Inductance	65
4.6	Normalization of the Analysis with Respect to the Tunnel Diode Parameters	68
4.7	Conductance Functions due to Square Wave Pump	70
4.8	Approximate Analysis	73
4.9	Dependence of Gain on the Pump Current	76
4.10	Damping Period	81
4.11	Frequency Response	84
4.12	Dependence of Gain on G_t	84
4.13	Dependence of Gain on the Diode Characteristics	86
4.14	Alternative Method of Analysis	90
4.15	Experimental Investigations	90
4.16	Conclusions	99

CHAPTER FIVE

	Regenerative Amplifier with Sine Wave Pump	
5.1	Introduction	101
5.2	Numerical Determination of Conductance Function	102
5.3	Approximate Methods	102
5.4	Dependence of Gain on Pump Frequency	109
5.5	Dependence of Gain on Pump Amplitude	115

		6.
5.6	Experimental Investigations	122
	5.6.1 Method of Measurement	122
	5.6.2 Low Frequency Measurements	125
	5.6.3 High Frequency Measurements	130
5.7	Conclusions	130
<u>CHAPTER SIX</u>	Cascaded Regenerative Amplifiers	
6.1	Introduction	133
6.2	Considerations for a Cascaded Amplifier	134
	6.2.1 Maximization of the First Stage	134
	6.2.2 Optimum Conditions for the Second Stage	136
	6.2.3 Unilateralization of Cascaded Stages	140
6.3	Grading of Diodes in Cascaded Amplifiers	142
6.4	Experimental Investigations	143
	6.4.1 Measurements on Cascaded Amplifier with Square Wave Pump	143
	6.4.2 Measurements on Cascaded Amplifier with Sine Wave Pump	145
6.5	Conclusions	148
<u>CHAPTER SEVEN</u>	Noise in Tunnel Diode Regenerative Amplifiers	
7.1	Introduction	149
7.2	Shot Noise in Tunnel Diodes	151
7.3	The Noise Figure of Regenerative Amplifier	153
7.4	Measurement of Amplifier Noise Figure	155
	7.4.1 Noise Generator Method	155
	7.4.2 C.W. Method	158
7.5	Conclusions	160
Conclusions		163
References		170
Appendices		
A.1.	The Effect of Series Inductance on the Input Conductance (G_{in})	173

A.2.	Method of Step by Step Integration	177
A.3.	Computer Programme For Square Wave Pump Calculations	179
A.4.	Computer Programme for Sine Wave Pump Calculations	183
A.5.	Measurement of i_{eq} for Tunnel Diodes	186

LOCATION OF FIGURES

<u>Fig.</u>	<u>Page</u>	<u>Fig.</u>	<u>Page</u>	<u>Fig.</u>	<u>Page</u>
1.1	15	4.8	72	5.12	120
1.2	15	4.9	72	5.13	121
1.3	17	4.10	74	5.14	123
1.4	17	4.11	74	5.15	123
2.1	21	4.12	76	5.16	124
2.2	21	4.13	78	5.17	124
2.3	24	4.14	80	5.18	128
2.4	26	4.15	82	5.19	129
2.5	27	4.16	83	6.1	135
2.6	29	4.17	86	6.2	137
2.7	31	4.18	87	6.3	138
2.8	31	4.19	89	6.4	139
2.9	34	4.20	91	6.5	141
2.10	34	4.21	92	6.6	144
2.11	34	4.22	94	6.7	146
3.1	38	4.23	96	7.1	150
3.2	38	4.24	96	7.2	152
3.3	39	4.25	97	7.3	152
3.4	39	4.26	98	7.4	156
3.5	41	5.1	103	7.5	156
3.6	46	5.2	104	7.6	159
3.7	50	5.3	106	C.1	168
3.8	53	5.4	108	A.1	174
4.1	60	5.5	110	A.2	175
4.2	60	5.6	112	A.3	187
4.3	63	5.7	113		
4.4	63	5.8	114		
4.5	67	5.9	116		
4.6	69	5.10	117		
4.7	71	5.11	119		

LOCATION OF TABLES

<u>Table</u>	<u>Page</u>
2.1	33
4.1	85
5.1	126

LIST OF PRINCIPAL SYMBOLS

A_m	Regenerative gain at the peak of output pulse (given by equations 3.30).
A_v	Gain factor (equation 3.31).
a	Negative-conductance area of conductance-time graph.
B	Bandwidth
C	Tunnel diode capacitance.
D	Time by which signal cycle is advanced w.r.t. pump current.
dp	Damping period.
F	Noise figure.
f_r	Frequency at which resistive part of tunnel diode impedance = 0.
$f(v)$	Tunnel diode current-voltage characteristic
G	Diode A.C. conductance
G_1	Magnitude of maximum negative-conductance of tunnel diode.
G_L	Load conductance
G_o	Circuit conductance at $v = 0$.
G_s	Source conductance.
G_t	Total external conductance seen by tunnel diode ($= G_s + G_L$).
$G(t)$	Circuit conductance-time characteristic.
$G'(t_1)$	Conductance slope of conductance-time graph at $t = t_1$.
$G'(t_2)$	Conductance slope of conductance time graph at $t = t_2$.
$G(v)$	Conductance-voltage characteristic of tunnel diode.
$G'(v_{x_1})$	Slope of conductance-voltage curve at $v = v_{x_1}$.
$G'(v_{x_2})$	Slope of conductance-voltage curve at $v = v_{x_2}$.
$G'(x_1)$	Conductance slope of conductance-time curve normalized to diode capacitance C at $x = x_1$.

$G'(x_2)$	Conductance slope of conductance-time curve normalized to diode capacitance C at $x = x_2$.
I_b	Amplitude of pump current.
I_E	Tunnel diode current from conduction band to the valence band.
I_p	Tunnel diode peak current.
I_s	Amplitude of signal current.
I_z	Tunnel diode current from valence band to conduction band
i_b	Pump current at a given instant.
i_d	Tunnel diode current at a given voltage.
i_{ego}	Excess pump current at the time $x = x_1$ when circuit conductance equals zero.
i_{eq}	Equivalent saturated diode current.
k	Boltzmann constant.
L_s	Tunnel diode series inductance.
P_{avs}	Maximum available power from signal source.
P_o	Power output into load.
P_T	Transducer gain.
q	Electron charge.
R_s	Tunnel diode series resistance.
R_t	Total resistance ($= \frac{1}{G_t}$)
t_1	Time at the beginning of regenerative period when $G(t) = 0$.
t_2	Time at the end of regenerative period when $G(t) = 0$.
μ	($= C\omega$), signal frequency normalized to diode capacitance.
μ_p	($= C\omega_p$), pump frequency normalized to diode capacitance.
μ_{pm}	Normalized angular pump frequency at which $G'(x_2)$ is a maximum.
μ_{po}	Normalized angular pump frequency at which $G'(x_2) = 0$.

V_p	Tunnel diode peak voltage
V_v	Tunnel diode valley voltage
v_{x_1}	Tunnel diode voltage at $x = x_1$.
v_{x_2}	Tunnel diode voltage at $x = x_2$.
v_y	Tunnel diode voltage (nearer the peak) where its negative conductance is maximum.
v_z	Tunnel diode voltage (nearer the valley voltage) where its negative conductance is the same as that at v_y .
W	Pump pulse width.
X	Period of pump cycle normalized to C .
x	Time normalized to C .
θ_1	Angle given by $\mu_p x_1$.
θ_2	Angle given by $\mu_p x_2$.
ω	Angular frequency of signal input.
ω_p	Angular frequency of pump input.

CHAPTER ONE

1. INTRODUCTION

1.1 Introductory Background

Very early in the history of Radio Engineering, regenerative amplifiers^{1,2} made a considerable contribution to the techniques of communications. By the early thirties of this century they were established as high frequency amplifiers and detectors not only for 'modern two way radio systems'³ but had found currency in the amateur repertoire of circuits.

The second world war saw super-regenerative circuits used widely in radar receivers. A considerable amount of effort was expended during this period towards the understanding and mathematical analysis of such amplifiers. Further work and de-classification of information after the war resulted in a large number of publications^{4,5,6,7} on the subject of the regenerative amplifiers.

While all the earlier work on the regenerative amplifiers employed the valve as an active device, with the advent of transistor and its acceptance later on as a respectable device, some work was reported^{8,9,10} on the 'transistor as a super-regenerative amplifier and detector'. When Esaki reported¹¹ the tunnel diode, it was expected that the two terminal negative-resistance, provided so simply by tunnel diodes, would find use amongst other applications in regenerative amplifiers.

1.2 Definitions

1.2.1 The regenerative principle

Regeneration is concerned with the build up of transients. In a valve or transistor this process is achieved by applying a part of the output energy to the input circuit in an appropriate phase relationship. An analysis and simplification of such valve or transistor regenerative circuits produce a simple equivalent circuit which consists of a time varying conductance and one or more reactive elements^{12,13}. The time varying conductance changes its sign from positive to negative and back again for every

completed transient.

Depending upon the magnitude and the type of reactive elements, the conductance and the initial conditions of the circuit, the regenerative circuit will be an oscillator, bi-stable switch or monostable switch etc. We will examine the conditions for these modes of operation in sections 2.5 and 2.6,

Tunnel diode is perhaps the simplest regenerative device. The conditions for regeneration can be achieved simply by the application of an appropriate bias.

1.2.2 The regenerative amplifier

The theory of the regenerative amplifier is concerned with the repeated build up and decay of transients. The circuit conductance is made alternately negative and positive by the application of periodic voltage from a quench or pump oscillator.

One type of regenerative amplifier is the well known super-regenerative amplifier. This type of amplifier goes into oscillations as the circuit conductance becomes negative and the oscillations are quenched as the conductance goes positive. The signal frequency is at or very near the frequency of oscillation. The pump voltage is at a much lower frequency but at a frequency at least twice as high as the maximum frequency of the modulation on the signal. The oscillations build up from the signal voltage developed across the circuit. When there is no signal present, the oscillations start from the level of the noise existing in the circuit. During the build up oscillations may become many times greater than the signal input and hence the gain of the amplifier.

The regenerative amplifier proposed in this thesis does not go into oscillations. The voltage transient across the circuit builds up from the signal voltage developed across the circuit. This build up is arrested by the pump input and then the voltage across the circuit decays. The transients build up from the signal level to a peak voltage before they are quenched. This peak voltage is proportional to the magnitude of the input signal and may be many times larger. In this resides the gain of the

regenerative amplifier.

The pump frequency, in this case, is at least twice as high as the frequency of the signal.

In both types of the amplifiers described above, it is essential that the signal transient should die away before the commencement of the next cycle. Otherwise the next cycle will build up from the dying transient instead of from the signal.

The choice of pump frequency, amplitude and waveform have a considerable influence on the characteristics of the regenerative amplifier. The actual choice is a complicated matter and is dealt with in later chapters.

There are two modes of operation according to whether or not the transients are allowed to build up to an equilibrium value before they are arrested. If the transient which builds up in a single cycle of pump is quenched before it reaches a limiting equilibrium amplitude, determined by the circuit conditions and the load, the peak amplitude of the transient is proportional to the signal or noise voltage from which the transient grew. The amplification in this case bears a linear relationship with the input. If, however, the build up is allowed to proceed for long enough, the transient reaches a steady amplitude before it decays. In this, the logarithmic mode, the effect of an applied signal is to modulate the phase of the transient.

The basic requirement of a regenerative amplifier thus is to provide by some means a conductance characteristic which oscillates between positive and negative conductance as a periodic control voltage is applied to the circuit. We shall see in Chapter 2, how tunnel diode provides this.

1.3 Early Experimental Work and the Origin of the Project

When this work was started, some work on linear negative-resistance amplifiers had been reported^{14,15,16,17}. A short report later gave some experimental results obtained with tunnel diode super-regenerative receivers¹⁸. It was decided to investigate the possibility of a new mode of amplification which would utilize the inherent advantages of a simple

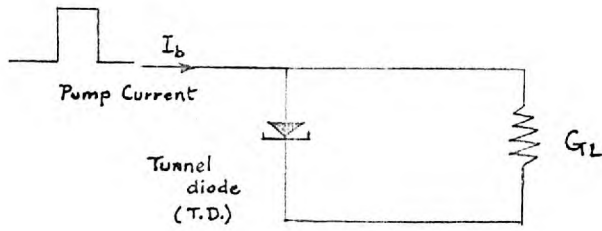


Fig. 1.1: Tunnel diode Switching Circuit.

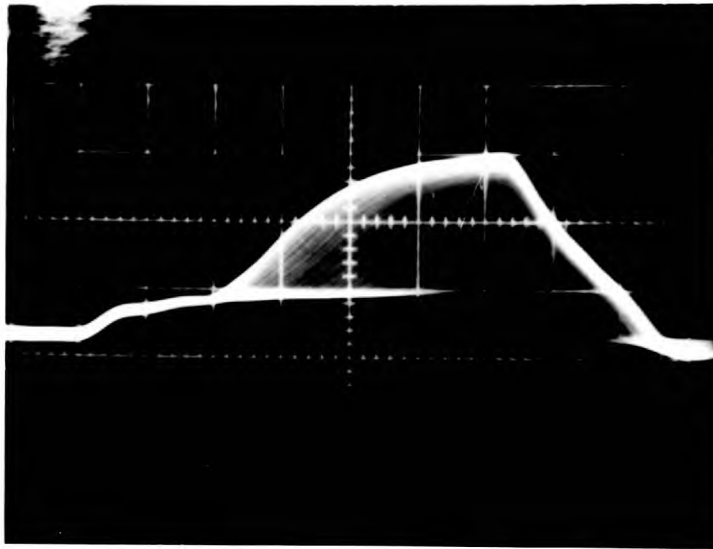


Fig. 1.2; Diode Voltage against time characteristics in the presence of sinusoidal signal.

two terminal device like a tunnel diode and at the same time it would try to overcome some of the disadvantages of the tunnel diode.

In the earlier work by the author on tunnel diode as a logic element, the dependence of the switching characteristics on the trigger current and the parasitic elements associated with the tunnel diode was investigated. The circuit used was that of Fig. 1.1. It was observed that the switching transient of a tunnel diode in this circuit could be modulated by the presence of a small signal along with the trigger. The signal would, in such a case, see a conductance which is made to alternate, by the trigger current, from positive to negative and back again.

Further, it was observed that if the trigger current was allowed to last for long enough the voltage across the tunnel diode reached a steady amplitude but the switching transient was advanced or retarded in time corresponding to the amplitude of the signal impressed (Fig. 1.2). On the other hand if the switching transient was not allowed to build up to the equilibrium amplitude then the peak voltage across the tunnel diode was proportional to the amplitude of the signal (Fig. 1.3) and the amplitude of the signal modulation on the peak voltage was many times the amplitude of the signal input.

The signal was thus sampled at the frequency of the trigger current (pump current from now on) and amplified at the same time (Fig. 1.4).

Tunnel diode is potentially a high frequency^x and low noise device. It was expected that in this mode of amplification signals upto very high frequencies could be sampled and amplified in a low noise stage. These arguments suggested that performance far exceeding that of any conventional techniques might be expected.

It seemed a very attractive and feasible proposition that such amplifier stages could also be cascaded to produce high gain. Tunnel diode is a two terminal device and thus completely bilateral. In cascaded amplifiers of this sort where every stage would be switched on and off by a

x

The advantages of a tunnel diode are discussed fully in Chapter 2.

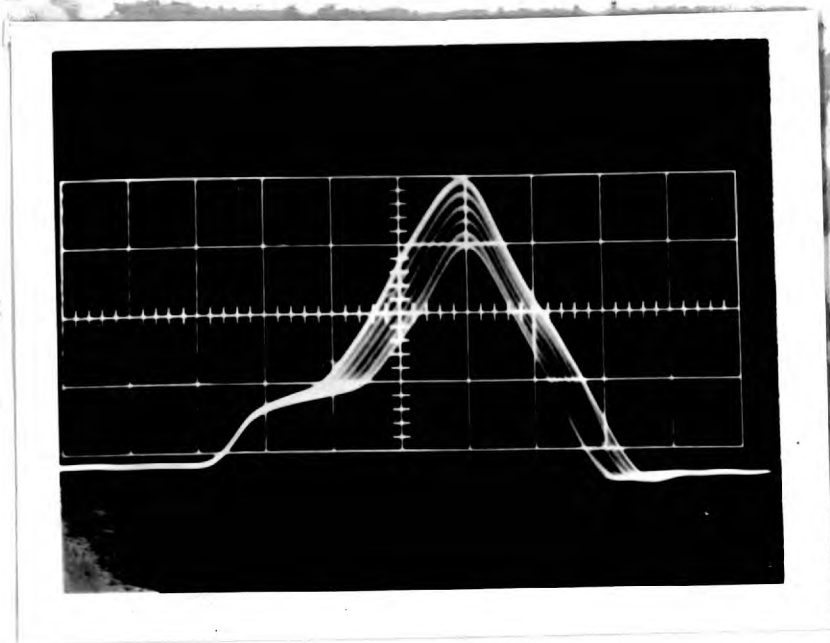


Fig. 1.3 : Diode Voltage Against Time

(Trigger Current Switched off at 0.4 μ sec.)

Horizontal - 100 ns/cm Vertical - 50 mV/cm

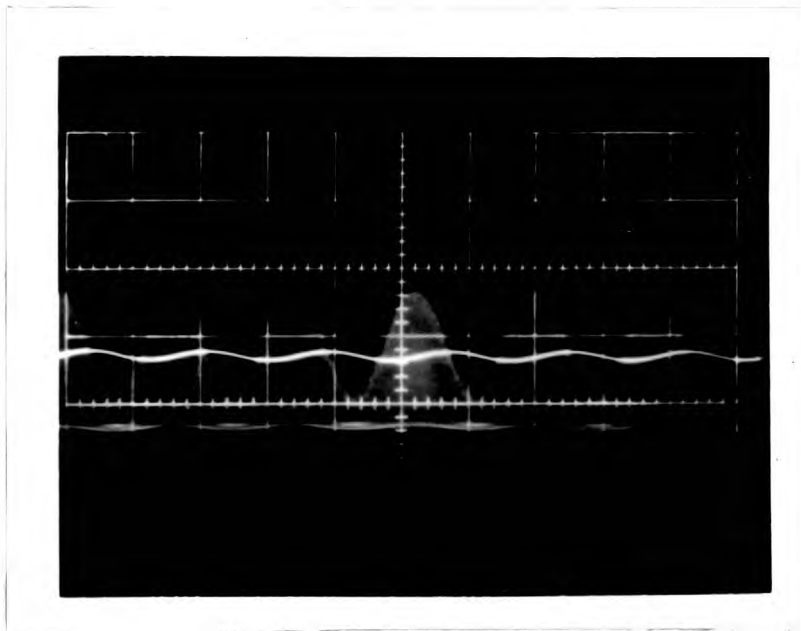


Fig. 1.4 : Signal Modulation on the Switching Transient
and the Signal Current Waveform.

pump current an appropriate phase delay introduced between the pump input to the consecutive stages would give us a flow of signal energy in one direction only by making sure that the first stage was in a quiescent state by the time second stage became regenerative and so on. In this way it seemed possible to overcome the major drawback of the tunnel diode due to its two terminal nature.

The components required for such an amplifier would be simple components like resistors, tunnel diode and short delays. It was expected that the simplicity of this configuration of amplification would make it possible to fabricate a low noise, wideband sampling amplifier in a very simple solid state construction.

1.4 Problem to be Investigated

In this work we will investigate tunnel diode regenerative amplifiers as defined earlier in section 1.2.2. The analysis and understanding of non-oscillatory linear regenerative amplifiers form the main part of this thesis. To this end it is necessary to develop the simplest possible equivalent circuit which will, however, represent the linear regenerative amplifier to an adequate degree of approximation (Chapter 2). This analysis, though being carried out with tunnel diode expressly in mind, is nevertheless accurately applicable to any circuits, using other active elements, which can be reduced to the simple equivalent circuit assumed in the analysis of Chapter 3.

It is intended to derive simple analytic expressions for the gain and the frequency response of regenerative amplifiers (Chapter 3). These expressions are to be obtained for a general conductance function. The conductance function corresponding to particular pump amplitude, frequency, waveform and other circuit conditions can be substituted later to obtain optimum gain and frequency response conditions (Chapters 4 and 5).

As far as possible effort would be made to avoid any numerical or graphical methods. It is intended to obtain analytic expressions which will help to further a qualitative understanding of the regenerative process and at the same time provide an approximate quantitative theory.

As mentioned in section 1.3, the cascading of such amplifier stages seems very promising and it should, therefore, be investigated (Chapter 6).

An important aspect of the evaluation of any small signal amplifier is its noise performance (Chapter 7). An accurate analysis of noise in a sampling amplifier is very complex. Only alternative to cumbersome digital computer calculations is to make some reasonable simplifying assumption and then to show that the predictions based on these assumptions are in good accord with the measurements.

It is important that while optimizing the amplifier with respect to its gain, frequency response and noise performance, the simplicity of fabrication is conserved.

1.5 Original Contributions in this Thesis

Except where reference is made to the work of others the research and conclusions reported in this thesis are original with the author. The work of sections 2.1, 2.2, 2.3 and 2.6 is well known and therefore only a few important references are given for these sections.

CHAPTER TWO2. TUNNEL DIODE AS A CIRCUIT ELEMENT2.1 Introduction

Esaki gave news of the discovery of the tunnel diode in June 1958¹¹. After a period of inertia, Sommers¹⁹ gave more details and suggested applications. Soon afterwards the tunnel diode was hailed as the greatest discovery after the transistor. A great deal of investigation was carried out in the field of tunnel diode circuits and many ingenious circuits were devised. The enthusiasm of the earlier days is no longer present. Nevertheless, the tunnel diode appears likely to take its place along with the transistor, the semiconductor diode and the ferrite core in the field of applications.

Tunnel diode can be employed in various circuits of which switches, converters, oscillators and amplifiers may be considered the most important. One of the main advantages tunnel diodes offer in these applications is the extremely wide range of frequencies in which the diode can be operated. The upper limit of oscillations obtained so far is of the order of 100 KMc/s, but it is believed that useful negative-resistance effects will also be available in millimeter wave range as the technology improves. This remarkable feature results from the fact that unlike most other semiconductor devices the tunnel diode operates on the principle of majority carrier transition. The transit time effect is, therefore, of no importance here and frequency limitations arise only from the relatively large capacitance of the junction and the parasitic reactances associated with the mount.

The low noise produced by the diode is another noteworthy feature. In the region of tunnel diode characteristic over which the diode current is due mainly to tunnel current the noise current is due to shot noise associated with diode current. One of the most impressive features of the tunnel diode is its relative insensitivity to a wide range of temperature variations. Significant resistance to radiation damage, greater reliability, small dimensions and a relatively simple fabrication process are other advantages of the tunnel diode.

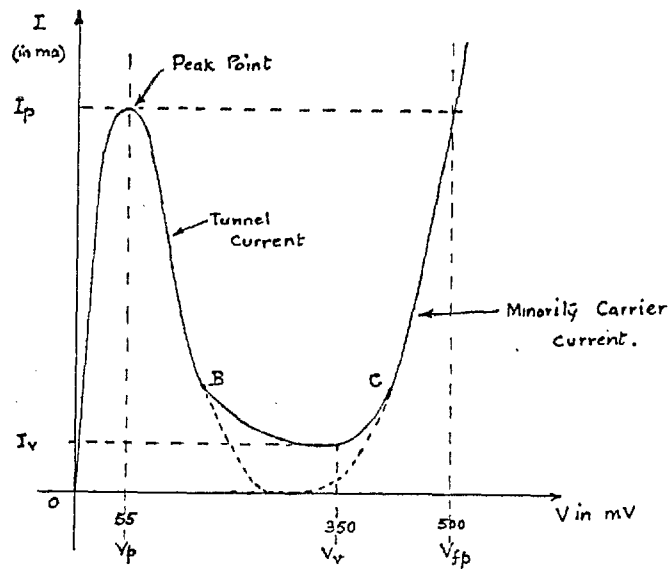


Fig. 2.1: Static Characteristic Curve of Germanium Tunnel diode

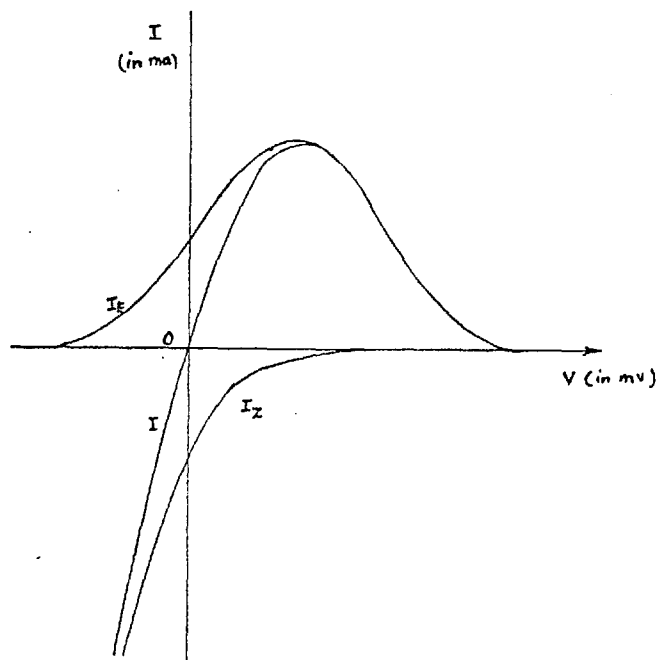


Fig. 2.2: Theoretical Tunnel diode characteristic

This device, unfortunately, has several drawbacks. The most important one is its two terminal nature which makes it completely bilateral. The design of multistage tunnel diode amplifier, for this reason, is not very easy.

It is a small power device. Whereas this is an advantage in some circuits (logic elements in a computer) it is also a great disadvantage when tunnel diodes are used as oscillators etc.

2.2 Tunnel Diode Voltage-Current Characteristics

The voltage-current characteristics for a germanium tunnel diode is as shown in Fig. 2.1. The important D.C. parameters are also indicated in this figure.

The dotted line in this figure shows a normal diode characteristic resulting from minority carrier current. In the range over 0.35 Volt in the forward direction, the voltage-current curve could be fitted quite accurately by the relation

$$I = I_s \left[\exp(qV/KT) - 1 \right]$$

In the lower voltage region below point C and in the reverse biased state the diode current consists of majority carriers which tunnel through the narrow p-n junction. Following Esaki¹¹, it can be assumed that there are two current streams flowing across the junction in opposite directions. The current flowing in the reverse direction is the familiar zener current (I_Z). The current in the forward direction can be called Esaki current (I_E). The Zener current I_Z from the valence band to the conduction band, and the Esaki current I_E flowing from the conduction band to the valence bands are taken as

$$I_E = A \int_{E_C}^{E_V} f_C(E) \rho_C(E) Z_{C \rightarrow V} \left[1 - f_V(E) \right] \rho_V(E) dE, \quad 2.1.$$

$$\text{and } I_Z = A \int_{E_C}^{E_V} f_V(E) \rho_V(E) Z_{V \rightarrow C} \left[1 - f_C(E) \right] \rho_C(E) dE, \quad 2.2.$$

where A is an appropriate constant

$Z_{C \rightarrow V}$ and $Z_{V \rightarrow C}$ are the probabilities of penetrating the gap.

$f_C(E)$ and $f_V(E)$ are the Fermi-Dirac distribution functions; namely, the probabilities that a quantum state is occupied in the conduction and the valence bands respectively.

$\rho_C(E)$ and $\rho_V(E)$ are the energy level densities in the conduction and valence bands respectively.

The net electron current flowing across the junction i_d is the difference between I_E and I_Z

$$i_d = I_E - I_Z \quad 2.3.$$

According to simplifications due to Pucel²⁰ and others

$$I_E = \frac{i_d}{1 - \exp \frac{-qV}{kT}} \quad 2.4.$$

$$\text{and} \quad I_Z = I_E \exp \frac{-qV}{kT} \quad 2.5.$$

These components of tunnel currents are plotted in Fig. 2.2.

In practice, the diode current is greater than the sum of the theoretical majority and minority currents between points B and C (Fig. 2.1). The current in this region is called the excess current and there have been some attempts at explaining its presence.

The peak point current (I_p) of a tunnel diode can be accurately controlled by etching the junction and tunnel diodes with a wide range of current ratings from microamperes to several amperes can be obtained.

The peak point voltage V_p , valley point voltage V_v and forward point voltage V_{fp} are determined by the semiconductor material and are largely fixed (see Fig. 2.1). For germanium these voltages are respectively 55 mV, 350 mV and 500 mV typically at 25°C.

If the shape of the voltage-current characteristic for tunnel diodes with different peak currents is assumed constant, their conductances at any point over the characteristic will be in the ratio of their peak currents;

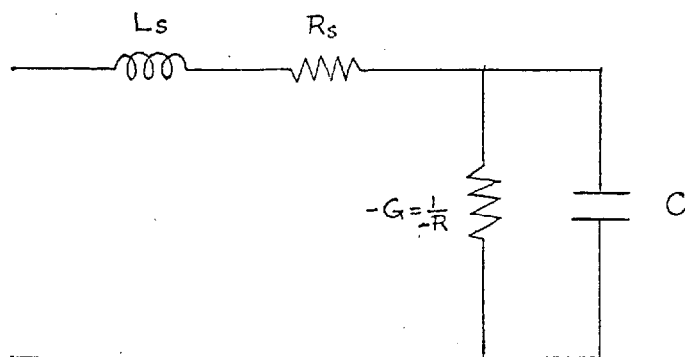


Fig. 2.3: Small signal Equivalent Circuit
for a tunnel diode

that is the ratio $\frac{I_p}{G}$ is constant. In practice $\frac{I_p}{G}$ varies approximately from 0.1v to 0.2v but most diodes have this ratio in the middle of this range.

2.3 Small Signal Operation of Tunnel Diodes

A complete equivalent circuit for a tunnel diode in the linear mode including both the effects of series inductance and dissipation is shown in Fig. 2.3. This equivalent circuit remains effective to extremely high frequencies.²¹

The diode a.c. conductance, G , is a function of bias voltage and can be either positive or negative (Fig. 2.4). The diode conductance varies very slowly with voltage in the reverse bias condition.

The capacitance, C , is also a function of bias but changes more gradually (Fig. 2.5). The capacitance is primarily due to the capacitance of the junction although a small portion of the capacitance is due to the leads and the package. As the junction capacitance is reduced the package capacitance becomes more and more important, however.

The inductance, L_s , is relatively low and is determined primarily by the inductance of the leads.

A small amount of series resistance, R_s , is also present and is determined by the bulk resistance of the semiconductor material.

Measurements techniques for these diode parameters are described in the literature^{22,23}.

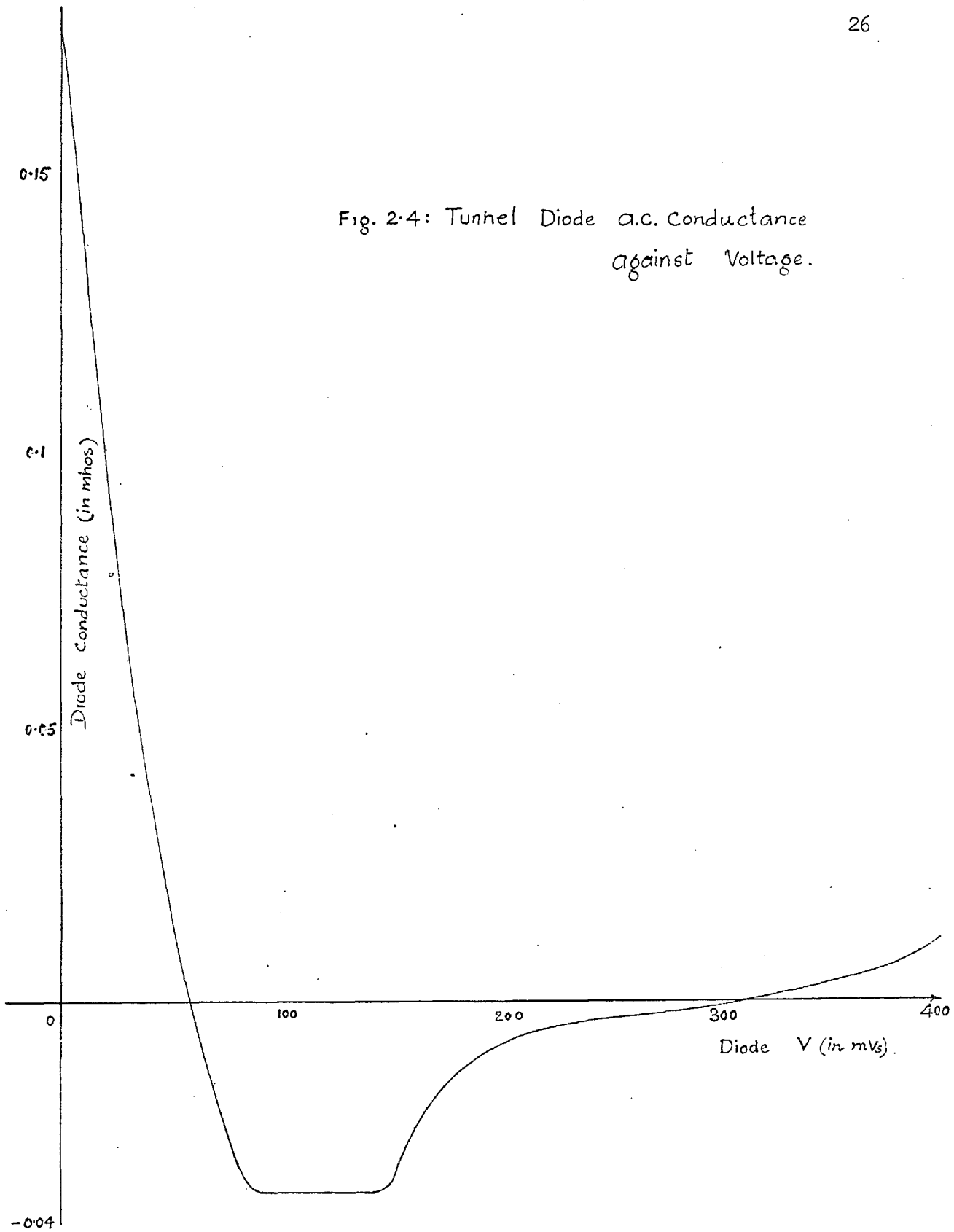
The small signal a.c. characteristics of the tunnel diode are described in terms of these equivalent circuit parameters L_s , C , R_s , $-R = \frac{1}{G}$ and of certain characteristic frequencies that are functions of these parameters.

The impedance Z_d of the diode is

$$Z_d = R_s + j\omega L_s + \frac{R}{j\omega RC - 1} \quad 2.6.$$

$$\therefore R_e = R_s - \frac{R}{1 + (\omega CR)^2} \quad 2.7.$$

Fig. 2.4: Tunnel Diode a.c. Conductance
against Voltage.



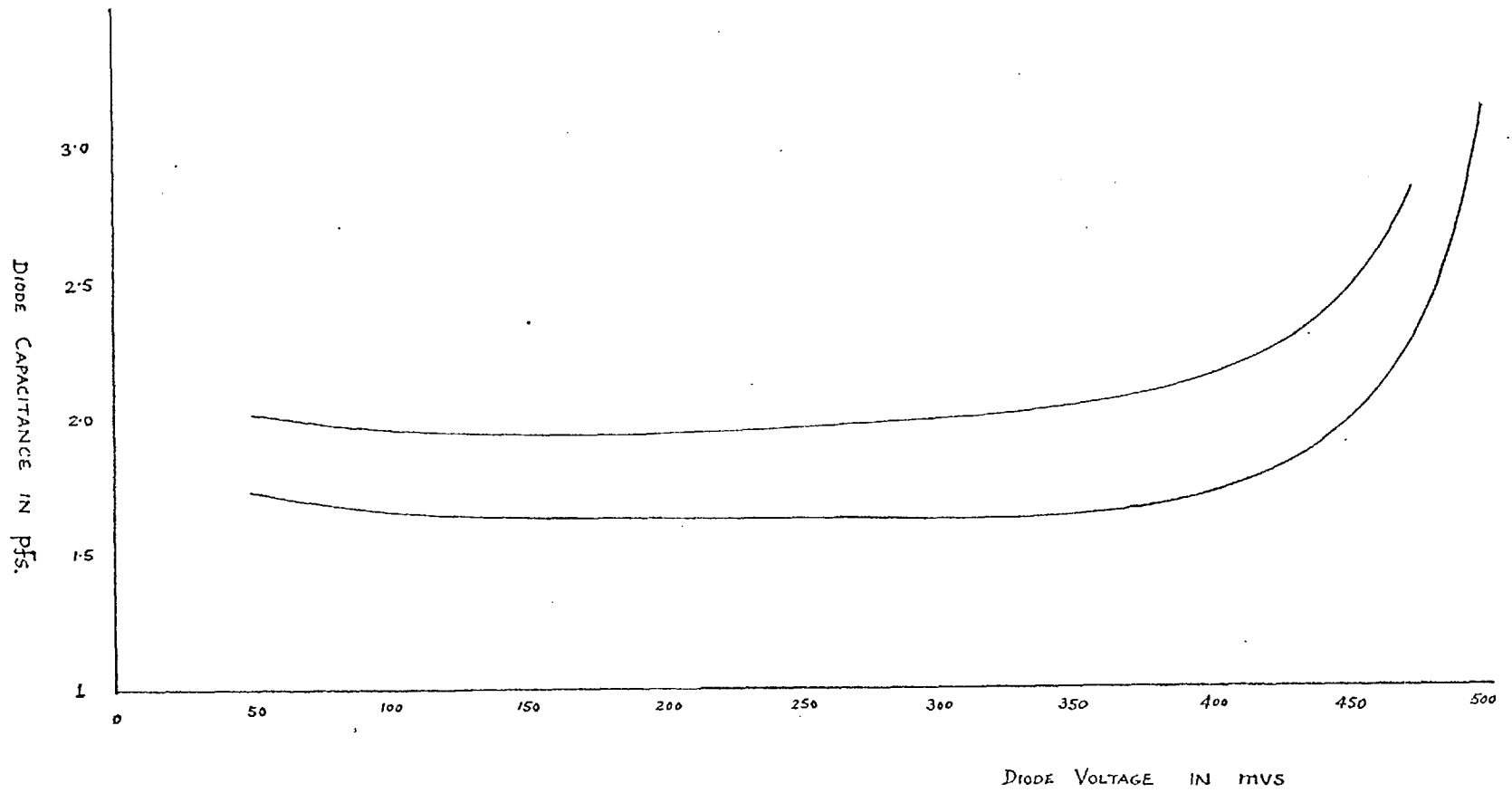


Fig. 2-5: Tunnel Diode Capacitance Vs Voltage.

$$\text{and } X_e = \omega L_s - \frac{\omega C R^2}{1 + (\omega C R)^2} \quad 2.8.$$

where R_e = the real part of Z_d
and X_e = the reactive part of Z_d .

The frequency at which the real part R_e of Z_d is zero is the resistive cut off frequency,

$$f_r = \frac{1}{2\pi RC} \left[\frac{R}{R_s} - 1 \right]^{\frac{1}{2}} \quad 2.9.$$

The frequency at which the reactive part $X_e = 0$ is the self resonant frequency

$$f_s = \frac{1}{2\pi RC} \left[\frac{R^2 C}{L_s} - 1 \right]^{\frac{1}{2}} \quad 2.10.$$

A third characteristic frequency sometimes referred to as the oscillation frequency which, by definition, is theoretically the frequency at which the diode will oscillate if short circuited

$$f_{osc} = \frac{1}{2\pi [L_s C]^{\frac{1}{2}}} \left[1 - \frac{R_s}{R} \right]^{\frac{1}{2}} \quad 2.11.$$

This is true only for low level oscillations.

Some typical values of the parameters for a tunnel diode are

$$\begin{aligned} I_p &= 4.7 \text{ mA} & L_s &= 6 \text{ nH} \\ R_s &= 0.5 \text{ ohm} & -R &= -33 \text{ ohms} \\ C &= 10 \text{ pF} \end{aligned}$$

and the corresponding characteristic frequencies are

$$\begin{aligned} f_r &= 3.88 \text{ KMc/s} \\ f_s &= 417 \text{ Mc/s} \\ f_{osc} &= 645 \text{ Mc/s} \end{aligned}$$

2.4 Large Signal Operation

The validity of the small signal tunnel diode model can be extended over a large signal range by incorporating the static terminal characteristics of the device into the model shown in Fig. 2.6. For most large signal applications the lead inductance L_s , the series body resistance, R_s , and

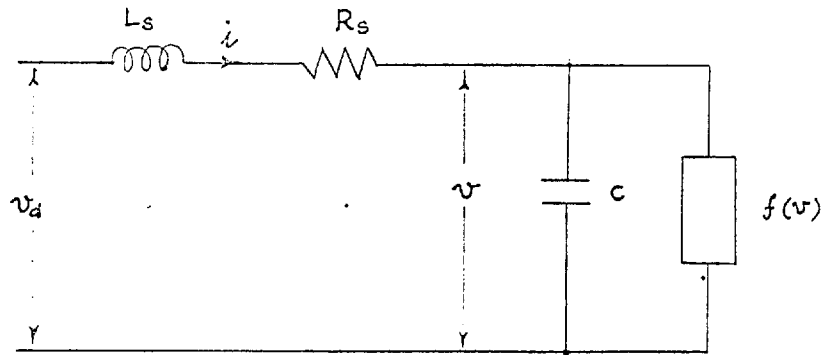


Fig. 2.6: Large Signal Equivalent Circuit

the barrier capacitance, C , can all be assumed to maintain constant values over the range of interest without introducing gross inaccuracy into the analysis.

The equations describing large signal operation of the tunnel diode are

$$v_d = v + i R_s + L_s \frac{di}{dt} \quad 2.12.$$

$$\text{and } i = C \frac{dv}{dt} + f(v) \quad 2.13.$$

where v = voltage across the junction

and $f(v)$ = static voltage-current relationship of tunnel diode junction.

2.5 Conditions for Regeneration

For a large number of applications including the regenerative amplifier of this work, of tunnel diodes, to the equivalent circuit of Fig. 2.3, a load resistance R_L and some associated lead inductance L_L are added. Then the equivalent circuit becomes as in Fig. 2.7. If series resistance R_s is neglected and the voltage generator of Fig. 2.7 is replaced by an equivalent current source, then the circuit of Fig. 2.7 can be represented by Fig. 2.8.

From the equivalent circuit (Fig. 2.7) we can write down the expression for the circuit impedance

$$\begin{aligned} Z(S) &= R_t + SL + \frac{1}{SC - G} \\ &= \frac{S^2 LC + (R_t C - LG)S + (1 - R_t G)}{SC - G} \end{aligned} \quad 2.14.$$

The zeros of this equation are

$$S_{1,2} = -\frac{1}{2} \left[\frac{R_t}{L} - \frac{G}{C} \right] \pm \left[\frac{1}{4} \left(\frac{R_t}{L} - \frac{G}{C} \right)^2 - \frac{1 - R_t G}{LC} \right]^{\frac{1}{2}} \quad 2.15.$$

$$\text{or } S_{1,2} = \alpha \pm (\alpha^2 + \beta)^{\frac{1}{2}} \quad 2.16.$$

$$\text{where } \alpha = -\frac{1}{2} \left[\frac{R_t}{L} - \frac{G}{C} \right]$$

$$\text{and } \beta = \frac{R_t G - 1}{LC}$$

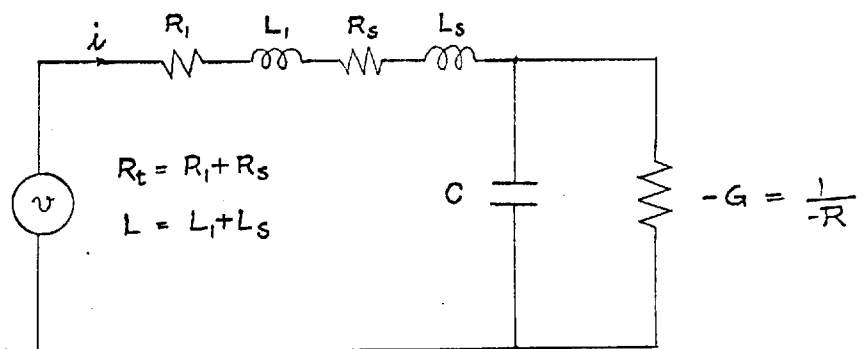


Fig. 2.7:

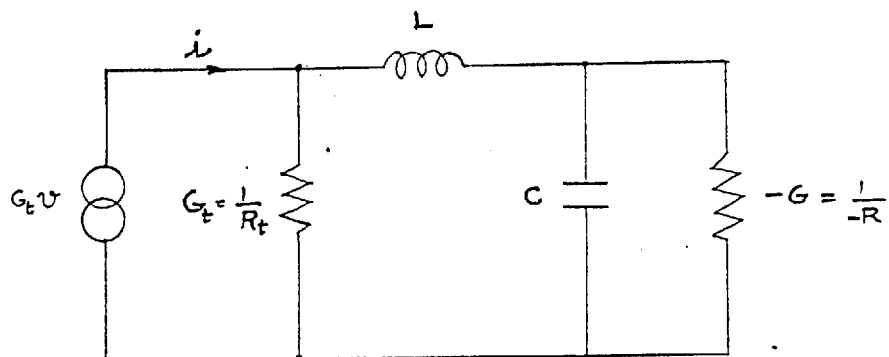


Fig. 2.8:

The current i in such a circuit for a step input would be described by

$$i = A_1 e^{S_1 t} + A_2 e^{S_2 t} + \theta(t)$$

where A_1 and A_2 are constants which depend upon the initial current in the inductor and charge on the capacitor.

The exponential factors S_1 and S_2 may be real, complex or imaginary depending upon the choice of the circuit parameters. If either of the roots S_1 or S_2 has a positive real part, the circuit will be regenerative. If the S 's are real, an initial disturbance will either grow or decay exponentially to the steady bias condition. If the S 's are complex, the transients will be growing or decaying sinusoids.

Equation 2.15 can be studied by the behaviour of the factors α and β in equation 2.16, for different relative magnitudes of the circuit parameters.

Table 2.1 gives the various circuit conditions possible for different values of R_t , L , C and G .

For the condition 3 i.e. $\frac{LG}{C} < R_t < \frac{1}{G}$ the roots S_1 and S_2 have negative real parts and the circuit is absolutely stable.

For all other combinations of α and β signs the circuit is regenerative because at least one of the roots have a positive real part.

If $R_t < \frac{1}{G}$, $R_t \leq \frac{LG}{C}$ and $\alpha^2 < |\beta|$ then the roots are complex and the circuit will be oscillatory. For all other conditions 1, 2 and 5 of Table 2.1 the circuit is regenerative but non-oscillatory.

2.6 Modes of Operation

There are various modes of operation possible for a tunnel diode depending upon the bias applied to the tunnel diode, the load resistance and the relative magnitudes of the reactive elements.

2.6.1 Bistable operation

If $R_t > \frac{1}{G}$ for all magnitudes of L and C the tunnel diode will have two stable states A and D (Fig. 2.9) which are defined by the load line and

	$R_t < \frac{1}{G}$	$R_t > \frac{1}{G}$	$R_t > \frac{LG}{C}$	$R_t < \frac{LG}{C}$	Roots S_1 and S_2	Circuit Condition.
1		$\beta +ve$	$\alpha -ve$		one +ve one -ve	Regenerative Bistable Switch.
2		$\beta +ve$		$\alpha +ve$	both +ve	Regenerative Bistable Switch
3	$\beta -ve$		$\alpha -ve$		both -ve or $-\alpha \pm j\gamma$	Stable [at $R_t = \frac{1}{G}$, Point of infinite Low frequency amplification].
4	$\beta -ve$			$\alpha +ve$	$\alpha \pm j\gamma$	Regenerative Oscillatory if $\alpha^2 < \beta $ if $\alpha = 0$ free Oscillations.
5	$\beta -ve$			$\alpha +ve$	one +ve one -ve	Regenerative no oscillations if $\alpha^2 > \beta $.

TABLE 2.1.

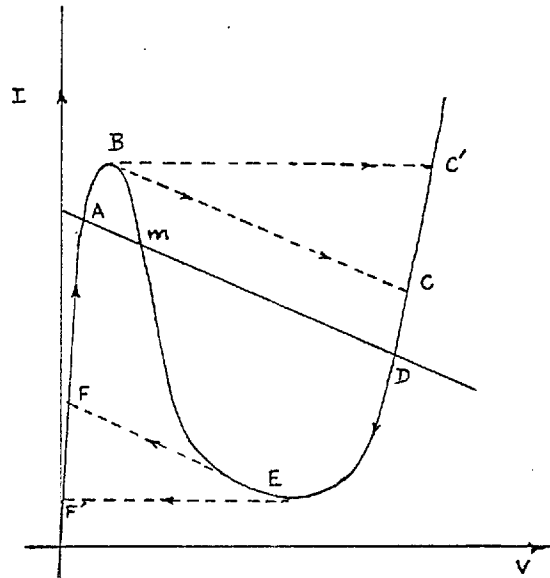


Fig 2.9: Bistable Operation of Tunnel diodes.

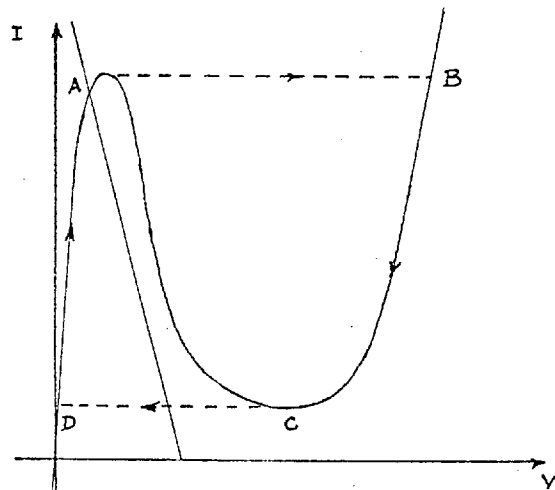


Fig 2.10: Monostable Operation.

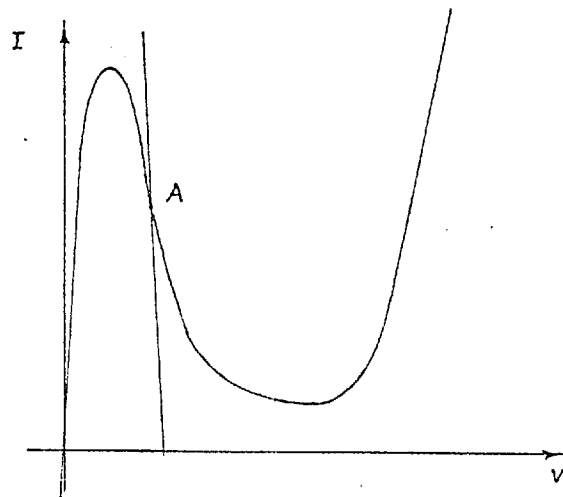


Fig 2.11: Bias condition for Amplifiers and Oscillators.

the bias.

If tunnel diode is biased at point A and $\frac{R_t}{L} \gg \frac{G}{C}$, a positive pulse of large enough magnitude applied to the tunnel diode will lift the biasing current above the peak current and if this lasts long enough to take the tunnel diode beyond the point m then the tunnel diode switches to the high voltage state D. Otherwise it will return to the point A. If the width of the pulse is greater than the time taken to switch from A to C then the trajectory followed will be ABC. When the triggering current ceases, the biasing point moves from C to the high voltage quiescent state D.

To switch back to the low voltage state, a negative trigger pulse is applied to the tunnel diode such that the tunnel diode current is reduced to below its valley current. The tunnel diode switches to F and then back to point A - when the trigger pulse ceases. The switching cycle is therefore ABCDEFA.

For bistable operation if $\frac{R_t}{L} \ll \frac{G}{C}$ then the load line is modified by the presence of the inductance. The trajectory in such a case is ABC'DEF'A.

2.6.2 Monostable operation

If a tunnel diode is biased such that the load line makes only one intersection with the tunnel diode characteristic as in Fig. 2.10 then the circuit has only one stable point.

If the inductance L is large enough, i.e. $\frac{R_t}{L} \ll \frac{G}{C}$, a trigger current which increases the diode current to more than the peak current will cause it to go through the trajectory ABCD.

If $\frac{R_t}{L} \gg \frac{G}{C}$ the voltage across the tunnel diode at any instant will be dependent on the amplitude of the trigger current at that instant.

2.6.3 Negative-resistance amplifiers and oscillators

In these types of applications R_t is restricted to be less than or equal to $\frac{1}{G}$ and the bias point is as shown in Fig. 2.11.

If $\frac{LG}{C} < R_t < \frac{1}{G}$, then the circuit will be stable and will act as a

linear negative-resistance amplifier.

If $R_t < \frac{1}{G}$, $R_t < \frac{LG}{C}$ and $\alpha^2 < |\beta|$ then as discussed in section 2.3 the circuit will be oscillatory.

2.7 Requirements of a Regenerative Amplifier

The requirements of a regenerative amplifier are twofold.

1) For a circuit to be regenerative it is necessary that at least one of the zeros of the immittance function of the circuit has a positive real part at some part of the pump cycle.

2) If such a regenerative circuit is to amplify a signal then the real part of its immittance function seen by the signal must be negative for a part of the pump cycle.

It is possible in some circuits to fulfill the requirements 1) and 2) above and at the same time a zero of the immittance function of such a circuit not only has a positive real part but the roots are complex. The circuit in this case is oscillatory and acts as the wellknown super-regenerative amplifier.

It is intended to restrict this work to the investigation of the non-oscillatory regenerative mode of amplification. The circuit of such an amplifier will have at least one positive real root.

A study of table 2.1 of section 2.5 shows that the first two rows of the table satisfy the conditions for regenerative amplification. Of these the circuit conditions $R_t > \frac{1}{G}$ and $R_t > \frac{LG}{C}$ are of greater interest as shown in appendix A.1.

CHAPTER THREE3. GENERAL THEORY OF REGENERATIVE AMPLIFIER3.1 Introduction

In the linear small signal mode of amplification, the regenerative amplifier can be represented by a very simple but adequate equivalent circuit. Fig. 3.1 shows the schematic representation of such an amplifier. i_p is the pump current which is very large compared with i_s , the signal current.

If the frequency band of operation is well below the resistive cut off and the self resonant frequencies, a considerable simplification in the analysis can be achieved by replacing the tunnel diode in Fig. 3.1, by the approximate circuit of Fig. 3.2. In this circuit the series inductance L_s and the series resistance, R_s , are neglected.

For linear negative-resistance amplifiers this model suffices to 500 Mc/s or so for the majority of the presently available diodes. However, this and the following chapters assume this equivalent circuit and it is worth emphasizing that the analysis is exactly applicable whenever the situation can be described in terms of a time varying conductance shunted by a parasitic capacitance.

A network model which includes the series inductance is studied later in section 4.5.

A further simplification can be made by handling the problem in two stages:

a) A large signal analysis. Here we obtain from the differential equations of the equivalent circuit of Fig. 3.3, the conductance-time characteristic produced by the action of the pump and study the effect of the pump frequency amplitude, waveform and the circuit parameters on the conductance-time characteristic.

b) A small signal analysis. Here we study the effect of a time varying conductance on the signal (Fig. 3.4). For this analysis we assume that the signal current is very small compared with the pump current.

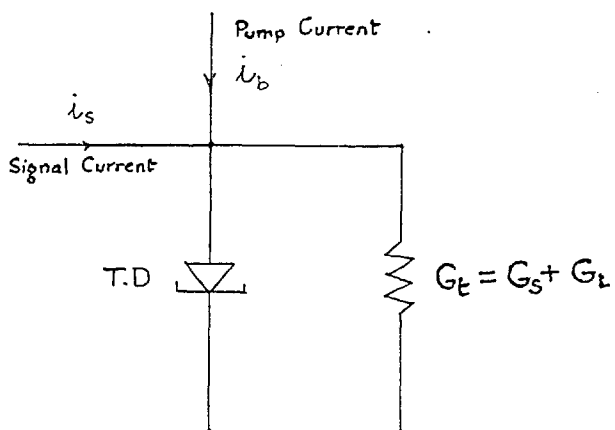


Fig. 3-1: Schematic Representation of Regenerative Amplifier.

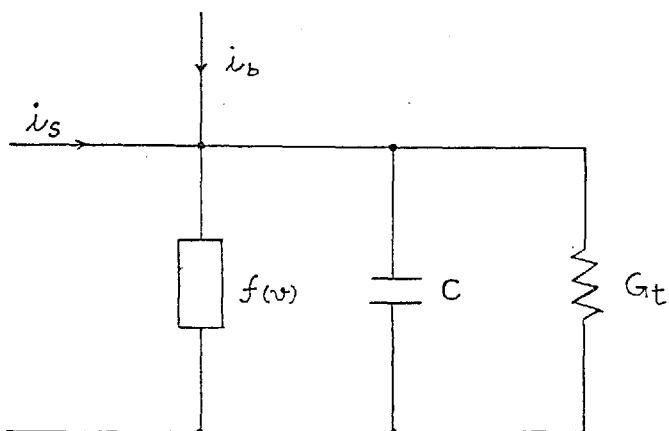


Fig 3-2. Simplified Equivalent Circuit of Regenerative amplifier.

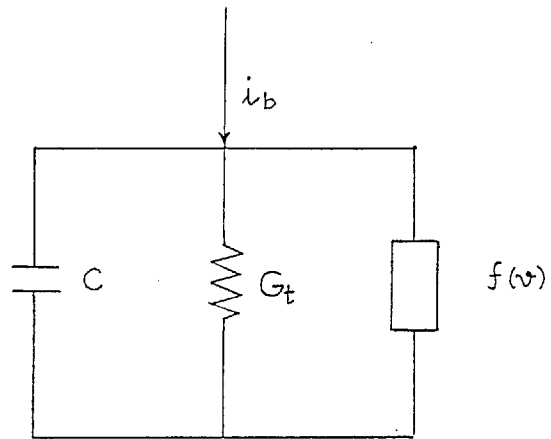


Fig. 3.3: Simplified large signal equivalent circuit for the determination of conductance function.

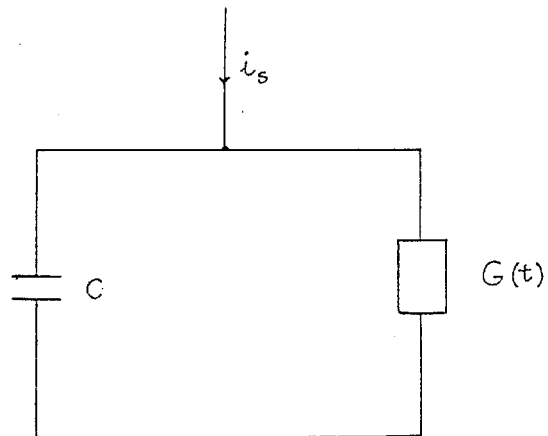


Fig 3.4: Equivalent circuit for small signal analysis of regenerative amplifier.

In this chapter we will investigate the part (b) for this purpose we assume a simple conductance function which is of the form

$$G(t) = G_0 [1 - F(t)]$$

It is possible to develop general formulae and understand the main properties of the regenerative amplifier on the basis of these assumptions.

In Chapter 4 the large signal analysis will be attempted and then we can substitute the conductance time function corresponding to a particular pump.

3.2 Qualitative Description of Regenerative Cycle

The operation of this amplifier can be best understood by tracing the various events that take place during a single cycle of pump. We will study the equivalent circuit of Fig. 3.2 in the presence of a square wave pulse of current of magnitude I_p . A typical voltage transient, across the tunnel diode, in response to a square wave current input, will be as shown in Fig. 3.5. From the conductance against voltage graph (Fig. 2.4) we can obtain the conductance-time curve (Fig. 3.5).

We can assume the circuit conductance for $V \leq 0$ to be a constant value G_0 . This will not introduce much inaccuracy in our analysis as conductance is a very slowly varying function of voltage in this region. Furthermore, as we shall see later, this section of conductance-time graph does not play a very important role in our analysis.

At time $t < 0$ and $G(t) = G_0$ (Fig. 3.5) the voltage across the circuit is that due to the applied signal current $i_s = I_s \sin \omega t$. When the tunnel diode is forward biased by the pump current (i.e. $t > 0$) the voltage across the tunnel diode capacitance slowly builds up to the peak voltage V_p . If i_b is large enough at this point to exceed $I_p + V_p G_0$ then the voltage will start increasing further. At time $t = t_1$, the value of circuit conductance has been reduced from G_0 to zero. At this point as $G(t)$ changes sign from positive to negative, regenerative build up starts. This build up goes on from the level of the signal to a maximum amplitude at the instant $t = t_2$, when the conductance is once again zero.

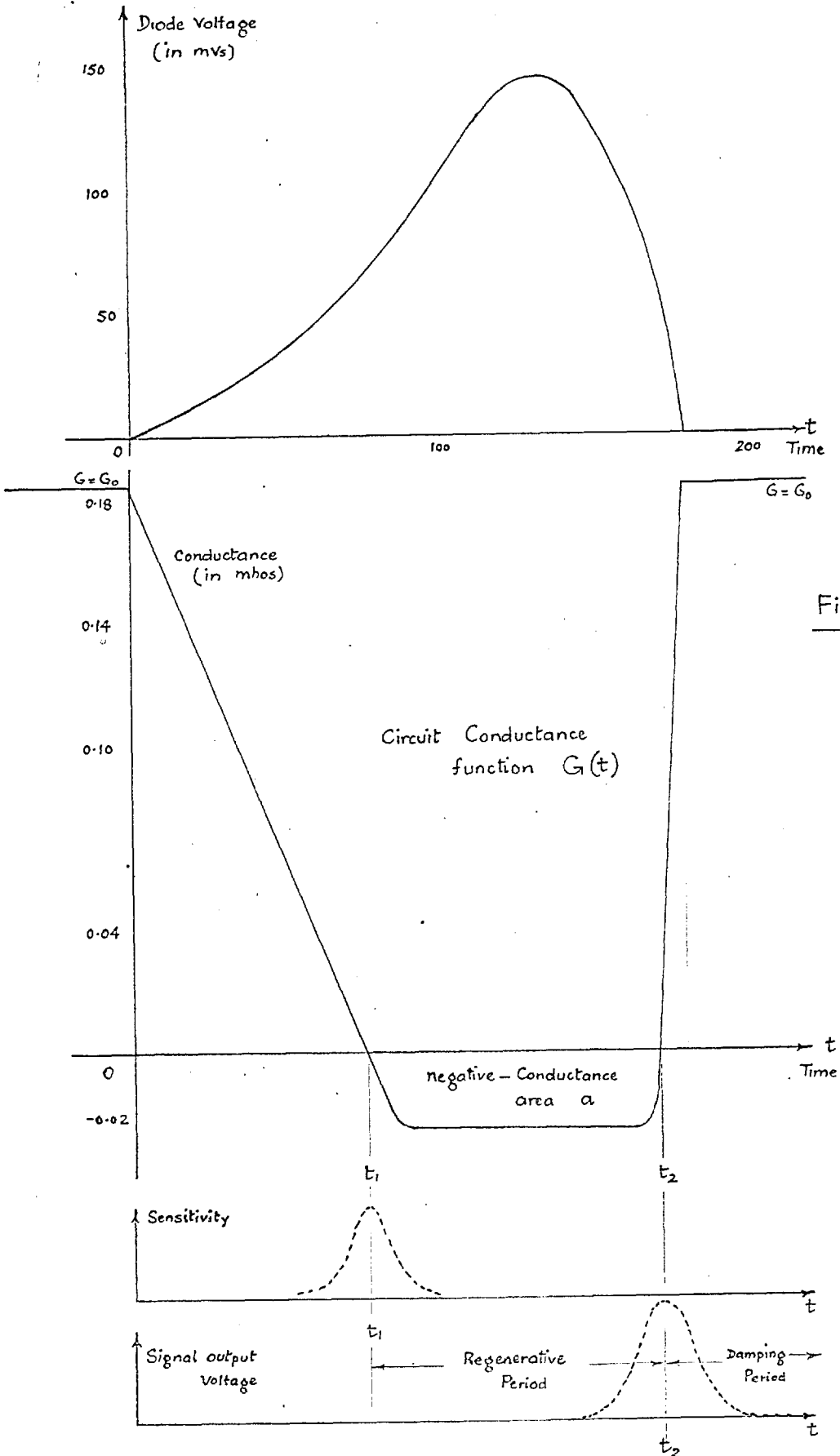


Figure 3.5.

After that the voltage, due to the signal, across the tunnel diode decays as the conductance goes positive. In order that the next regenerative cycle builds up from the level of the signal the voltage across the tunnel diode due to the signal must decay to the signal level.

3.3 Sampling Process

At the point $t = t_1$ and $G(t) = 0$, the current-voltage curve for the circuit goes through a maximum. At this point in the cycle there is a minimum amount of charge flowing into the diode capacitance C . Any small signal current impressed at this instant makes a significant contribution to the total charge available to build up the voltage across the diode capacitance. At an instant before or after $t = t_1$ the signal impressed makes a much less significant contribution. The signal input is thus sampled for a short period around t_1 (when conductance changes from positive to negative).

The sample of signal during the sensitive period of the pump determines the amplitude to which the signal voltage across the tunnel diode can rise before being quenched.

The way in which sampling sensitivity varies during a pump cycle depends on the pump, the tunnel diode and the circuit parameters.

The signal is sampled once for every cycle of the pump. The maximum frequency of amplification is thus restricted to half that of the pump.

From this qualitative description it is easy to see that the gain of a regenerative amplifier would, to a large extent, be dependent upon the characteristics of the amplifier in the sensitive period. It is not obvious as to what would be the determining influence on the frequency response except that the tunnel diode capacitance would be one major factor and the conductance, in some way, another.

3.4 Analysis of the Linear Regenerative Amplifier

An approximate mathematical analysis of the circuit of Fig. 3.4, should

describe the main properties of the regenerative amplifier.

Equating the currents in the circuit, the differential equation for the circuit is

$$C \dot{v} + G(t) v = I_s \sin \omega t \quad 3.1.$$

where C = the diode capacitance

$I_s \sin \omega t$ = signal current at an angular frequency ω .

and $G(t) = G_0 [1 - F(t)]$

Rewriting 3.1.

$$\dot{v} + \frac{G(t)}{C} v = \frac{I_s}{C} \sin \omega t \quad 3.2.$$

This equation is of the form

$$\dot{y} + G(x) y = H(x) \quad 3.3.$$

This equation can be solved readily by multiplying both sides by an integrating factor, $\exp(\int G(x) dx)$.

Equation 3.3. now becomes

$$\left[\dot{y} + G(x) y \right] \exp\left(\int G(x) dx\right) = H(x) \exp\left(\int G(x) dx\right)$$

which is the same as

$$\frac{d}{dx} \left[y \exp\left(\int G(x) dx\right) \right] = H(x) \exp\left(\int G(x) dx\right)$$

$$\therefore y = \exp\left(-\int G(x) dx\right) \left[\int H(x) \exp\left(\int G(x) dx\right) + K \right]$$

where K is an appropriate constant which depends on the initial conditions of the circuit.

The solution of equation 3.2. therefore, is

$$\begin{aligned} v &= K \exp\left(-\frac{1}{C} \int G(t) dt\right) + \exp\left(-\frac{1}{C} \int G(t) dt\right) \cdot \int \frac{I_s}{C} \exp\left(\frac{1}{C} \int G(t) dt\right) \sin \omega t dt \\ &= v_0 + v_1 \end{aligned} \quad 3.4.$$

The formula 3.4. for the voltage across the circuit is applicable to any variations of conductance. The signal voltage v at any time $t > 0$ consists of two parts. v_0 can be regarded as the steadystate voltage and

v_1 is due to the effect of the signal input on the time varying conductance.

For a time $t < 0$, the voltage v across the circuit is the steady state voltage. This assumes that signal from the previous cycle has decayed to the steady state value. At time $t = 0$, $G(t) = G_0$, and therefore, the equation 3.2. for this region is

$$\dot{v} + \frac{G_0}{C} v = \frac{I_s}{C} \sin \omega t \quad 3.5.$$

The steady state solution of this equation is

$$v = \frac{I_s}{C \left[\omega^2 + \left(\frac{G_0}{C} \right)^2 \right]} \left[\frac{G_0}{C} \sin \omega t - \omega \cos \omega t \right] \quad 3.6.$$

The value of the constant K in equation 3.4. can now be determined from the boundary condition at $t = 0$. The voltage v is continuous through $t = 0$ i.e.,

$$v \Big|_{-0} = v \Big|_{+0} \quad 3.7.$$

From 3.6.

$$v \Big|_{-0} = \frac{-I_s \omega}{C \left[\omega^2 + \left(\frac{G_0}{C} \right)^2 \right]}$$

From 3.4.

$$v \Big|_{+0} = K$$

Consequently using equation 3.7.

$$K = \frac{-I_s \omega}{C \left[\omega^2 + \left(\frac{G_0}{C} \right)^2 \right]} \quad 3.8.$$

From equations 3.4. and 3.8. we are now in a position to write the expression for v_0 .

$$v_0 = \frac{-I_s \omega}{C \left[\omega^2 + \left(\frac{G_0}{C} \right)^2 \right]} \exp \left(-\frac{1}{C} \int G(t) dt \right) \quad 3.9.$$

but $\left(\frac{G_o}{C}\right)^2 \gg \omega^2$ and therefore,

$$v_o = \frac{-I_s \omega C}{G_o^2} \exp\left(-\frac{1}{C} \int G(t) dt\right) \quad 3.10.$$

We will see later that the relative importance of the steady state voltage v_o and the transient voltage v_1 depends upon the period t_1 which is the time required for the circuit conductance to reduce from G_o to zero.

3.5 Sensitivity of the Amplifier to Signal Input

The qualitative description of section 3.3 shows us that the sensitivity of the circuit to signal input is greatest at $t = t_1$.

From the equation 3.4, we may write the value of v_1 in the form

$$v_1 = \frac{I_s}{C} \exp\left(-\frac{1}{C} \int_0^t G(t) dt\right) I_1$$

where

$$I_1 = \int_0^t \exp\left(\frac{1}{C} \int_0^t G(t) dt\right) \sin \omega t dt. \quad 3.11.$$

We can proceed now to evaluate I_1 . For this it is necessary to substitute a general conductance function with the important characteristics of the conductance curve of Fig. 3.5. An appropriate conductance function is

$$G(t) = G_o [1 - F(t)] \quad 3.12.$$

$$\text{At } t = 0, G(t) = G_o \quad \therefore F(0) = 0,$$

$$\text{At } t = t_1, G(t_1) = 0 \quad \therefore F(t_1) = 1 \quad 3.13.$$

$$\text{and At } t = t_2, G(t_2) = 0 \quad \therefore F(t_2) = 1$$

and we note further that

$$\int_0^t G(t) dt = G_o [t - \phi(t)] \quad 3.14.$$

$$\text{where } \phi(t) = \int_0^t F(t) dt \quad 3.15.$$

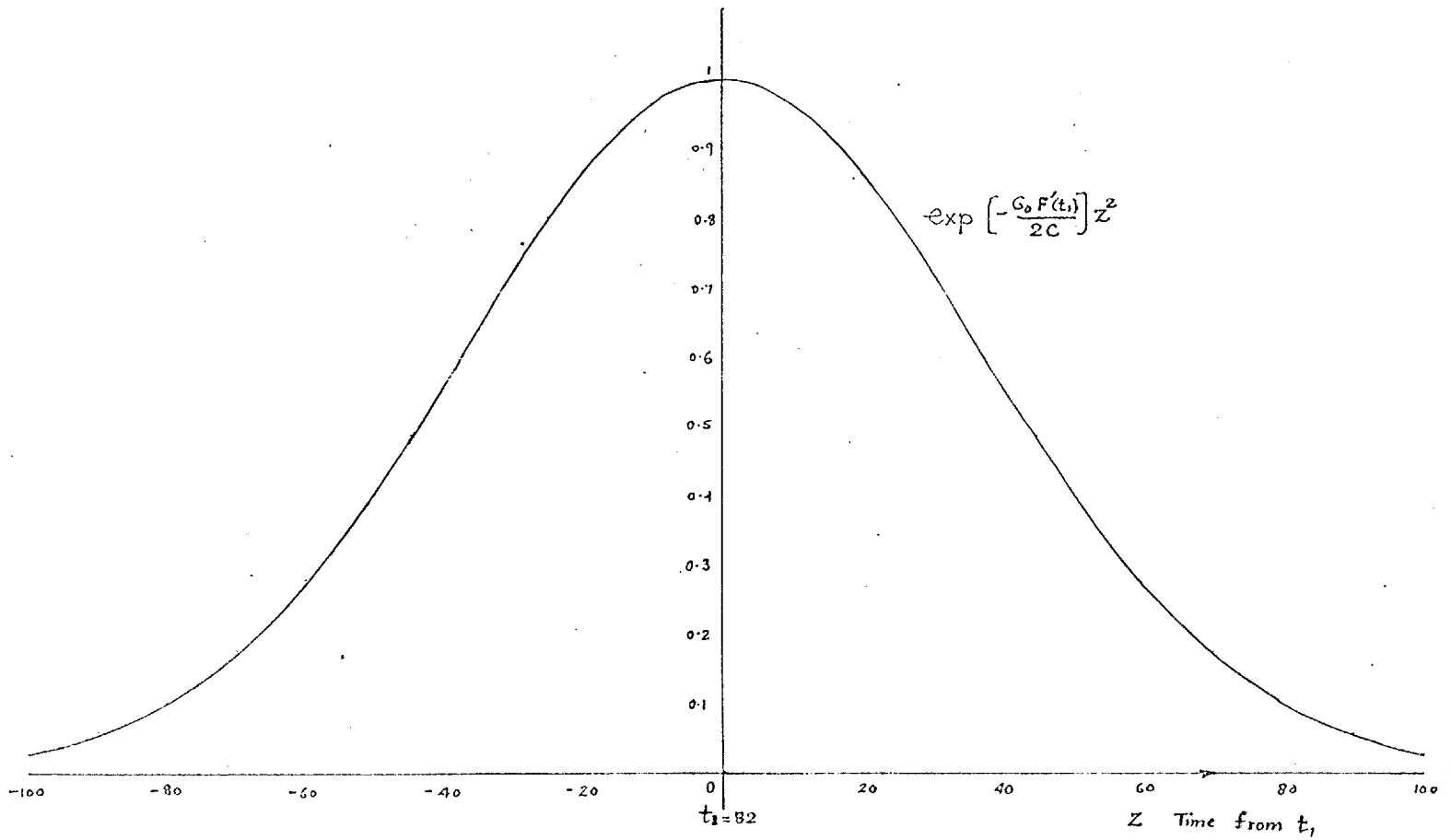


Fig. 3.6: Sensitivity factor against time.
 $G'(t)/c = 0.00071$

Making the substitutions in equation 3.11. from equation 3.14,

$$I_1 = \int_0^t \exp \left[\frac{G_0}{C} \{ t - \phi(t) \} \right] \sin \omega t \, dt$$

To study the sensitivity of the amplifier this equation should be studied at and around $t = t_1$.

Changing the origin from $t = 0$ to $t = t_1$ and the time variable from t to $Z = t - t_1$, now I_1 becomes

$$I_1 = \int_{-t_1}^{t-t_1} \exp \left[\frac{G_0}{C} \{ (Z+t_1) - \phi(Z+t_1) \} \right] \sin \omega(Z+t_1) \, dz \quad 3.16.$$

The exponential under the integral is a maximum at $t = t_1$ and falls off on either side of it. We can reach a reasonable approximation to the value of integral I_1 by expanding the exponential expression about the instant $t = t_1$ and neglecting the unimportant terms

$$\phi(Z+t_1) = \phi(t_1) + Z F(t_1) + \frac{1}{2} Z^2 F'(t_1)$$

and because $F(t_1) = 1$

$$\phi(Z+t_1) = \phi(t_1) + Z + \frac{1}{2} Z^2 F'(t_1)$$

Consequently the exponential becomes

$$\begin{aligned} \exp \left[\frac{G_0}{C} \{ (Z+t_1) - \phi(Z+t_1) \} \right] &= \exp \left[\frac{G_0}{C} \{ t_1 - \phi(t_1) \} \right] \exp \left[- \frac{G_0 F'(t_1)}{2C} \right] Z^2 \\ &= \exp \left(\frac{1}{C} \int_0^{t_1} G(t) \, dt \right) \exp - \frac{G_0 F'(t_1)}{2C} Z^2 \end{aligned} \quad 3.18.$$

The factor $\exp - G_0 F'(t_1) Z^2 / 2C$ is plotted in Fig. 3.6. It has the form of a gaussian error curve with a maximum at $Z = 0$ i.e. at $t = t_1$.

The amplifier is most sensitive to signal at the time $t = t_1$ and the sensitivity falls off quite rapidly for an instant before or after time $t = t_1$.

3.6 Expression for Signal Voltage

The fact that the sensitivity factor in 3.18. is important only for

values of t near t_1 leads to a considerable simplification in the evaluation of equation 3.16.

Now $\sin \omega(Z+t_1) = \sin \omega Z \cos \omega t_1 + \cos \omega Z \sin \omega t_1$. The first term on the right hand side is very small near $Z = 0$ and therefore, can be neglected. So that

$$I_1 = \exp\left[\frac{1}{C} \int_0^{t_1} G(t) dt\right] \sin \omega t_1 \int_{-t_1}^{t-t_1} \exp\left[-\frac{G_0 F'(t_1)}{2C} Z^2\right] \cos \omega Z dZ. \quad 3.19.$$

If the limits of integration can be replaced by $\pm \infty$ then the integral is a standard one which can be solved by simple means. This assumption is justified because the sensitivity falls off quite rapidly on both sides of $Z = 0$.

$$\left. \begin{array}{l} \text{Provided } \frac{G_0 F'(t_1)}{2C} t_1^2 > 3 \\ \text{and } t > 2t_1 \end{array} \right\} \quad 3.20.$$

the sensitivity factor in which case would have fallen to less than 5 per cent of its peak value. If these conditions are satisfied, the error involved in changing the limits of integration is negligible.

$$\begin{aligned} \therefore I_1 &= \exp\left[\frac{1}{C} \int_0^{t_1} G(t) dt\right] \sin \omega t_1 \int_{-\infty}^{\infty} \exp\left[-\frac{G_0 F'(t_1)}{2C} Z^2\right] \cos \omega Z dZ \\ &= \exp\left[\frac{1}{C} \int_0^{t_1} G(t) dt\right] \left[\frac{2 \pi C}{G_0 F'(t_1)}\right]^{\frac{1}{2}} \exp\left[-\frac{C \omega^2}{2 G_0 F'(t_1)}\right] \sin \omega t_1 \end{aligned}$$

$$\text{Now } G_0 F'(t_1) = G'(t_1).$$

The signal voltage v_1 now is given by

$$v_1 = I_s \sin \omega t_1 \left[\frac{2 \pi}{C G'(t_1)}\right]^{\frac{1}{2}} \exp\left[-\frac{C \omega^2}{2 G'(t_1)}\right] \exp\left[\frac{1}{C} \int_{t_1}^t G(t) dt\right] \quad 3.21.$$

In this expression $\exp\left[-\frac{C \omega^2}{2 G'(t_1)}\right]$ is the frequency dependent term. As

we shall see later this expression is very nearly equal to unity over the frequency band of amplification. $\sin \omega t_1$ appears in the equation only to signify that a sample of signal $I_s \sin \omega t$ is taken at the instant $t = t_1$.

Now we are in a position to compare the relative magnitudes of v_1 and v_o . From equations 3.10. and 3.21.

$$\frac{v_1}{v_o} = \left[\frac{2\pi}{C G'(t_1)} \right]^{\frac{1}{2}} \frac{G_o^2}{\omega C} \exp \left[\frac{1}{C} \int_0^{t_1} G(t) dt \right] \quad 3.22.$$

For v_o to be less than one per cent of v_1 , the right hand expression should be greater than 100. In practice, this expression has a value of 1000 or more. Therefore, neglecting v_o

$$v = v_1 = I_s \left[\frac{2\pi}{C G'(t_1)} \right]^{\frac{1}{2}} \exp \left[\frac{-C \omega^2}{2 G'(t_1)} \right] \exp \left[-\frac{1}{C} \int_{t_1}^t G(t) dt \right] \sin \omega t_1 \quad 3.23.$$

3.7 Signal Output Waveshape

Further simplification of equation 3.23 is possible and can be made to yield very useful information regarding the waveshape of the output signal voltage.

We know from qualitative description of section 3.2 that the signal builds up in amplitude to the point $t = t_2$ when the circuit conductance reduces to zero from its negative value. For $t > t_2$ the circuit conductance goes positive and the signal voltage decays. Hence the signal output voltage is a maximum at $t = t_2$.

The only part of expression 3.23. which can describe the shape of the output is the exponential factor $\exp \left[-\frac{1}{C} \int_{t_1}^t G(t) dt \right]$

$$\text{and } \exp \left[-\frac{1}{C} \int_{t_1}^t G(t) dt \right] = \exp \left[-\frac{1}{C} \int_0^t G(t) dt \right] \exp \left[\frac{1}{C} \int_0^{t_1} G(t) dt \right]$$

but $\exp \left[-\frac{1}{C} \int_0^t G(t) dt \right]$ can be expanded around the time $t = t_2$

$$\text{At } t = t_2 \quad G(t_2) = 0 \quad F(t_2) = 1$$

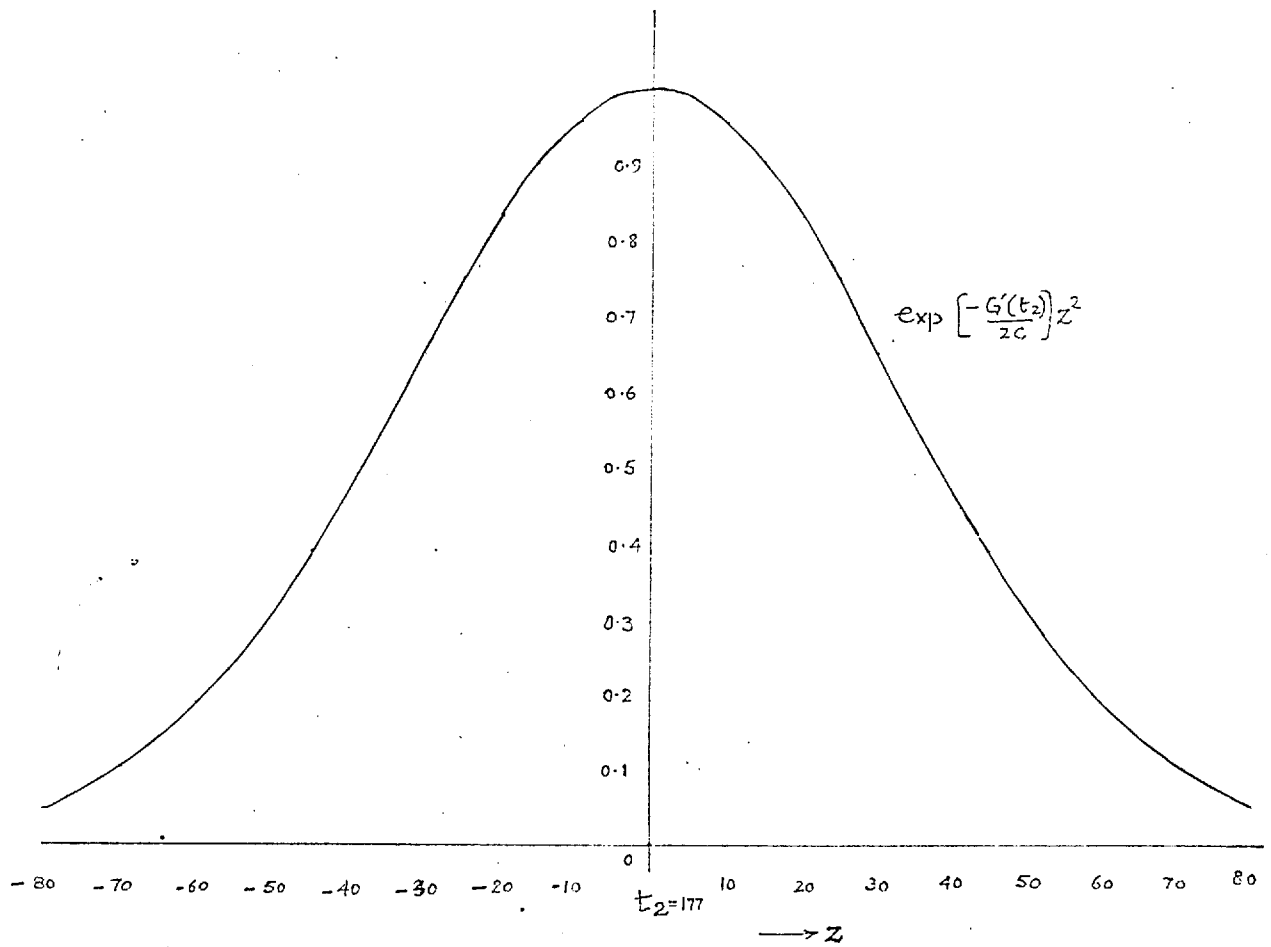


Fig. 3.7: Wave Shape of Signal Output voltage.

$$\frac{G'(t_2)}{C} = 0.000925$$

Changing the variables once again from t to $Z = t - t_2$, we obtain

$$\begin{aligned} \exp \left[-\frac{1}{C} \int_0^t G(t) dt \right] &= \exp \left[-\frac{G_0}{C} \{t - \phi(t)\} \right] \\ &= \exp \left[-\frac{G_0}{C} \{(Z+t_2) - \phi(Z+t_2)\} \right] \end{aligned}$$

$$\text{Now } \phi(Z+t_2) = \phi(t_2) + Z F(t_2) + \frac{1}{2} Z^2 F'(t_2)$$

We neglect higher terms of the expansion and this makes the exponential factor

$$\begin{aligned} \exp \left[-\frac{1}{C} \int_0^t G(t) dt \right] &= \exp \left[-\frac{G_0}{C} \left\{ t_2 - \phi(t_2) - \frac{1}{2} Z^2 F'(t_2) \right\} \right] \\ &= \exp \left[-\frac{1}{C} \int_0^{t_2} G(t) dt \right] \exp \frac{-G'(t_2)}{2C} Z^2 \end{aligned} \quad 3.24.$$

The factor $\exp \frac{-G'(t_2)}{2C} Z^2$ gives us the shape of the output pulse and is a gaussian error curve. The peak of the output voltage occurs at the time $t = t_2$ and falls off quite rapidly on both sides of it. This factor is plotted in Fig. 3.7.

Substituting from equation 3.24 and 3.21 the output voltage across the circuit is

$$v = I_s \left[\frac{2\pi}{C G'(t_1)} \right]^{\frac{1}{2}} \exp \left[\frac{-C \omega^2}{2 G'(t_1)} \right] \exp \left[-\frac{1}{C} \int_{t_1}^{t_2} G(t) dt \right] \exp \frac{-G'(t_2)}{2C} Z^2 \quad 3.25.$$

Before embarking upon a further study of the constituent terms of this expression we can normalize it to a new time variable x such that

$$x = \frac{t}{C}$$

Then normalizing other time dependent factor in expression 3.25. with respect to C we have

$$G'(t_1) = \frac{G'(x_1)}{C}$$

$$G'(t_2) = \frac{G'(x_2)}{c}$$

$$-\frac{1}{c} \int_{t_1}^{t_2} G(t) dt = - \int_{x_1}^{x_2} G(x) dx = a = \text{negative-conductance area.}$$

$$\text{and } \omega^2 = \frac{\mu^2}{c^2}$$

Then the normalized expression for output voltage is

$$v = I_S \left[\frac{2\pi}{G'(x_1)} \right]^{\frac{1}{2}} \exp \left[-\mu^2 / 2G'(x_1) \right] \exp a \exp \left[\frac{-G'(x_2)}{2} (dx_2)^2 \right]$$

3.26.

where dx_2 is normalized time deviation from the instant $x = x_2$

3.8 Frequency Response

The only frequency dependent term in the expression 3.26. is the term

$$\exp -\mu^2 / 2G'(x_1) \quad 3.27.$$

The value of this expression is unity for $\mu = 0$ and falls off at higher frequencies. This term is drawn in Fig. 3.8.

In the regenerative amplifier, the maximum frequency of amplification is restricted to half the frequency of sampling. If $\frac{\mu_p}{2\pi}$ is the frequency of the pump

$$\text{then the frequency band of amplification} = \frac{\mu_p}{4\pi} \quad 3.28.$$

If the gain in this frequency band is not to fall by greater than 10% below the gain at the low frequency end

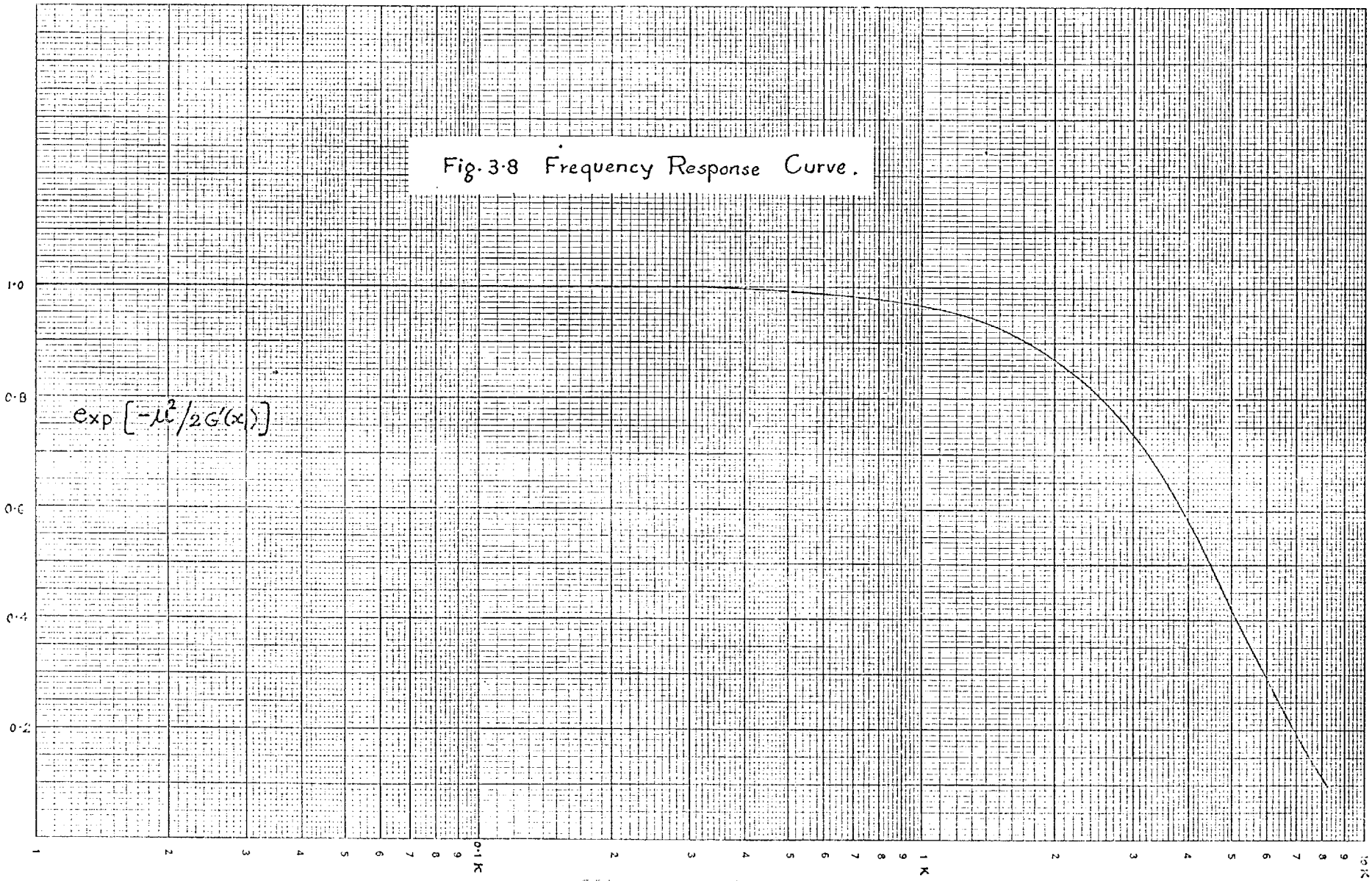
$$\text{then } \exp -\mu^2 / 2G'(x_1) > 0.9$$

$$\mu^2 / 2G'(x_1) < 0.105$$

$$\mu^2 < 0.21 G'(x_1)$$

$$\text{or } \mu_p^2 < 0.84 G'(x_1) \quad 3.29.$$

Fig. 3-8 Frequency Response Curve.



$$\exp\left[-\frac{\mu^2}{2G(x)}\right]$$

$\frac{\mu}{2\pi}$ →

This condition relate the two factors which determine the frequency response of the amplifier. In practice, as we will see in chapter 4, this condition 3.29 is more than satisfied and drop in gain in the frequency band of amplification is even less than 5%.

3.9 Regenerative Amplifier Gain

The linearity of the regenerative amplifier is evident from the fact that the signal output voltage v at any time during the regenerative cycle is directly proportional to the signal input current I_s .

The regenerative gain A_m of the amplifier measured at the time t_2 , at the peak of the output pulse and in the frequency band such that the expression 3.27 is unity, is given by

$$A_m = G_t \left[\frac{2\pi}{G'(x_1)} \right]^{\frac{1}{2}} \exp a \quad 3.30.$$

$$= G_t A_v$$

$$\text{where } G_t = G_s + G_L$$

$$\text{and } A_v = \left[2\pi/G'(x_1) \right]^{\frac{1}{2}} \exp a \quad 3.31.$$

A_v in this expression 3.31 depends upon the conductance function $G(t)$ and thus on G_t . A_v can be maximized with respect to G_t and then the gain A_m in equation 3.30. is at a maximum.

As far as the current and voltage gains and the voltage across the circuit are concerned, they are affected only by the total conductance G_t and not by the individual values of source conductance G_s or load conductance G_L . But the current input and thus also the current output depend upon the relative magnitudes of G_s and G_L .

$$\begin{aligned} \text{The maximum current input} &= I_s \text{ when } G_s = 0 \\ &\text{i.e. } G_t = G_L \end{aligned}$$

$$\text{The current gain } A_i = A_v G_t = A_v G_L$$

$$\text{and the maximum output current} = I_s A_v G_L \quad 3.32.$$

In an active two port which has infinite or zero input impedance, the amplification ratio (ratio of voltage or current out to voltage or current in)

is a very useful measure of performance. However, for a two terminal network with its input and output ports common or for a network which requires power at the input port, it is much more significant to measure performance in terms of the flow of power in the circuit.

The most important measure of power flow is the quantity called the transducer gain (P_T). Transducer gain is defined by the formula

$$\begin{aligned} P_T &= \frac{\text{Power delivered to the load.}}{\text{Power available from the source}} \\ &= \frac{P_o}{P_{avs}} \end{aligned} \quad 3.33.$$

Its importance arises from the fact that it compares the power which the active network delivers to the load with that which the generator alone could deliver under optimum conditions of the load and the source impedances, and therefore it measures the efficacy of using the active device.

$$\begin{aligned} \text{Power output into load at any instant} &= v^2 G_L \\ \text{Average power output over one cycle} &= \frac{1}{X} \int_0^X v^2 G_L dx \end{aligned} \quad 3.34.$$

where X = duration of one cycle.

$$\begin{aligned} \text{But } v &= I_s A_v \exp \left[\frac{-G'(x_2)}{2} (dx_2)^2 \right] \\ \text{Power available from the source} &= I_s^2 / 4G_s \end{aligned} \quad 3.35.$$

$$\text{Therefore } P_T = \frac{4 G_s G_L}{X} A_v^2 \int_0^X \left[\exp \left\{ \frac{-G'(x_2)}{2} (dx_2)^2 \right\} \right]^2 dx$$

Changing the limits of integration to $\pm \infty$ (This does not involve any inaccuracy because the expression under the integral falls in value to much below 5 per cent at the limits of integration i.e. $x = 0$ and $x = X$,

$$\therefore P_T = \frac{4 G_s G_L A_v^2}{X} \left[\frac{\pi}{G'(x_2)} \right]^{\frac{1}{2}} \quad 3.36.$$

The terms A_v and $\left[\frac{\pi}{G'(x_2)} \right]^{\frac{1}{2}}$ depend upon the external total conductance G_t and not on the individual values of G_s and G_L . These terms can be maximized with respect to G_t .

The remaining factor $\frac{4 G_s G_L}{X}$ in the expression 3.36. for P_T is a

maximum with respect to the source and the load conductance when

$$G_S = G_L = \frac{G_t}{2} \quad 3.37.$$

3.10 The Damping Period

In section 3.4 we made the assumption that at the end of each cycle the circuit reaches its steady state. It is necessary that each cycle must start from the level of the input signal. Otherwise the voltage transient would build up from the decaying transient of the previous cycle.

It is obvious from equation 3.36. that shorter the period X compatible with the circuit condition the higher the power gain P_T . But if the period X is reduced indefinitely the above assumption will not be justified.

If we can ensure that the transducer gain drops to -20 db at $x = X$, the power due to regenerative amplification would have dropped to 5 per cent of the signal power available from the source. For this

$$\begin{aligned} P_T &= 0.05 \quad \text{at } x = X \\ &= 4 G_S G_L A_v^2 \exp \left[\frac{-G'(x_2)}{2} (X - x_2)^2 \right]^2 \\ \therefore \exp \left[\frac{-G'(x_2)}{2} (X - x_2)^2 \right] &= \left[\frac{0.05}{4 G_S G_L A_v^2} \right]^{\frac{1}{2}} \quad 3.38. \end{aligned}$$

This condition must be satisfied if the analysis of this chapter is to hold valid. In practice this condition is satisfied very easily, specially when the pump waveshape is a practical one of a sinusoid.

3.11 Conclusions

It has been shown in the preceding analysis that the properties of the linear small signal amplifier can be described in terms of simple formulae. The usefulness of these formulae is not impaired to any degree (if anything it is enhanced) by basing the analysis on a general conductance function.

The parameters of great importance are the time t_1 , t_2 and the

conductance slopes $G'(t_1)$ and $G'(t_2)$ at the beginning and the end of the regenerative period respectively. The negative-conductance area a is another parameter of great significance. The frequency response is dependent upon the conductance slope at the beginning of the regenerative period. The gain of the amplifier is determined by the conductance slopes at the beginning and the end of the regenerative period and the negative-conductance area in the regenerative period.

The lower the $G'(t_1)$ the higher the gain but this is at the expense of the frequency response of the amplifier. Whereas an increase in negative-conductance area can achieve the same objective without any restrictions on the frequency response.

A reduction of $G'(t_2)$ increases the duration of the signal output pulse and hence the gain too but the period T has to be increased to ensure adequate damping.

CHAPTER FOUR

4. REGENERATIVE AMPLIFIER WITH SQUARE WAVE PUMP

4.1 Introduction

The general theory of the linear regenerative amplifier developed in the last chapter assumes a general conductance function. The expressions that result are sufficient to describe the operation of the amplifier under the restrictions imposed in the analysis.

In this chapter we consider conductance functions due to square wave pump, ^{when applied to a tunnel diode.} The analysis of regenerative amplifier with square wave pump is comparatively simple and is considered before sine wave pump (Chapter 5). However, square wave pump is more difficult to generate at higher frequencies than sine wave pump.

The study of a regenerative amplifier with a given pump entails a study of the response of a tunnel diode to the pump amplitude, frequency and waveform. It is also important to study the influence of tunnel diode internal parameters and the external circuit elements like the load conductance on this response. It is necessary, finally, to show how the gain and the frequency response depend upon the pump and the circuit elements. Only then will it be possible to suggest any optimization techniques that may be available to us.

The theoretical analysis of this regenerative amplifier using a specified pump is necessarily approximate. The corresponding conductance function depends upon the current-voltage characteristic of the tunnel diode. This characteristic is a very complicated non-linear function, but it remains the same in essential form from one tunnel diode to another and therefore, it is possible to normalize the analysis with respect to tunnel diode parameters.

The analytical method is only convenient when the pump current is a simple function of time and even then it is necessarily approximate and tedious. When a greater accuracy is desired or when the pump current cannot be easily expressed analytically, graphical or numerical methods are the only choice.

It is shown that some analytical methods can be used to get design data for rectangular pump currents. The numerical analysis gives more accurate results but it is not very convenient for optimization. Once approximate

* The rise time of the square wave pump is assumed to be small compared with its pulse width.

optimization has been carried out, the numerical analysis can then be used to provide accurate design information.

4.2 Types of Conductance Cycles

The tunnel diode conductance-voltage relationship can be calculated from its static characteristic, $i = f(v)$. To obtain $G(x)$, all that is required is to determine the tunnel diode voltage against time relationship. The tunnel diode voltage in the presence of pump current depends upon the magnitude, frequency and waveform of the pump along with the characteristics of the tunnel diode and the load conductance. In general, there are two distinct types of conductance function possible as shown in Figures 4.1 and 4.2.

If the tunnel diode voltage due to the pump is arrested as in Fig. 4.1, the conductance characteristic seen by the signal is similar to the one assumed for the discussion and analysis of Chapter 3. The signal in this case is sampled at $x = x_1$, is amplified to a peak level at $x = x_2$ and for $x > x_2$, the amplified signal decays. If the damping period is long enough, the signal voltage across the tunnel diode would decay to the signal input level before the commencement of the next regenerative cycle.

The conductance function of Fig. 4.2 on the other hand is a more complicated one. The signal input sees a negative-conductance area a_1 when the voltage across the tunnel diode, due to the pump, is building up and it sees another negative conductance area a_2 when the voltage across the tunnel diode, due to the pump, decays. Depending upon the length of time, δx , that elapses between the two negative-conductance areas, a_1 and a_2 , two possibilities exist.

- 1) If δx is small enough the amplified signal pulse across the tunnel diode does not decay to the signal input level before it is amplified again due to second negative-conductance area a_2 .
- 2) If δx is large enough, the amplified peak of signal at $x = x_2$, decays to the level of the signal input present. In this case another sample is taken of the signal at $x = x_1'$. This sample is amplified due to a_2

Fig 4.1.

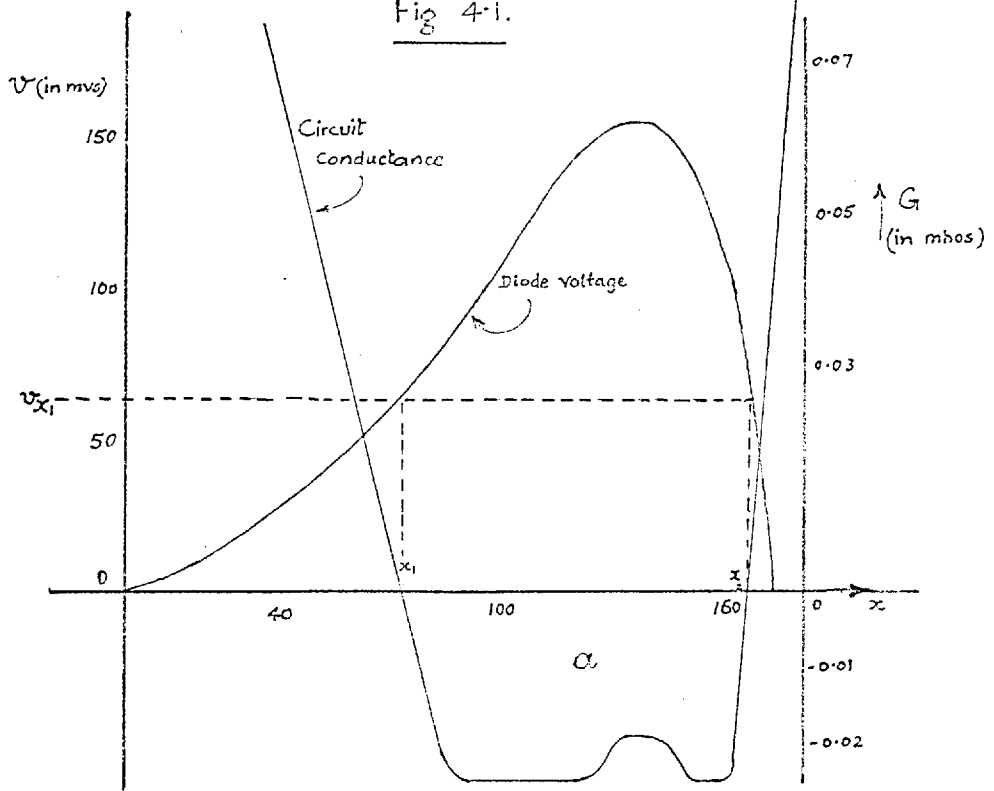
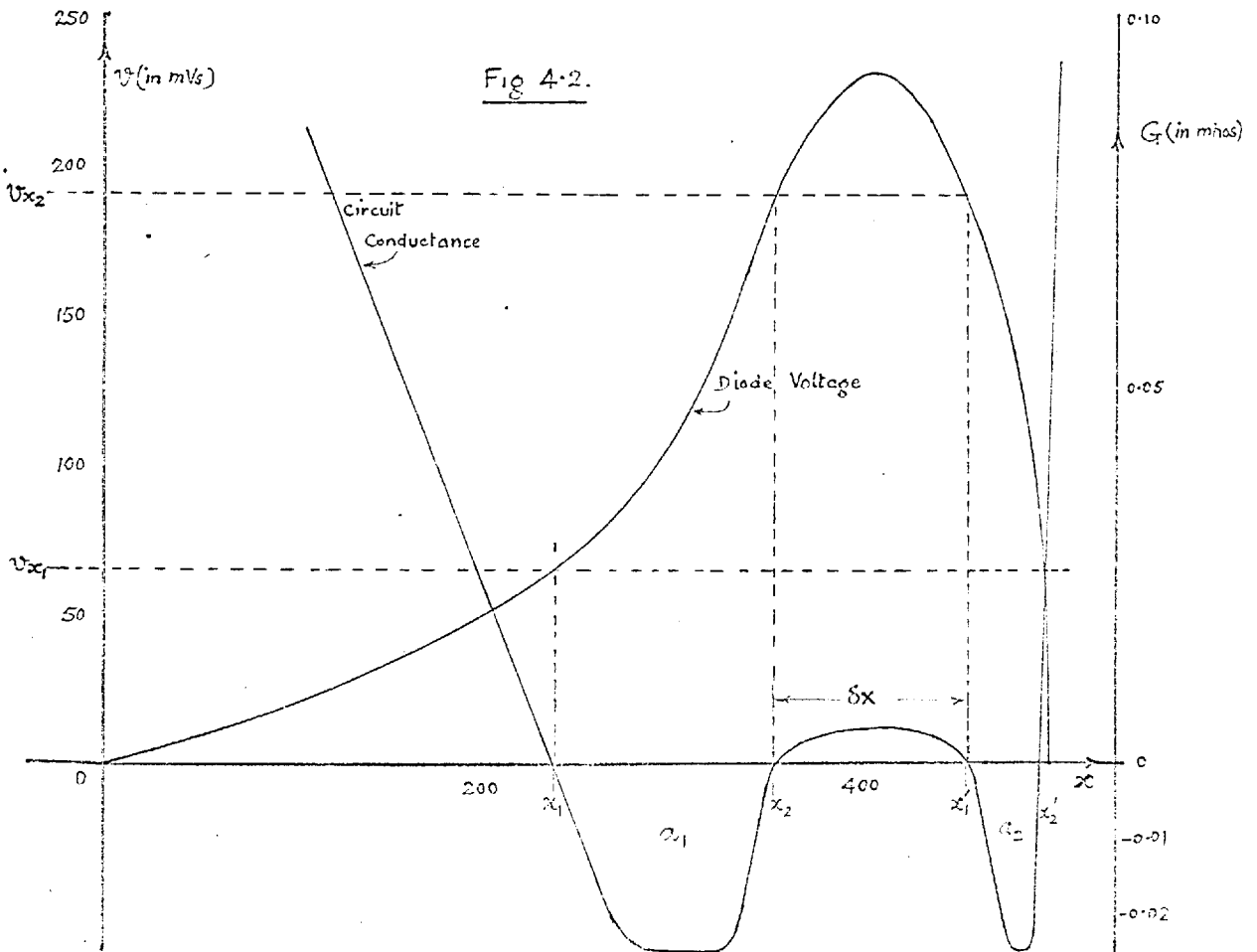


Fig 4.2.



and reaches a peak amplified level at $x = x_2'$ and so on. Thus two independent samples of the signal are taken and amplified during the period of one pump cycle and the two samples may each experience different amount of amplification.

For both the above mentioned conditions, if the area a_2 is small enough and its associated conductance slopes large enough then the amplification of the signal due to the second negative-conductance area may be insignificant. In such a case we can neglect the effect of the area a_2 .

If the amplification due to a_2 is comparable with that due to a_1 and the condition (1) above exists, then the power gain P_T will be increased. But if the amplification due to a_2 is comparable with that due to a_1 and the condition (2) above exists then the situation is a much more complicated one and will not be considered in this work.

The amplification due to a_2 can be made very very small in comparison with that due to a_1 if the decay of the tunnel diode voltage due to the pump is speeded up. This can be achieved very simply by letting the pump current go negative (as for a sinusoidal pump current) during the switch off portion of the tunnel diode voltage transient. In practice, then, $a_2 \ll a_1$ and can, therefore, be neglected.

4.3 Amplifier Output

In the regenerative amplifier there are two transient process taking place simultaneously. Due to the pump current, the tunnel diode voltage builds up, reaches a peak amplitude and then decays to the quiescent state. The signal voltage, similarly, builds up reaches a peak amplitude and then decays to the quiescent state. The relative position in time of the two peaks is not directly of any significance if the output of the amplifier is desired to be in the form of an amplified replica of the input signal. In such a case, we would endeavour to maximise the transducer gain P_T and the frequency response of the amplifier. The second negative-conductance area a_2 , discussed in Section 4.2, does make a contribution, though not a very significant one, to the transducer gain.

Other application of the regenerative amplifier, of this thesis, is to obtain amplified samples of the signal. The amplified signal appears as the envelope of the peaks of the voltage across the tunnel diode. To obtain a maximum signal modulation of the output pulses the two peaks must coincide in time.

The signal amplitude for a time $x > x_1$ depends upon the magnitude of the negative-conductance area traversed upto that time x . The circuit conductance is zero at the time x_1 when $v = v_{x_1}$ and becomes zero again at $v = v_{x_1}$ if the voltage transient is of the form shown in Fig. 4.1. but becomes zero at $v = v_{x_2}$ if the voltage transient is of the form shown in Fig. 4.2. Maximum negative-conductance area would have been traversed upto the peak voltage if the peak voltage is to be $v = v_{x_2}$ (i.e. $\delta x = 0$ for Fig. 4.2). The signal in this case reaches a peak value at $v = v_{x_2}$. The diode voltage due to pump current decays after this and the circuit conductance goes negative once again. This second excursion into negative-conductance region amplifies the signal further and the peak of the signal will rise to above the level of the signal at $v = v_{x_2}$ but the diode voltage due to pump current is lower than the peak value of v_{x_2} . The sum of the voltage due to signal and the voltage due to pump current could rise above that at $v = v_{x_2}$ only if 1) a_2 were to grow very quickly with time and

2) the voltage transient due to pump were to decay slowly.

These conditions have not been encountered in practice.

To achieve a maximum modulation of the diode voltage peak due to pump, by the amplified signal, the diode voltage transient should be arrested at $v = v_{x_2}$. For square wave pump this is very easy to arrange by restricting the width of the square wave, $W = x_2$, where x_2 is the time taken to reach $v = v_{x_2}$. But for sine wave pump it is much more complicated. In any case for an application of this type, the second negative-conductance area a_2 plays no significant role and need not, therefore, be considered.

4.4 Large Signal Operation of Tunnel Diodes

To study the voltage transient across a tunnel diode in the circuit of Fig. 4.3, the equivalent circuit of Fig. 4.4 is employed. In this circuit,

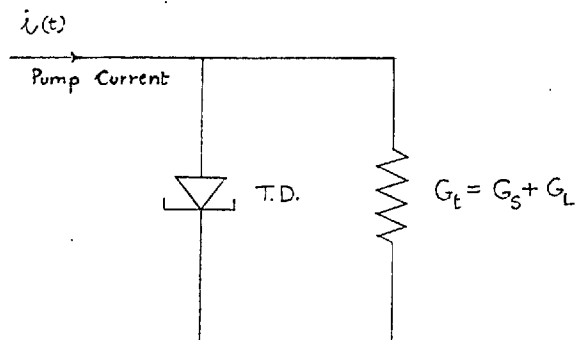


Fig. 4.3.

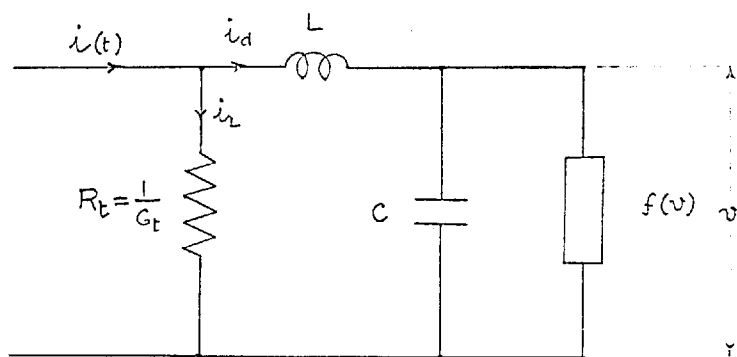


Fig. 4.4 Large Signal Equivalent Circuit

the tunnel diode is replaced by its static current voltage characteristic shunted by its junction capacitance C . L is the parasitic inductance in series with the junction and G_t is the external conductance seen by the diode. The series resistance R_s of the diode is very small for most germanium tunnel diode and it is neglected in the following analysis. The capacitance C is assumed constant with respect to diode voltage over the range of interest.

The differential equations for the circuit of Fig. 4.4 are

$$i_d = C \frac{dv}{dt} + f(v) \quad 4.1.$$

$$L \frac{di_d}{dt} = [i(t) - i_d] R_t - v \quad 4.2.$$

From 4.1. substituting for i_d in 4.2.

$$L \frac{di_d}{dt} = i(t) R_t - v - R_t C \frac{dv}{dt} + R_t f(v) \quad 4.3.$$

Again differentiating 4.1. and multiplying by L , we get

$$L \frac{di_d}{dt} = LC \frac{d^2v}{dt^2} + L G(v) \frac{dv}{dt} \quad 4.4.$$

$$\text{where } G(v) = \frac{d}{dv} f(v)$$

= the tunnel diode dynamic
conductance characteristic.

From the equations 4.3. and 4.4.

$$LC \frac{d^2v}{dt^2} + [R_t C + L G(v)] \frac{dv}{dt} + v + R_t f(v) = i(t) R_t \quad 4.5.$$

The solution of this equation 4.5. would give us the voltage time relationship for the tunnel diode in terms of the circuit parameters and the pump current. This is possible only if $f(v)$ is a simple function of voltage and $i(t)$ is a simple function of time.

$f(v)$ for a tunnel diode is a very complicated function and can be expressed to a reasonable degree of approximation only by a double exponential

of the form

$$Ave^{-Bv} + C [\exp(qv/kT) - 1]$$

(where A, B and C are constants of a given diode)

or by a polynomial. The polynomial approximation is good only if terms upto at least the fifth power are taken into consideration.

With these approximation to $f(v)$, the equation 4.5. is intractable by any simple means other than numerical or graphical. The complexity of mathematics demands that the static characteristic be approximated by piece-wise linearization of the characteristic. Then the voltage-time relationship can be obtained for every linearized region by solving equation 4.5. for the region in question. As we shall see later a mixture of piece-wise linear and other approximations are adequate to give us most of the design parameters.

4.5 Effect of the Series Inductance on the Conductance Cycle

In the analysis of Chapter 3, the series inductance L in the equivalent circuit of the tunnel diode was neglected. In this section we will study the effect of series inductance on the conductance cycle and determine the conditions which the circuit parameters must satisfy to minimize the effect of the inductance.

The equation 4.5. is of the form

$$A \frac{d^2 v}{dt^2} + B \frac{dv}{dt} + \phi(v) = D \quad 4.6.$$

where $A = LC$, $B = R_t C + L G(v)$,

$\phi(v) = v + R_t f(v)$ and $D = i(t)R_t$.

To simplify and study the equation 4.6. we can assume $i(t) = \text{constant}$, then if $z = \frac{dv}{dt}$

$$\begin{aligned} \frac{d^2 v}{dt^2} &= \frac{dz}{dt} = \frac{dz}{dv} \cdot \frac{dv}{dt} \\ &= Z \frac{dz}{dv} \end{aligned} \quad 4.7.$$

Substituting 4.7. into equation 4.6. we have

$$Az \frac{dz}{dv} + Bz + \phi(v) = D \quad 4.8.$$

For any particular value of $\frac{dz}{dv}$ this is a relationship between z and $\phi(v)$.

$$\text{Let } \frac{dz}{dv} = M \quad 4.9.$$

From equations 4.8. and 4.9.

$$z = \frac{D - \phi(v)}{AM + B}$$

or substituting for A, B, D and $\phi(v)$

$$z = \frac{i(t) R_t - v - R_t f(v)}{LCM + R_t C + L G(v)} \quad 4.10.$$

A family of isoclinals can be drawn for different values of M and then the integral curves can be obtained by graphical means as in Fig. 4.5.

From the equations 4.5. and 4.10. it is obvious that the effect of L is negligible if $\frac{R_t C}{|G(v)|} \gg L$

The tunnel diode conductance $G(v)$ is a maximum at $v = 0$ and as v increases, $G(v)$ reduces in magnitude and it never attains the same magnitude in the cycle except at the end of the cycle when it returns to the same magnitude as at $v = 0$. Therefore, if $\frac{R_t C}{G(v)} \gg L$ at $v = 0$, we can neglect L altogether.

If $|L G(v)|$ is of the same order of magnitude as the product $R_t C$ and $R_t > \frac{1}{G}$, the effect of L on $z = \frac{dv}{dt}$ is similar to that shown in Fig. 4.5. When $G(v)$ is positive, i.e. from $x = 0$ to $x = x_1$, the term $L G(v)$ adds to the term $R_t C$ and $\frac{dv}{dt}$ is reduced; the voltage transient is slowed down in this region by the presence of the inductance.

As the circuit goes into the negative conductance region ($x > x_1$), $R_t C$ is reduced by the amount $|L G(v)|$, thus speeding up the transient in the negative conductance region. The effect of the presence of series inductance

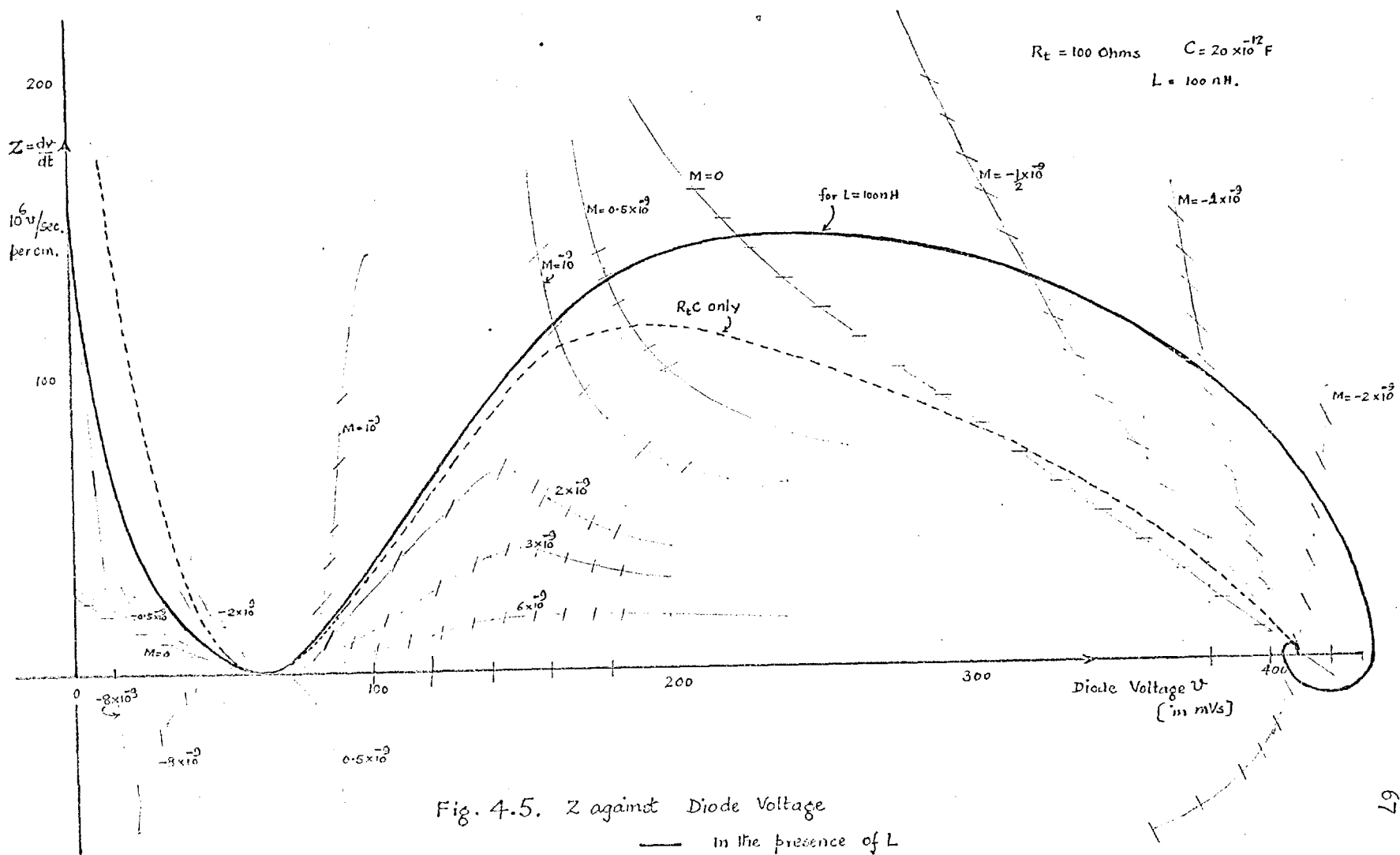


Fig. 4.5. Z against Diode Voltage

— in the presence of L
 ---- No L present.

is to reduce the time taken to traverse the negative-conductance region, thus reducing the negative-conductance area, a , and increasing the conductance slopes $G'(x_1)$ and $G'(x_2)$.

Further, the negative conductance seen by the signal reduces in magnitude as L is increased. (Appendix A.1.).

Both these effects tend to reduce the gain of the amplifier. This result is an important one to consider while designing practical amplifiers. It is necessary to reduce the spurious series inductance to a minimum so that the gain and the frequency response predicted in the subsequent analysis can be obtained. In the analysis that follows it is assumed^x that $|L G(v)| \ll R_t C$ i.e. the inductance L is neglected.

4.6 Normalization of the Analysis with Respect to the Tunnel Diode Parameters

If the condition derived in the last section, i.e. $R_t C \gg L G(v)$ is satisfied, the analysis is considerably simplified. The circuit of Fig. 4.4. reduces to that of Fig. 4.6.

Equating the currents

$$C \dot{v}(t) = i(t) - f(v) - G_t v \quad 4.11.$$

Normalizing with respect to the diode capacitance C

$$\dot{v}(x) = i(t) - f(v) - G_t v \quad 4.12.$$

A study of this equation reveals that it is possible to normalize it with respect to the diode peak current I_p , provided we can assume that all tunnel diodes have the same shape of static characteristics, $f(v)$, whatever their peak current. This assumption is not strictly true in practice. Nevertheless, we can obtain useful approximate results from the analysis on the basis of it. If equation 4.12. is solved, we obtain voltage against time x graph for a diode with a peak current I_p , a conductance G_t and a pump current $i(t)$. This voltage against time graph would be the same for another circuit which has a diode with its peak current

$$I_{p_n} = m I_p, \quad 4.13.$$

^x This is possible to achieve in practice. See Section 4.15.

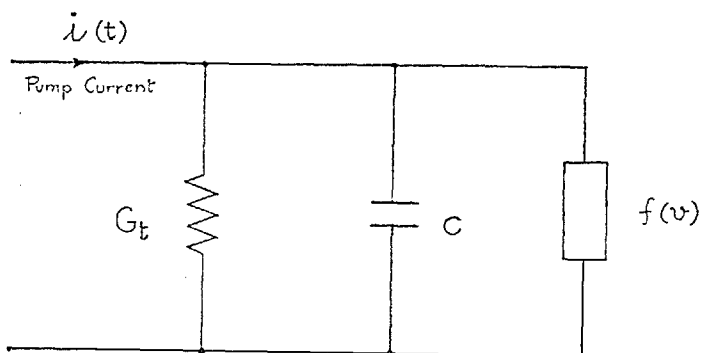


Fig. 4.6 Simplified Equivalent Circuit
for the large signal Analysis.

$$\text{A conductance } G_{t_n} = m G_t \quad 4.14.$$

$$\text{and a pump current } i_n(t) = m i(t) \quad 4.15.$$

if the time scale is multiplied by $\frac{1}{m}$

$$\text{i.e. the new time } x_n = \frac{x}{m}$$

Thus calculations and optimization carried out on a tunnel diode with a given I_p can easily be transferred to a diode with a different I_p if the conditions of load conductance, frequency and other design requirements of a practical amplifier are more appropriate to the conditions offered by the second diode.

4.7 Conductance Functions Due to Square Wave Pump

We shall now examine the conductance function due to square wave pump. The analysis for square wave pump is, perhaps, the simplest by numerical means. The equation 4.12. for square wave pump becomes

$$\dot{v}(x) = I_b - f(v) - G_t v \quad 4.16,$$

where I_b is the amplitude of the pump current.

This equation can be solved to a sufficient degree of accuracy and in a useful form by a step by step integration for different values of I_b . This process is very simple but tedious. A method of calculation is described in Appendix A.2. A digital computer programme to do the same is given in Appendix A.3.

The graphs of voltage against time x of Fig. 4.7. are drawn for a circuit with the following specification:

The tunnel diode static characteristic, assumed for these calculations and the calculations in the following sections of this Chapter, was that of Fig. 4.8.

$$\begin{aligned} \text{Tunnel diode } I_p &= 4.7 \text{ mA} \\ V_p &= 60 \text{ mV} \\ G_t &= 0.01 \text{ mhos.} \end{aligned}$$

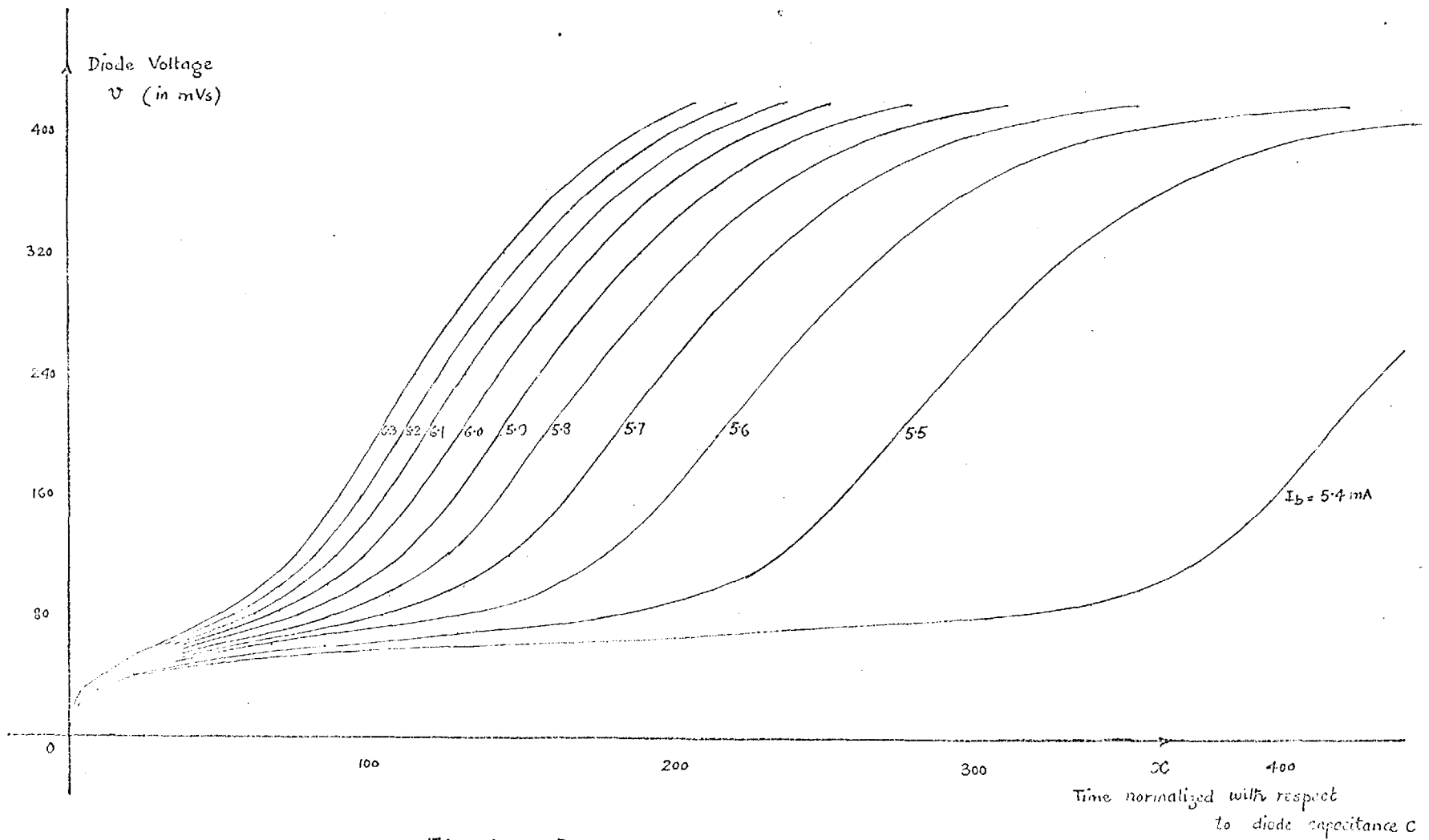


Fig. 4.7. Diode Voltage Against Time for different values of Pump Current I_b .

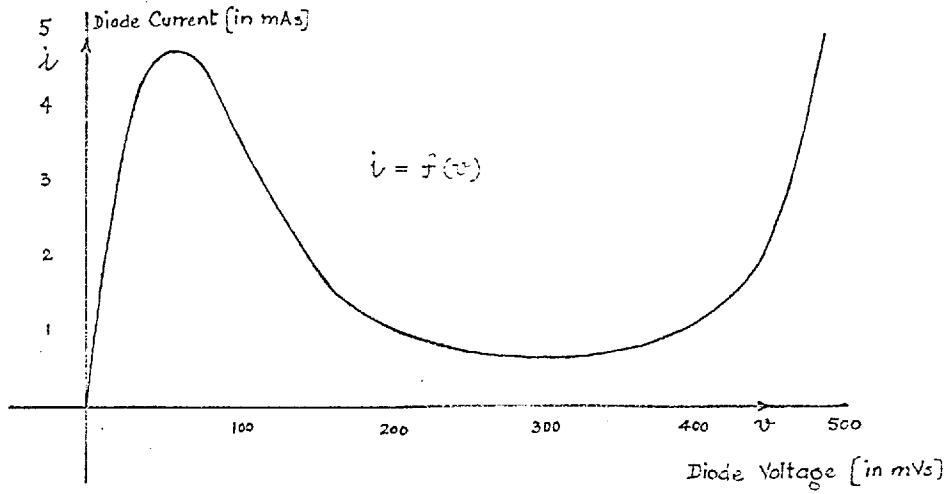


Fig. 4.8. Tunnel diode Static Characteristic.

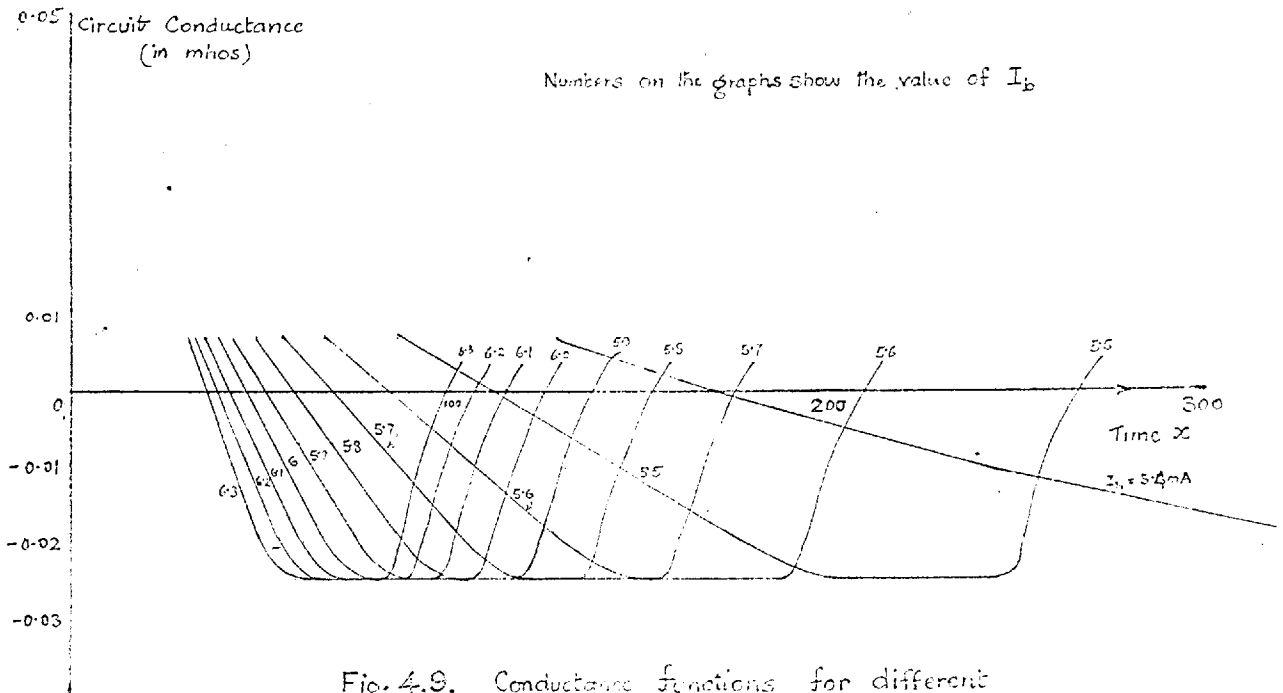


Fig. 4.9. Conductance functions for different values of pump current.

Fig. 4.9 gives the corresponding conductance functions for different values of I_b . Only the sections of conductance curves of direct interest are shown.

4.8 Approximate Analysis

At first sight it seems plausible that a piece-wise linearization of the diode static characteristic would lead to a considerable simplification of the analysis. The expressions obtained as solutions for the differential equations of the different linearized regions are cumbersome and so far as the understanding of this mode of application is concerned, are no more lucid and informative than the computer calculations.

As shown in Sec. 3.11, it is not necessary for us to know the complete conductance function to determine the properties of the regenerative amplifier; the parameters of interest are the time x_1 , the conductance slopes $G'(x_1)$ and $G'(x_2)$ and the negative conductance area a .

$G'(x_1)$ is highly dependent on the conditions that exist at the point $x = x_1$ and piece-wise linear approximation results in grossly inaccurate values of $G'(x_1)$. Similarly, $G'(x_2)$ will be far from accurate.

The following method gives the design parameters directly. The intersections of the $G(v)$ characteristic of the tunnel diode and the external conductance G_t (Fig. 4.10.) are at the voltages v_{x_1} and v_{x_2} where the circuit conductances $G(x_1) = G(x_2) = 0$.

From the equation 4.16.

$$\dot{v}]_{x_1} = I_b - f(v_{x_1}) - G_t v_{x_1} \quad 4.17.$$

$$\begin{aligned} \text{and } G'(x_1) &= \frac{d}{dx} G(v) \quad \text{at } v = v_{x_1} \\ &= G'(v_{x_1}) \dot{v}]_{x_1} \end{aligned} \quad 4.18.$$

where $G'(v_{x_1})$ is the slope of conductance-voltage curve at $v = v_{x_1}$.

From the equation 4.17. and 4.18. and the diode characteristics, $G'(x_1)$ can be determined readily.

$v_{x1} = 64mV$	$f(v_{x1}) = 4.67mA$	$G'(v_{x1}) = 0.00145$
$v_y = 90mV$	$f(v_y) = 4.0mA$	$G'(v_{x2}) = 0.00055$
$v_z = 150mV$	$f(v_z) = 1.85mA$	
$v_{x2} = 190mV$	$f(v_{x2}) = 1.12mA$	

$G_t = 0.01mhos$ $G_o = 0.185mhos$ $G_l = 0.035mhos$

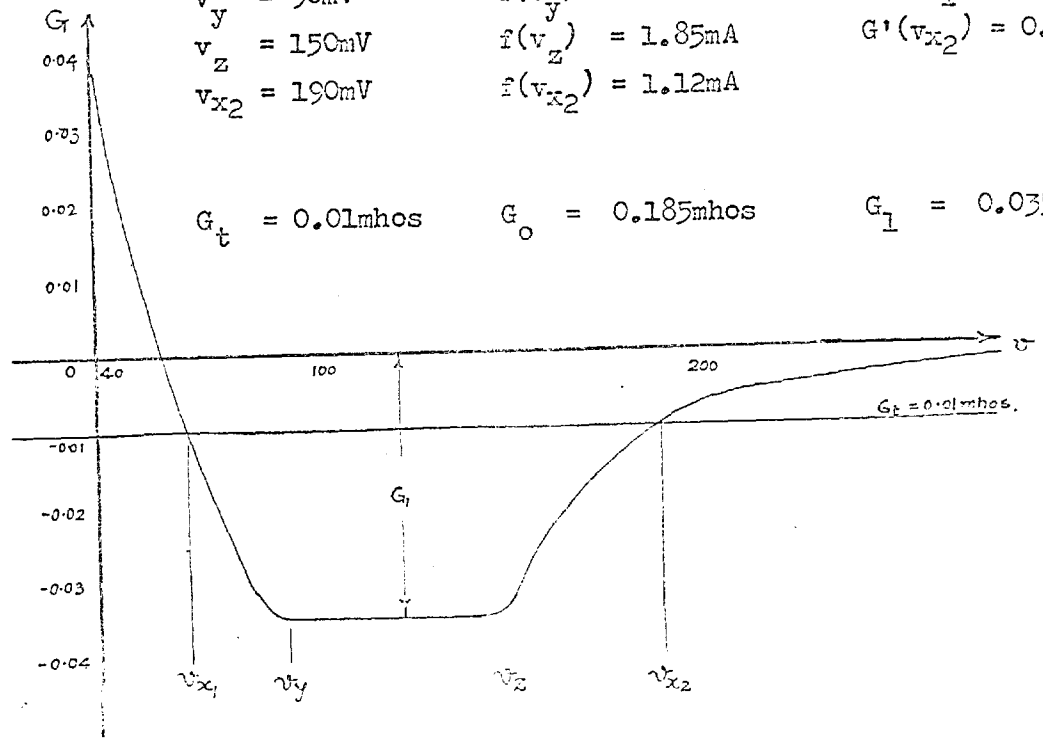


Fig. 4-10

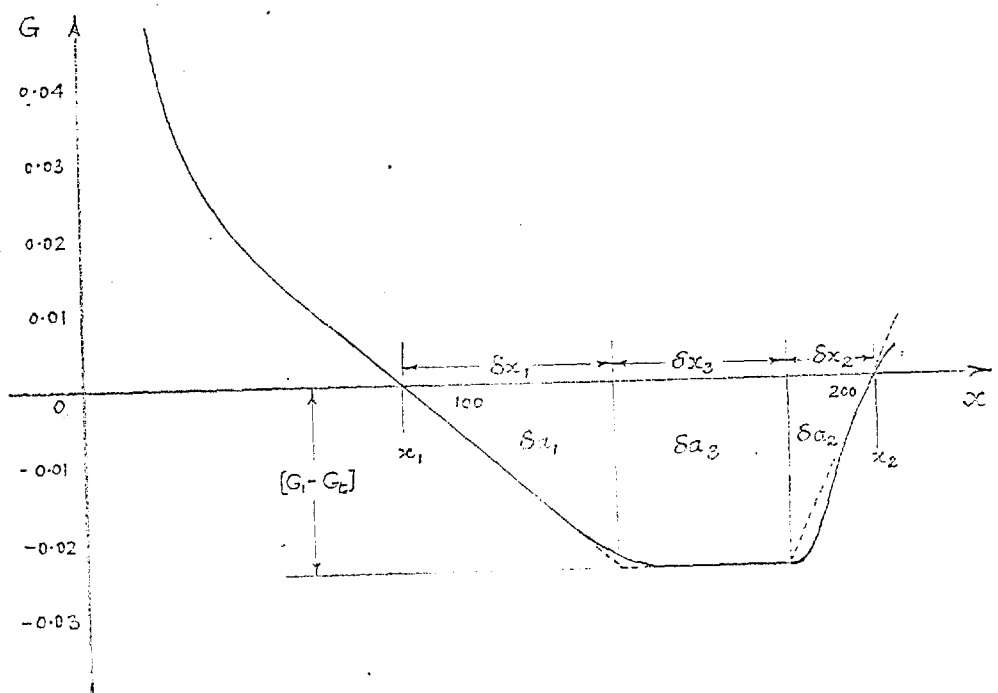


Fig. 4-11.

Similarly

$$\bar{v}]_{x_2} = I_b - f(v_{x_2}) - G_t v_{x_2} \quad 4.19.$$

$$\text{and } G'(x_2) = G'(v_{x_2}) \bar{v}]_{x_2} \quad 4.20.$$

In this way both the conductance slopes can be calculated accurately.

The negative conductance area a can be determined by simple approximations based on a study of the conductance curves of Fig. 4.9. The area a can be divided into three parts as shown in Fig. 4.11. The conductance slope $G'(x)$ is very nearly equal to $G'(x_1)$ from the point $x = x_1$ to $x = x_1 + \delta x_1$. At the point x_1 the circuit conductance $G = 0$ and \wedge the point $x = x_1 + \delta x_1$ the circuit conductance is $G_t - G_1$ where $(-G_1)$ is the maximum negative conductance of the diode.

$$\text{Then the time } \delta x_1 = \frac{|G_t - G_1|}{G'(x_1)}$$

and the triangular area

$$\begin{aligned} \delta a_1 &= \frac{\delta x_1}{2} \cdot |G_t - G_1| \\ &= \frac{|G_t - G_1|^2}{2 G'(x_1)} \end{aligned} \quad 4.21.$$

The rectangular area δa_3 (Fig. 4.11.) is

$$\delta a_3 = \delta x_3 |G_t - G_1|$$

δx_3 is the time required to traverse the voltage range v_y to v_z over this range circuit conductance is constant at $G_t - G_1$

From equation 4.11,

$$\begin{aligned} \delta x_3 &= \int_{v_y}^{v_z} \frac{dv}{I_b - [f(v) - (|G_t - G_1|)v]} \\ &= \frac{1}{|G_t - G_1|} \ln \frac{I_b - f(v_z) - G_t v_z}{I_b - f(v_y) - G_t v_y} \end{aligned} \quad 4.22.$$

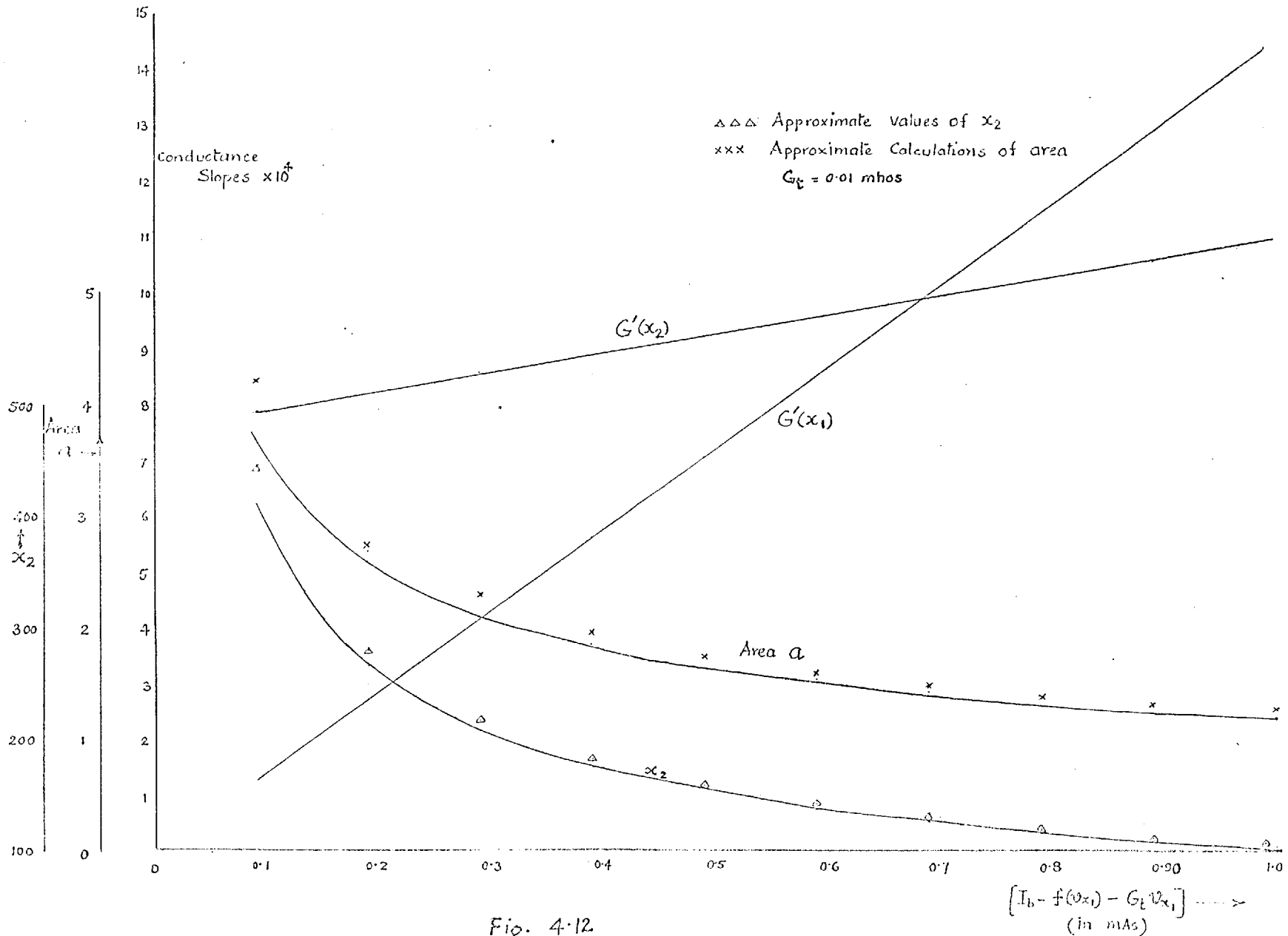


Fig. 4.12

$$\therefore \delta a_3 = \ln \frac{I_b - f(v_z) - G_t v_z}{I_b - f(v_y) - G_t v_y} \quad 4.23.$$

The area δa_2 is comparatively small and can be determined to a reasonable accuracy by a similar assumption to that for the area δa_1 ; the conductance slope is assumed constant at $G'(x_2)$ from v_z to v_{x_2} (Figs. 4.10 and 4.11).

Therefore

$$\begin{aligned} \delta a_2 &= \frac{|G_t - G_1|}{G'(x_2)} \\ \text{and } \delta a_2 &= \delta x_2 \cdot \frac{G_t - G_1}{2 G'(x_2)} \\ &= \frac{|G_t - G_1|^2}{2 G'(x_2)} \quad 4.24. \end{aligned}$$

From the equations 4.21, 4.23 and 4.24

$$\text{the total area } a = \frac{|G_t - G_1|^2}{2} \left[\frac{1}{G'(x_1)} + \frac{1}{G'(x_2)} \right] + \ln \frac{I_b - f(v_z) - G_t v_z}{I_b - f(v_y) - G_t v_y} \quad 4.25.$$

The time x_1 can be accurately obtained by integrating the equation 4.16. This integration can be carried out by the step by step method of Appendix A.2.

The time x_2 is then given by

$$x_2 = x_1 + \delta x_1 + \delta x_2 + \delta x_3 \quad 4.25A.$$

The values of the conductance slopes $G'(x_1)$, $G'(x_2)$, the area a and the time x_2 are given in Fig. 4.12. for different values of the expression $I_b - f(v_{x_1}) - G_t v_{x_1}$. The area a and the time x_2 , as determined by the approximate method of this section, are a little higher than those computed from accurate calculations of Section 4.7, but the error involved is less than 10 per cent.

4.9 Dependence of Gain on the Pump Current

Equation 4.16. equates the current flowing into the diode capacitance,

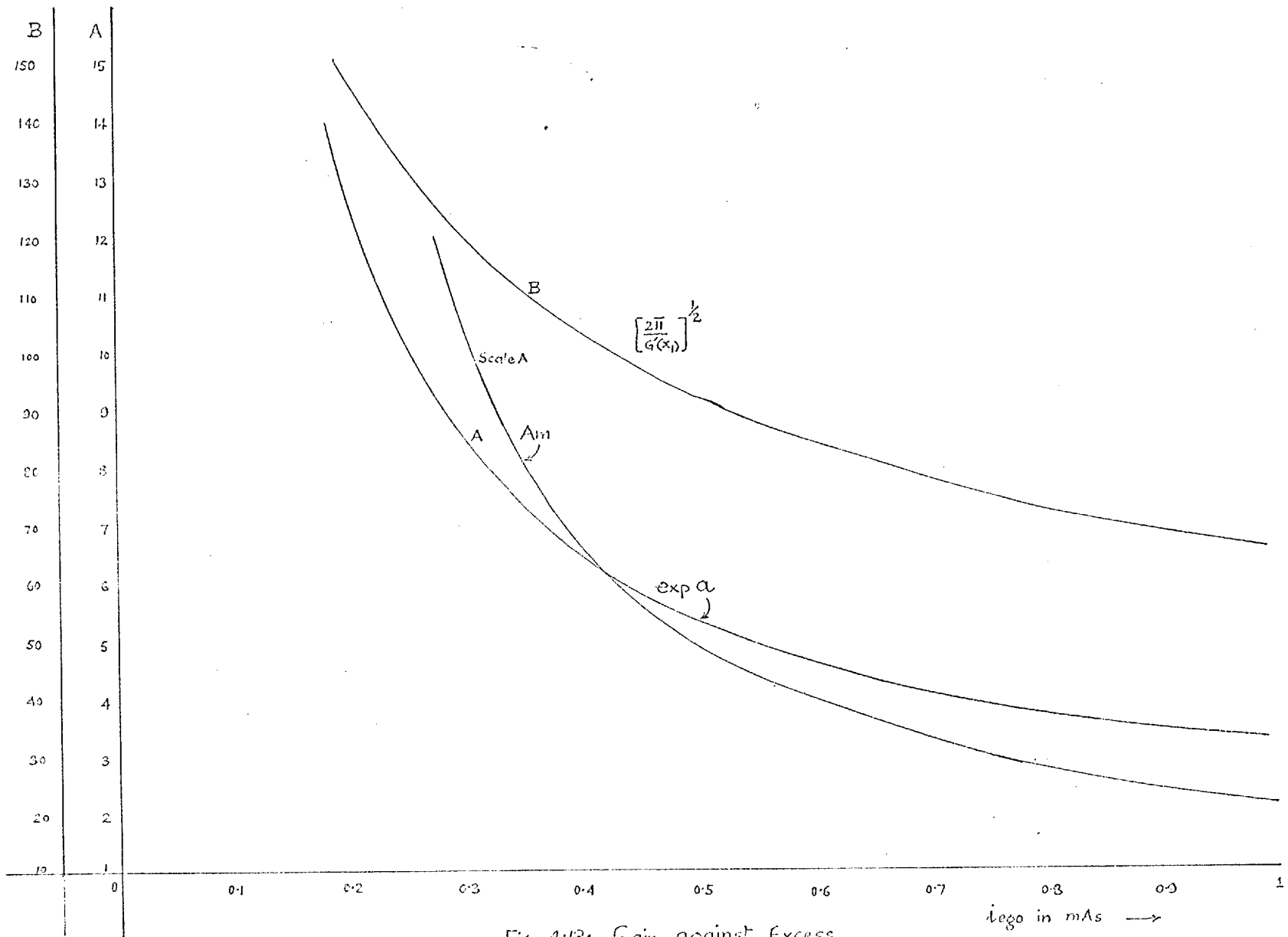


Fig. 4.13. Gain against Excess Pump Current

to the excess of pump current over the part of the pump current that flows into the conductance part of the circuit. We shall call it the excess pump current and denote it by i_e . If i_e is very small, the voltage transient across the diode builds up very slowly and its excursion into the negative conductance region takes a very long time thus increasing area a and hence the gain. On the other hand if i_e is very large the transient builds up very quickly and the area a is reduced.

The excess pump current available at the time $x = x_1$ determines to a considerable degree the performance of the amplifier. The equation 4.18. gives the conductance slope, $G'(x_1)$, at the beginning of the regenerative cycle. This can be rewritten as

$$G'(x_1) = i_{ego} \cdot G'(vx_1) \quad 4.26.$$

where i_{ego} is the excess pump current at the time $x = x_1$.

For values of $i_{ego} < 0$, no regenerative build up takes place.

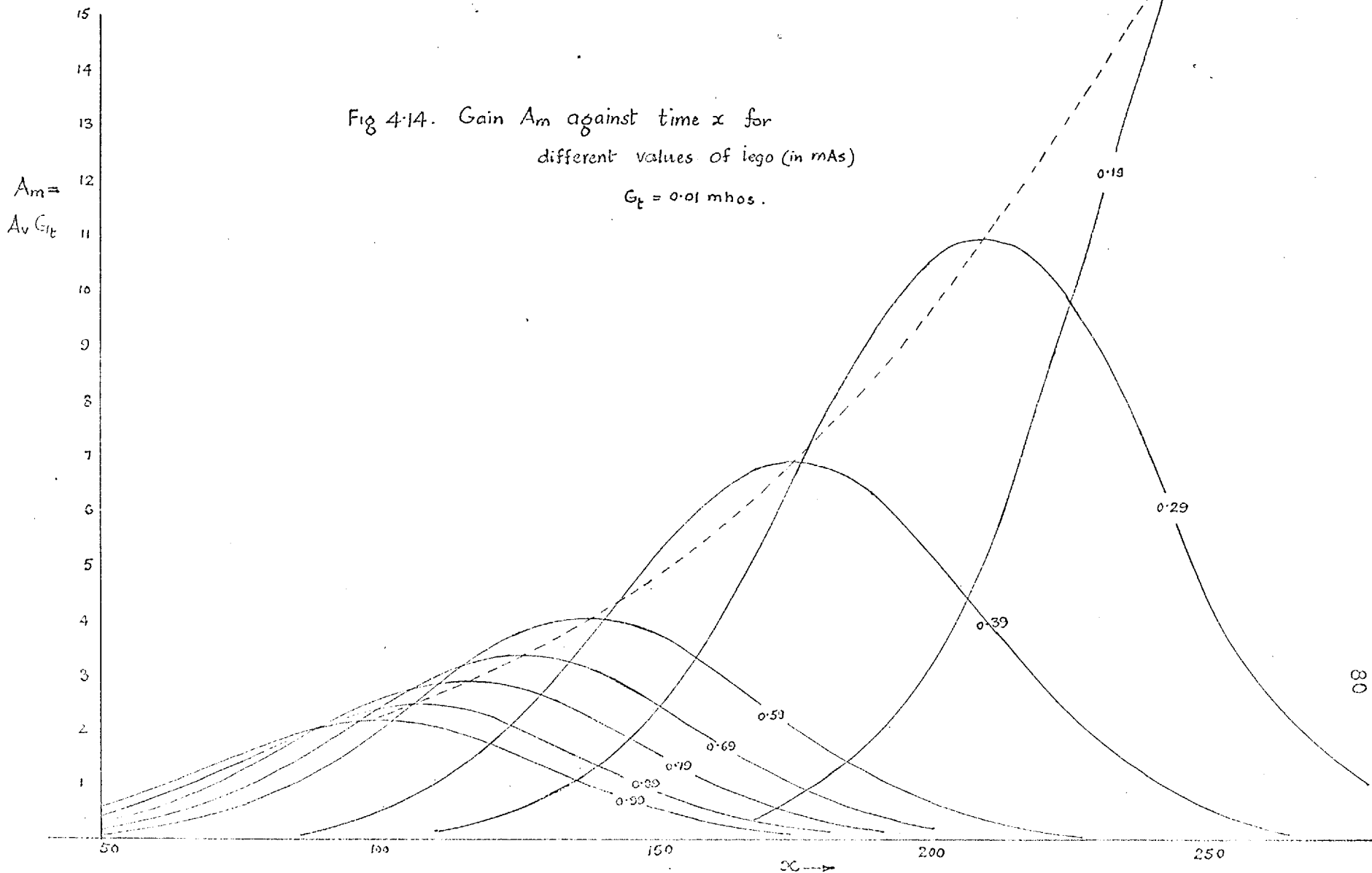
For $i_{ego} > 0$ but very small, $G'(x_1)$ is small and the area a large. The gain of the amplifier under such conditions is very high (Fig. 4.13.) and a small change in i_{ego} causes a large change in gain. i_{ego} is dependent upon the magnitude of the pump current I_b , the tunnel diode static characteristics $f(v)$ and the conductance G_t . Any spurious variations in these circuit parameters have a direct effect on the excess pump current i_{ego} . When i_{ego} is very small a small change in circuit parameters produces a large change in i_{ego} . Thus gain of an amplifier, with a small value of i_{ego} , is highly sensitive to any spurious variations in the circuit parameters and the pump amplitude.

The larger the i_{ego} , the lower the gain and the amplifier performance is less sensitive to the spurious variations in the circuit conditions. A compromise is therefore necessary between the magnitude of the amplifier gain and its stability with respect to the circuit tolerances.

The curves of Fig. 4.14. show the shape of the output pulse for different values of the excess pump current i_{ego} . The peaks of the signal output, for each value of i_{ego} , occur at the time x_2 corresponding to it. If the pulse width of the pump is larger than the corresponding x_2 , the modulation

Fig 4-14. Gain A_m against time x for
different values of i_{e0} (in mAs)

$G_t = 0.01$ mhos.



of the voltage transient due to the pump by the signal is reduced according to the curves of Fig. 4.14. If the pump pulse width is restricted to less than x_2 , the gain A_m is again less than that at $x = x_2$. To achieve the maximum value of A_m , the width of the square wave pump pulse should therefore be restricted to the period x_2 .

The maximisation of transducer gain, on the other hand, is very complicated. Equation 3.36 for transducer gain shows that it is dependent upon $A_v G'(x_2)$ and the period X . A_v is dependent upon the negative conductance area and is therefore determined by i_{ego} and the pump pulse width W . Once again $G'(x_2)$ is dependent upon i_{ego} and W . The period X of the square wave is equal to $W + d_p$. The damping period d_p is calculated from the equation 3.38 and is therefore dependent upon $G'(x_2)$ and A_v . All these factors are interdependent in determining transducer gain but the excess pump current i_{ego} is an important parameter in the determination of transducer gain.

The graph of Fig. 4.15. shows transducer gains for different values of i_{ego} . For this graph we have assumed that $G_s = G_L = \frac{G_t}{2}$ and $X = 2x_2$. We note from this graph that under the conditions assumed the transducer gain increases rapidly when i_{ego} is reduced to small values. If the transducer gain of the amplifier is not to be unduly sensitive to the circuit tolerances and spurious variations in the various circuit elements then transducer gains of not much higher than 10 db. can be achieved.

4.10 Damping Period

The frequency response and the power gain of the amplifier are both dependent on the period X for a complete cycle of the pump. If the width of the square wave pump pulse is W , the period X must at least be

$$X = W + d_p \quad 4.27.$$

where d_p is the damping period.

In Section 3.10, we have derived the condition 3.38 which must be satisfied for adequate damping. The Fig. 4.16 shows the damping period calculated from the condition 3.38, for different values of i_{ego} . The corresponding values of x_2 are also shown in Fig. 4.16.

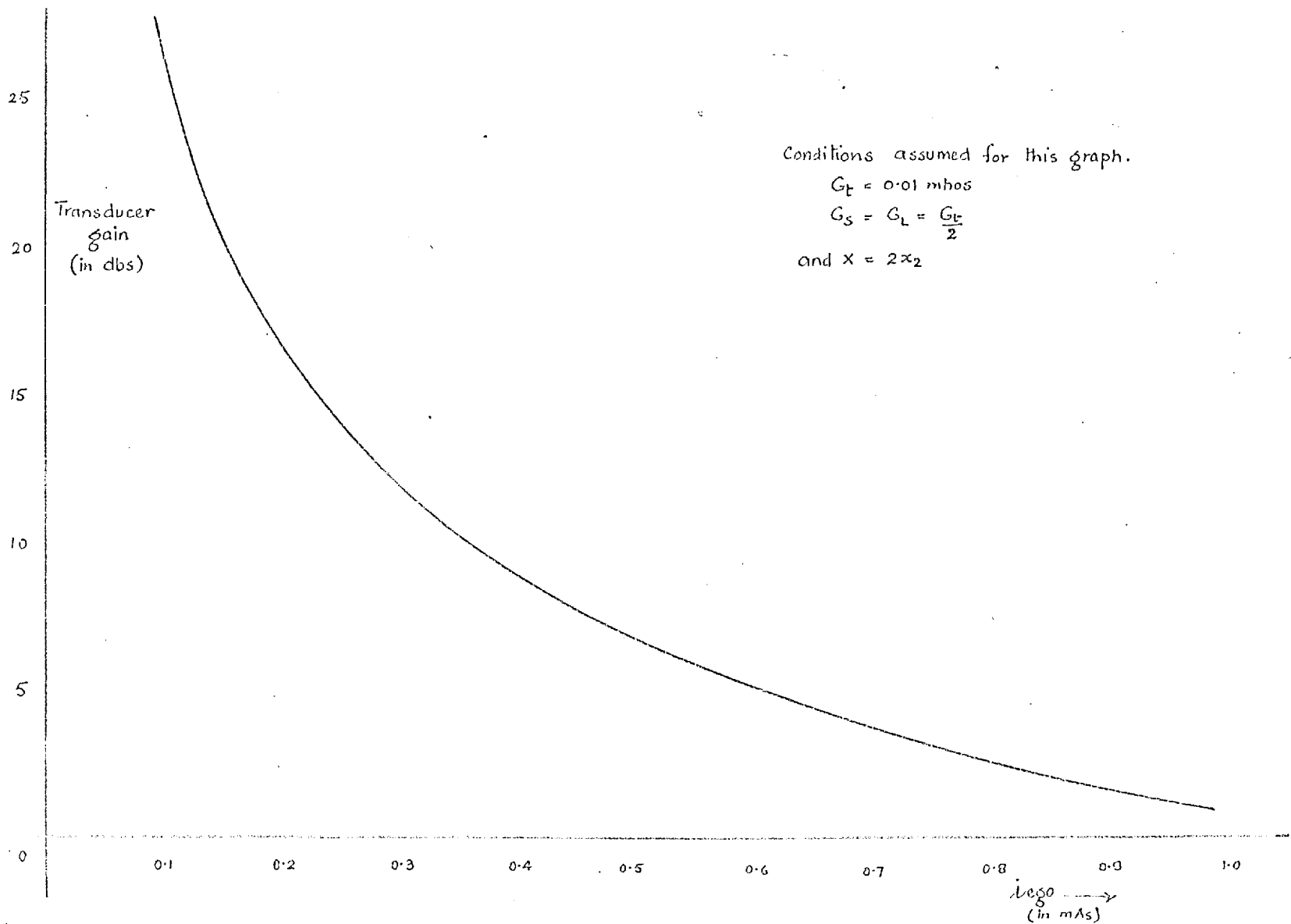


Fig 4.15 Transducer gain for different values of excess pump current i_{eo}

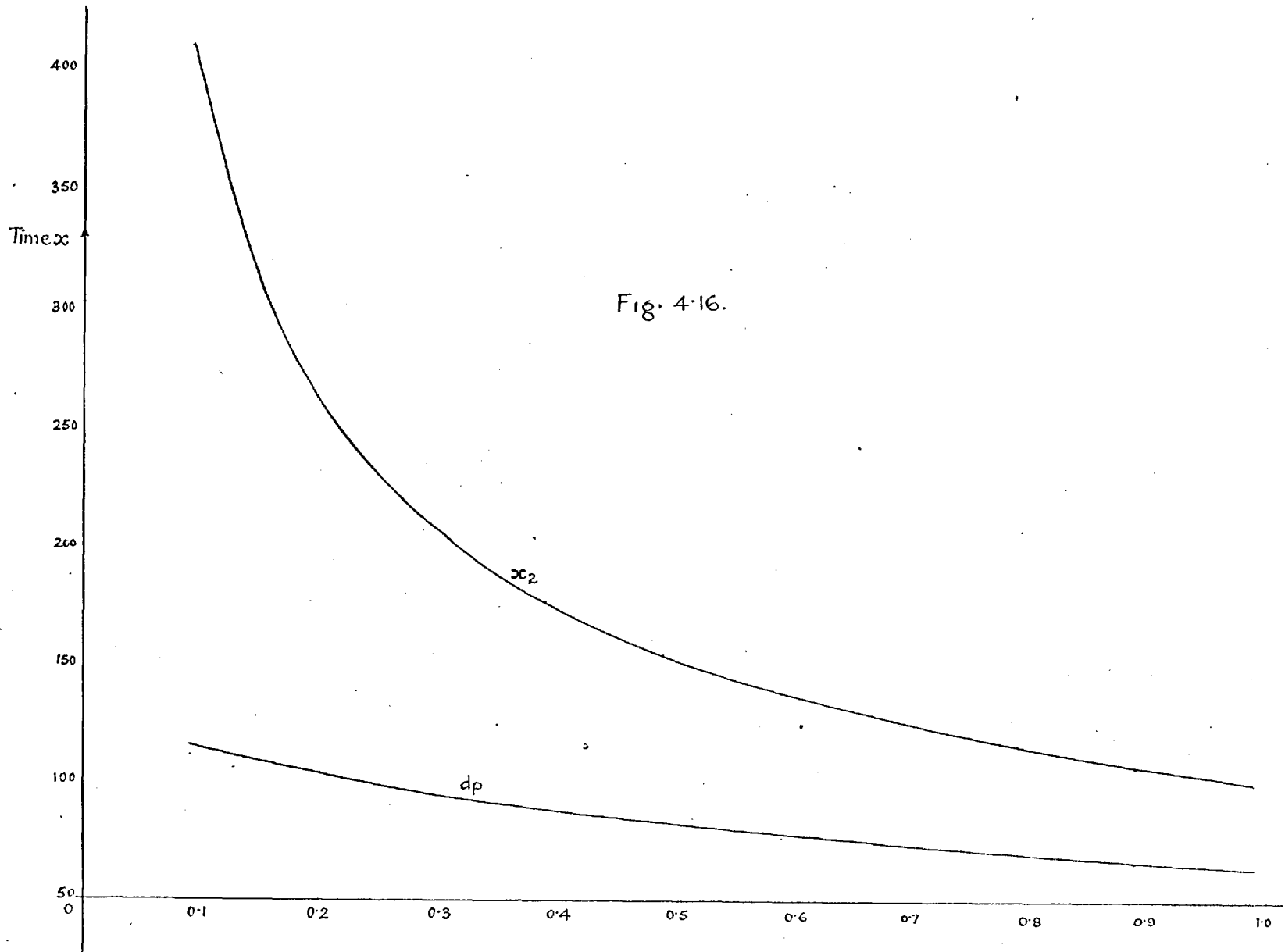


Fig. 4.16.

Excess pump Current i_{epo} . (in mA)

In a practical amplifier, the period X may be dictated by the difficulty of obtaining the required waveshape. In practice, $X = 2x_2$ more than satisfies the requirements of adequate damping period.

4.11 Frequency Response

As discussed in section 3.8, the frequency response of the regenerative amplifier is determined by two factors; the term $\exp -\mu^2/2G'(x_1)$ is one factor. This term is shown as a function of μ for different values of i_{ego} in Fig. 4.17. The frequency response of the amplifier is dependent also upon the sampling rate and hence on the period X .

If $\frac{\mu_p}{2\pi}$ is the pump frequency normalized to the diode capacitance

$$\frac{\mu_p}{2\pi} = \frac{1}{X}$$

$$= \frac{1}{2x_2}$$

if we assume $X = 2x_2$

$$\text{therefore } \mu_p = \frac{\pi}{x_2}$$

The frequency band of amplification will therefore be not greater than $\frac{\mu_p}{4\pi} = \frac{1}{2X}$. The gain of this frequency band will not fall by more than 10 per cent below the gain at the low frequency end if the condition 3.29 is satisfied. The table 4.1 shows the various factors calculated for different values of i_{ego} and we note that the condition 3.29 is more than satisfied.

4.12 Dependence of Gain on G_t

This study can best be performed by keeping some circuit conditions constant and then studying the influences of G_t on the gain. It is possible by changing G_t to modify $G'(x_1)$, a and $G'(x_2)$. For a practical design the permissible value of the conductance slope $G'(x_1)$ is specified by the circuit tolerances. Once $G'(x_1)$ is specified, the frequency response of

Table 4.1.

i_{ego}	$G'(x_1)$	$0.84 G'(x_1)$	x_2	$\mu_p^2 = \frac{\pi^2}{x_2^2}$
	$\times 10^{-4}$	$\times 10^{-4}$		$\times 10^{-4}$
0.09	1.31	0.95	411	0.587
0.19	2.76	2.32	268	1.37
0.29	4.2	3.63	210	2.24
0.39	5.65	4.75	176	3.19
0.49	7.1	5.96	154	4.17
0.59	8.55	7.18	138	5.15
0.69	10.0	8.4	126	6.15
0.79	11.47	9.6	116	7.3
0.89	12.9	10.8	107	8.65
0.99	14.39	12.1	100	9.86

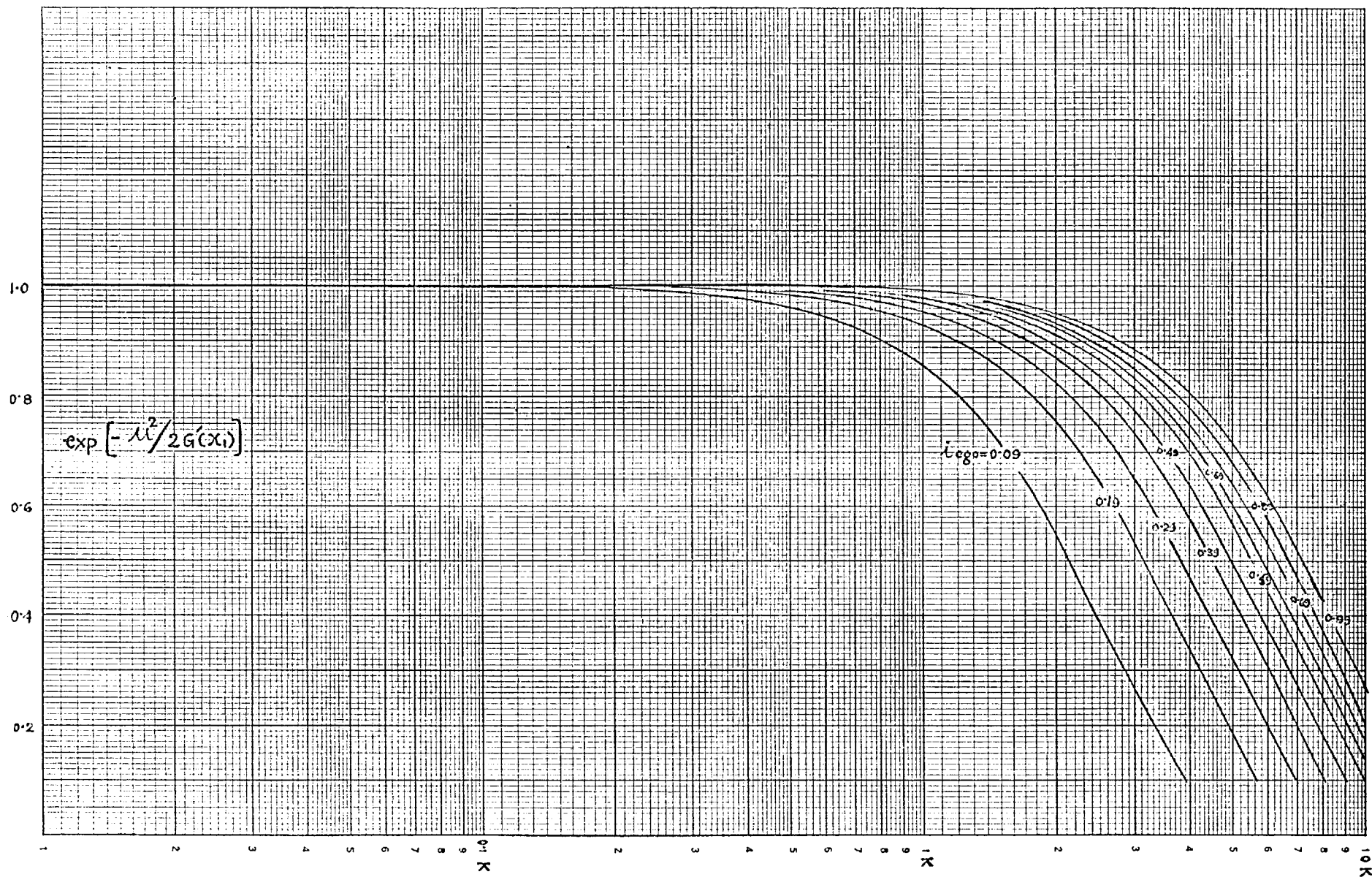


Fig. 4.17.

$\frac{\mu}{2\pi}$ →

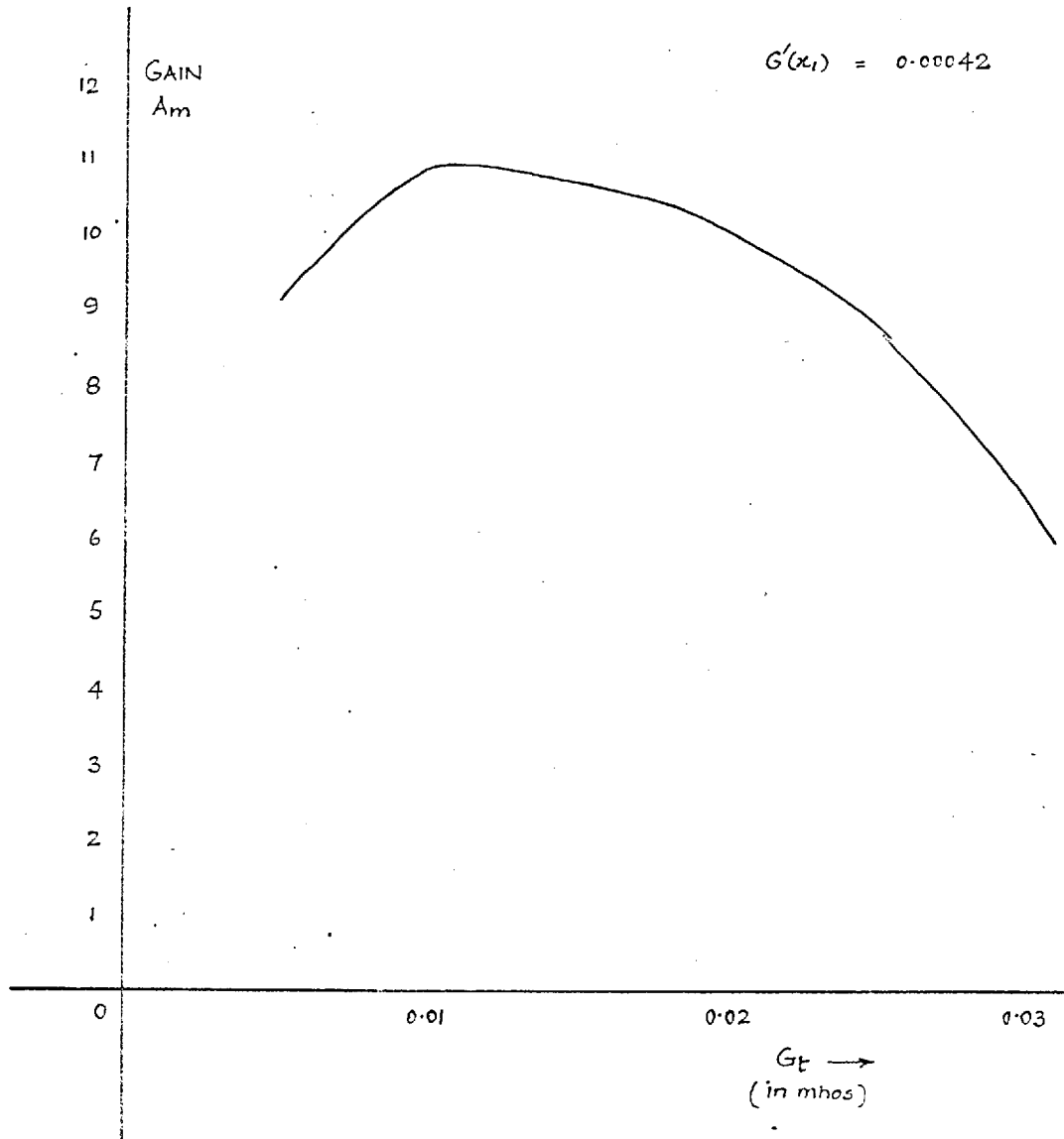


Fig. 4-18. Dependence of the gain A_m on G_t .

the amplifier is largely defined too. With $G'(x_1)$ fixed, we can proceed with the study of the effect of G_t on the gain of the amplifier.

There are two opposing effects of the total external conductance, G_t , seen by the tunnel diode in the circuit of the regenerative amplifier. The smaller the conductance G_t the faster is the tunnel diode transition through the negative conductance region but the total effective negative-conductance ($G_t - G_1$) is increased in magnitude. While the former effect tends to reduce the area a , the latter tends to increase it.

Fig. 4.18 is a plot of the gain A_m against different values of conductance G_t . For the values of G_t in the range of 0.0067 to 0.02 mhos the gain A_m is within 10% of the peak. For values of conductance higher than 0.02 mhos the gain falls off rather rapidly because ($G_t - G_1$) is reduced much more rapidly and the transit time through the negative-conductance region is not increased appreciably.

4.13 Dependence of Gain on the Diode Characteristics

The conductance slope $G'(x_1)$ and the negative-conductance area a are both dependent upon the diode characteristics. The amplifier gain can be increased by reducing the conductance slope $G'(x_1)$ and or by increasing the area a .

A reduction in $G'(x_1)$ can be accomplished by reducing $G'(v)$ at $v = vx_1$ or by reducing i_{ego} . A reduction in i_{ego} as discussed in section 4.9 is not suitable because the amplifier becomes more sensitive to the spurious variations in the circuit conditions. A reduction in $G'(vx_1)$ is possibly only by making the diode static characteristic, $i = f(v)$, broader at the peak.

This method of increasing gain by reducing the conductance slope $G'(x_1)$, works at the expense of the frequency response - (section 4.11 . (Fig.4.17)). Further, the gain factor $[2\pi/G'(x_1)]^{\frac{1}{2}}$ increases slowly compared with the gain factor $\exp a$.

The area a can be increased by increasing the effective negative-conductance. Fig. 4.19 shows the gain A_m against $|-G_1|$.

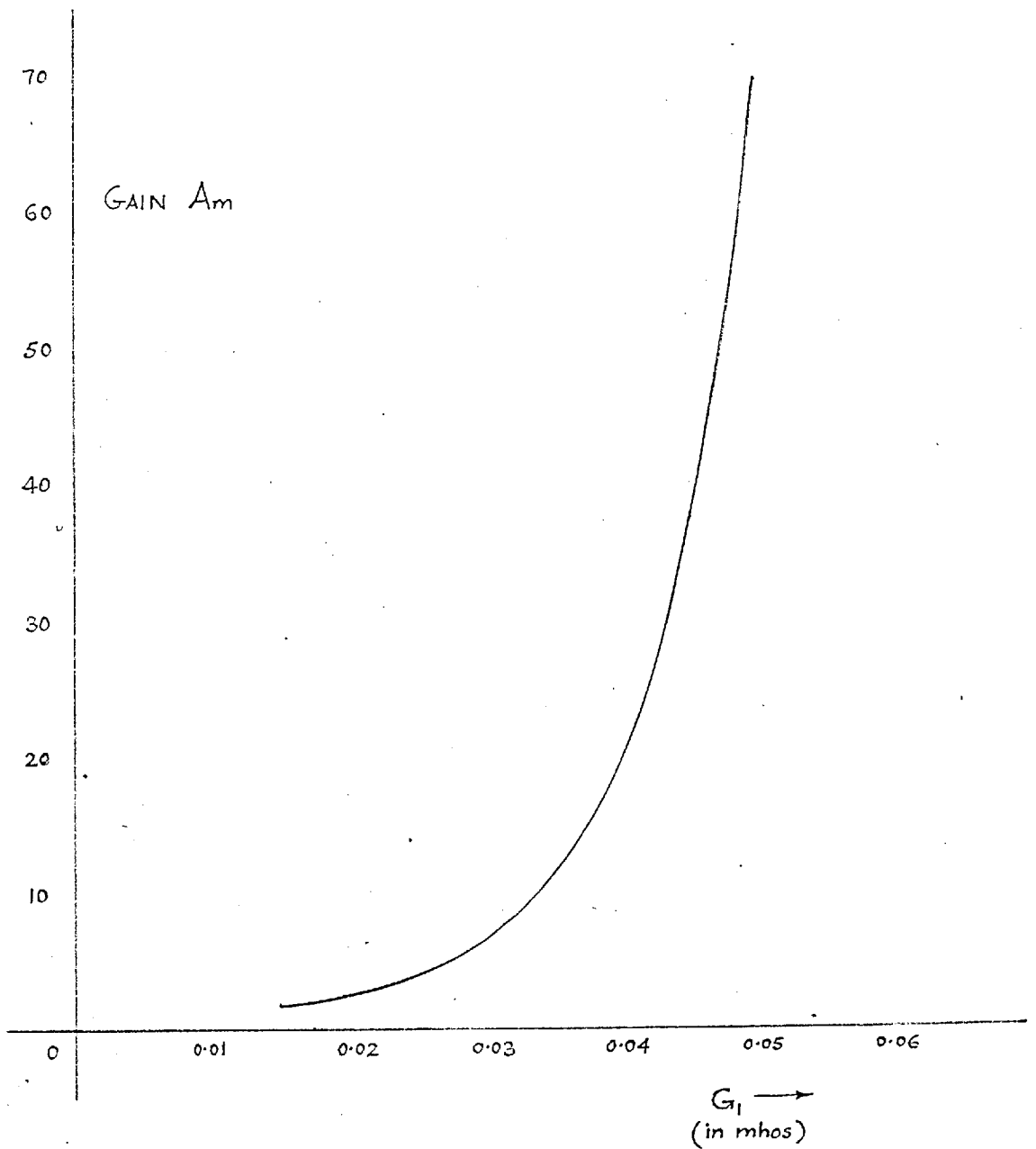


Fig. 4.19. Dependence of the gain A_m
on $-G_1$

$G'(x_1)$ was kept constant
at 0.00042
and $G_E = 0.01$ mhos.

Thus tunnel diodes with higher ratios I_p/I_v will give higher gains. The lower the $I_p/|-G_1|$ of a tunnel diode for the regenerative amplifier the higher the gain figure.

4.14 Alternative Method of Analysis

The method of analysis developed in Chapter 3, and employed in the study of the properties of the regenerative amplifier in the preceding sections of this chapter, gives us an understanding of the processes involved but a number of calculations are necessary before we arrive at the results. At the outset of this work, a much simpler method, of arriving at the gain A_m and the shape of the signal output pulse, was used.

From the solutions of equation 4.16 for various values of pump current I_p , the corresponding voltage against time graphs of Fig. 4.7 were drawn. From Fig. 4.7, we can obtain the graphs of $v G_t$ against i_{ego} for constant values of time x (Fig. 4.20).

$$\text{If } v G_t = i_o$$

$$\text{Gain } A_m = \frac{di_o}{di_{ego}}$$

This can be calculated for different values of x and i_{ego} . Fig. 4.21 shows the gain against time x graphs for different values of i_{ego} . These graphs, as is expected, are similar to those of Fig. 4.14. Thus we obtain some of the results by fairly simple means. But this method is entirely graphical and the accuracy of the predictions deteriorates as the number of graphical steps required to get the final results increases. This approach is again very limited because it is too mechanical to be of assistance in the study and the understanding of the processes involved. Nevertheless a comparison of the graphs of Fig. 4.21 with those of Fig. 4.14 shows that the results, obtained by the graphical and the analytical means, are in good accord.

4.15 Experimental Investigations

The circuit of Fig. 4.22 was employed to verify the theory of the

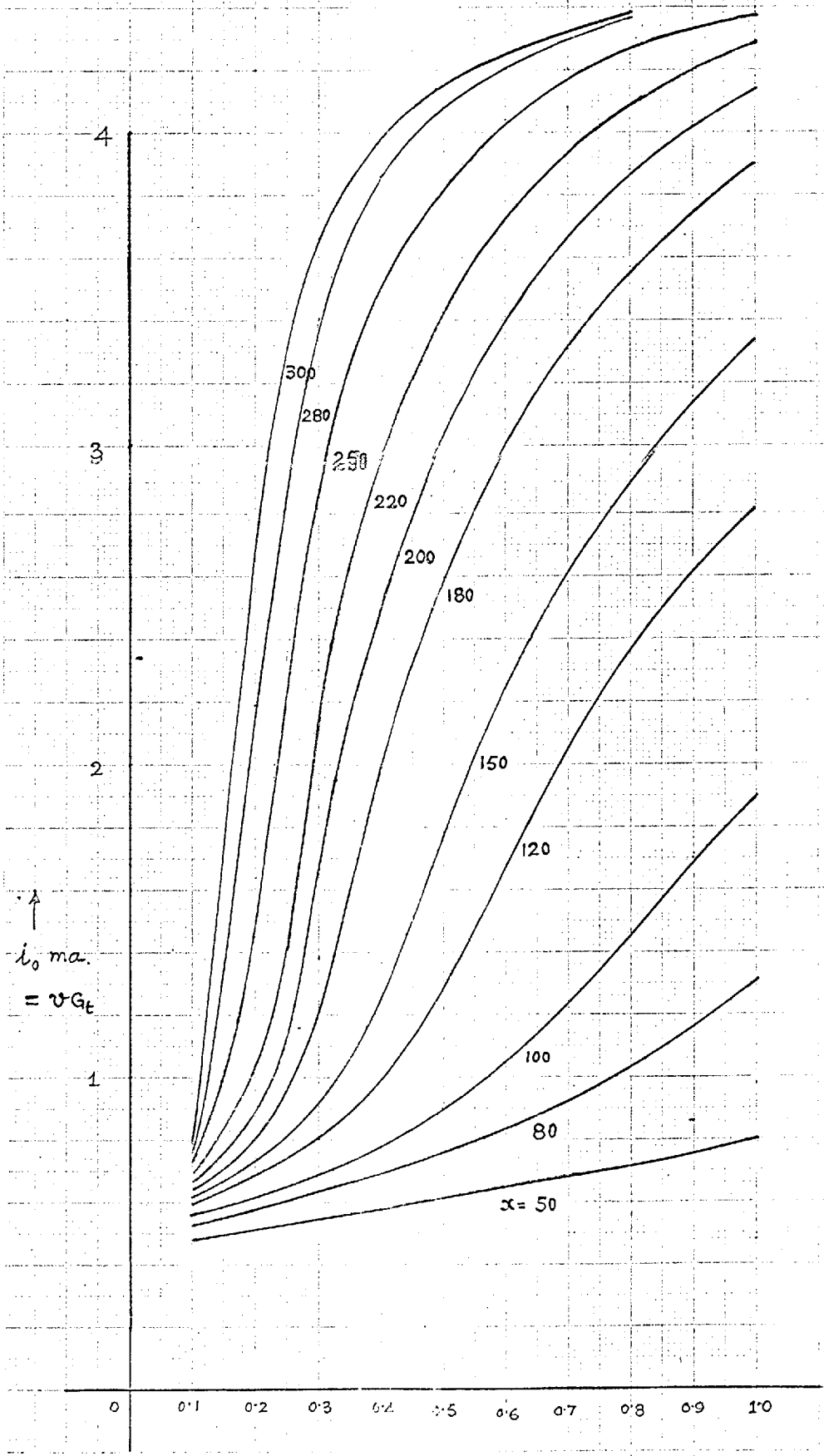
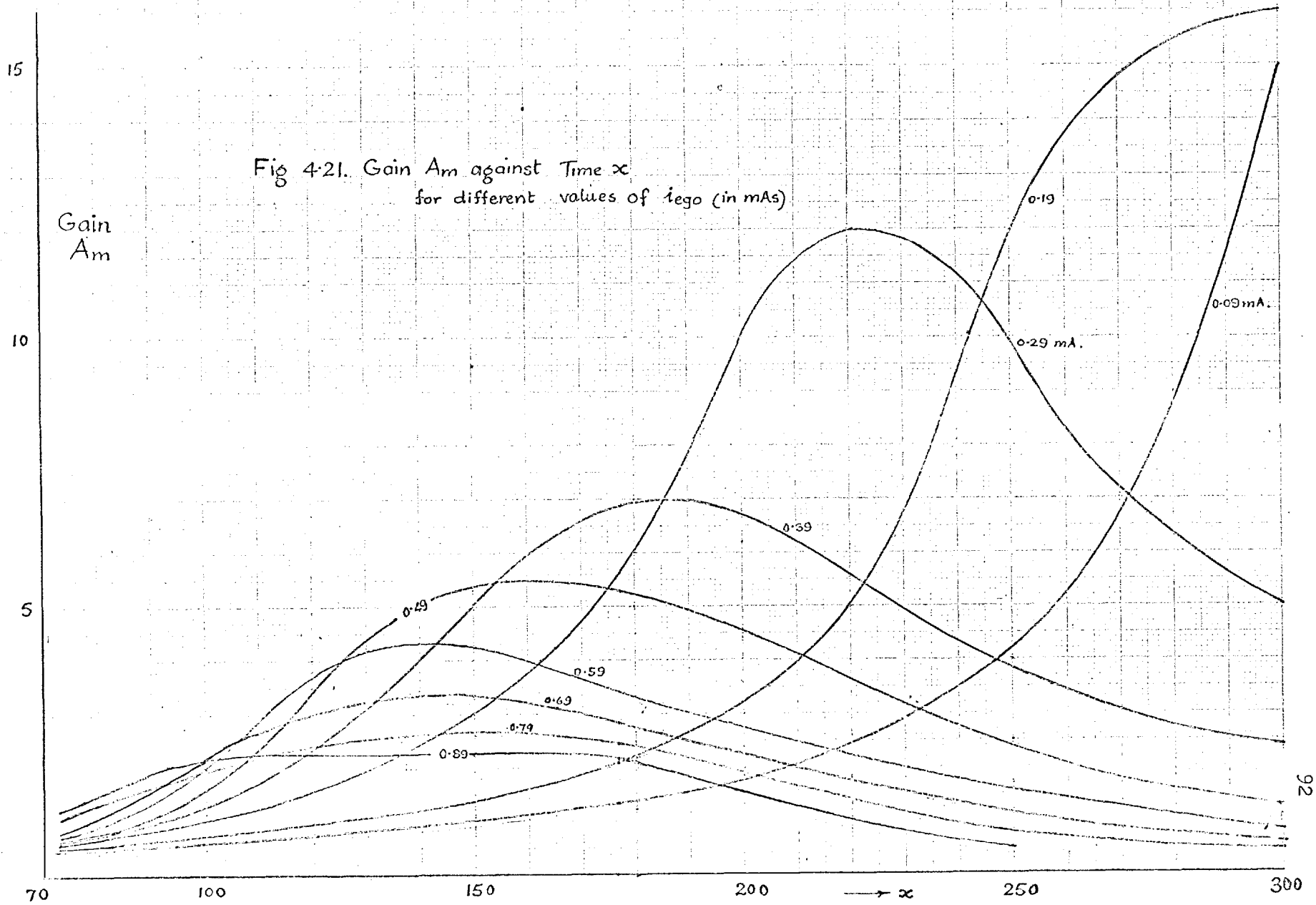


Fig. 4.20.

i_{00} mA \rightarrow



regenerative amplifier. The measurements were carried out at low frequencies to suit the available equipment.

A representative set of measurements was for an $I_b = 5.7$ mA. The diode used for these experiments has static characteristics of Fig. 4.8.

Other circuit parameters are

$$G_L = 0.01 \text{ mhos}$$

$$G_S = (0.00045)^2 = 0.0009$$

$$G_L \gg G_S.$$

If we assume $G_L = G_t = 0.01$ mhos then the graphs of Fig. 4.7 and the subsequent calculations apply to the circuit of Fig. 4.22.

The signal peak will be at x_2 corresponding to the circuit conditions. If the width of the square wave pump pulse is adjusted to this value, the peak of the voltage across the tunnel diode due to the pump current will coincide with the peak of the signal.

Fig. 4.7. gives the voltage against x graphs for different pump current. x_2 is the time taken to reach the voltage v_{x_2} . From Fig. 4.10. this is found to be at 190 mV. Therefore from Fig. 4.7.

$$x_2 = 177$$

For a pump pulse width of 0.4μ sec the capacitance C is given by

$$t_2 = Cx_2$$

$$\text{or } C = \frac{t_2}{x_2} = \frac{0.4 \times 10^{-6}}{177} = 2260 \text{ pf.}$$

The tunnel diode capacitance was increased to this value by the addition of an external capacitance of 2200 pF.

Great care was taken to keep the leads short so that the series inductance should be low. The external component like capacitors and resistors were of small size and connected to the tunnel diode very close to its base. Even then it was estimated that the series inductance could amount to as high as 30 nH.

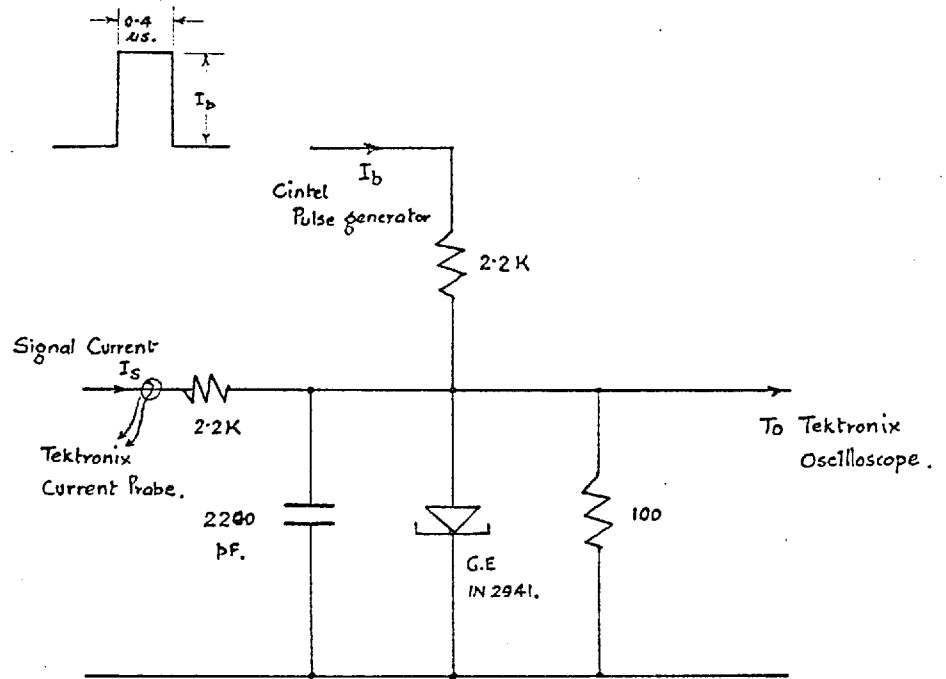


Fig. 4-22. Circuit for the measurements on the regenerative Amplifier.

To check if these conditions conform to the condition $LG \ll R_t C$, so that the circuit inductance can be neglected

$$R_t C = 2.26 \times 10^{-7}$$

$$\text{and } LG(v) = 30 \times 10^{-9} \times 0.175 = 5.25 \times 10^{-9}$$

$$\text{where } G(v) = 0.175 \text{ at } v = 0.$$

therefore, $LG(v) \ll R_t C$ and the effect of the inductance can be neglected.

In the calculation above we have employed the value of circuit conductance at the point $v = 0$. This part of the conductance cycle is of no significance as far as the gain of the amplifier is concerned. The significant part of the cycle is in the negative-conductance region (from x_1 to x_2). The circuit conductance and hence the factor $LG(v)$ are an order of magnitude lower in this region compared with those at $v = 0$.

$LG(v)$ at the point of maximum negative-conductance

$$\begin{aligned} |LG(v)| &= 30 \cdot 10^{-9} |(-G_1)| \\ &= 30 \times 10^{-9} \times 0.035 \\ &= 1.05 \times 10^{-9} \end{aligned}$$

In this experiment ordinary components were used. The tunnel diode used were mounted in TO 18 cans. Even with the leads cut very short the inductance of the leads is of the order of 6 nH. The resistor leads and the configuration of connection give rise to extra inductance.

If operation at very much higher frequencies is desired, the inductance can be reduced to very small values of the order of 1 nH or smaller by using strip line techniques. The series inductance of the diode itself can be reduced to less than 0.25 nH by mounting the diode between brass plates (known as pill type construction).

If the capacitance in the amplifier circuit of Fig. 3.22 is reduced to a thousandth, the pump pulse width will be 0.4 n sec. If $L = 1$ nH

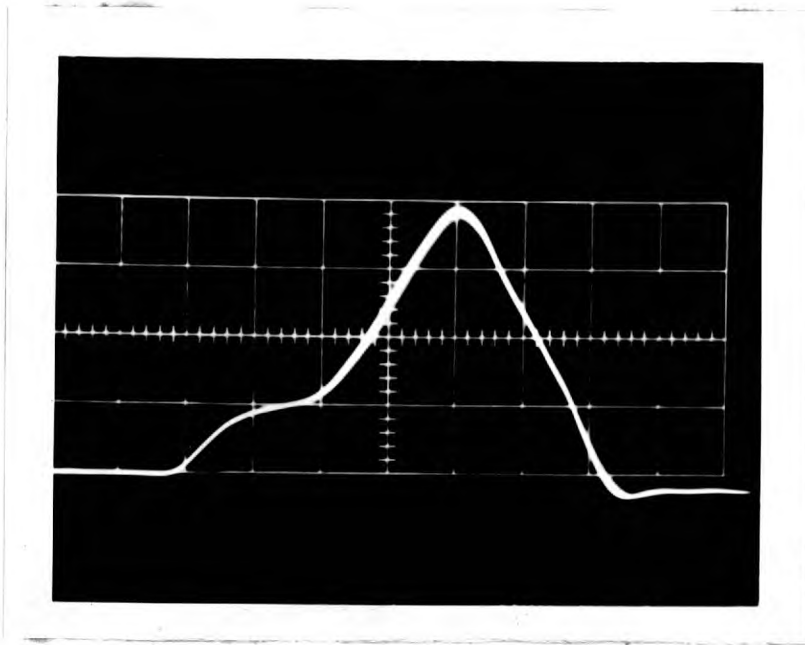


Fig. 4.23 : Tunnel Diode Voltage Against Time (For $I_b = 5.7 \text{ ma}$).
50 mV/cm Vertical. 100 nsec./cm horizontal.

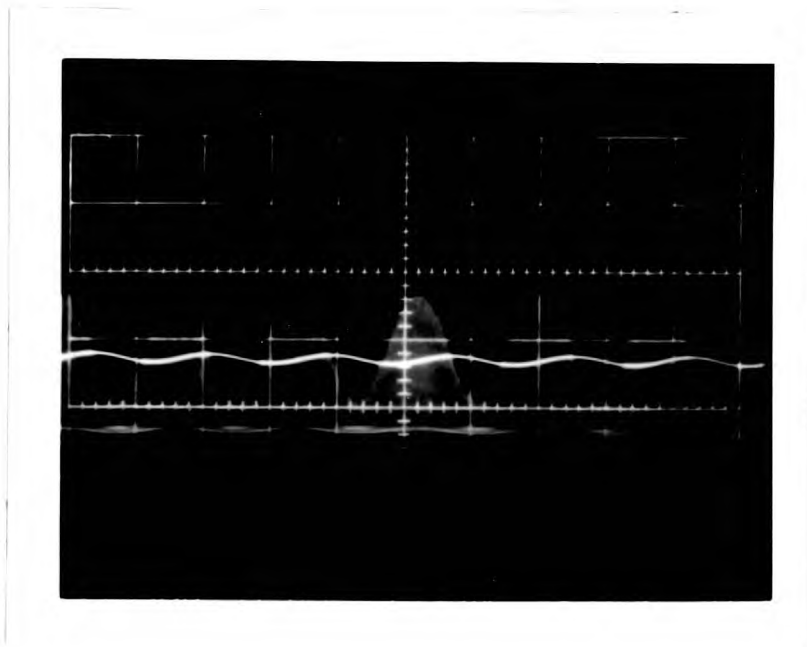


Fig. 4.24 : Peaks of the Tunnel Diode Voltage and the Signal
Current Against Time.
Tunnel Diode Voltage 10 mV/cm (i.e. for $G_t = 0.01, 0.1 \mu\text{A/cm}$)
Signal Current 0.1mA/cm.

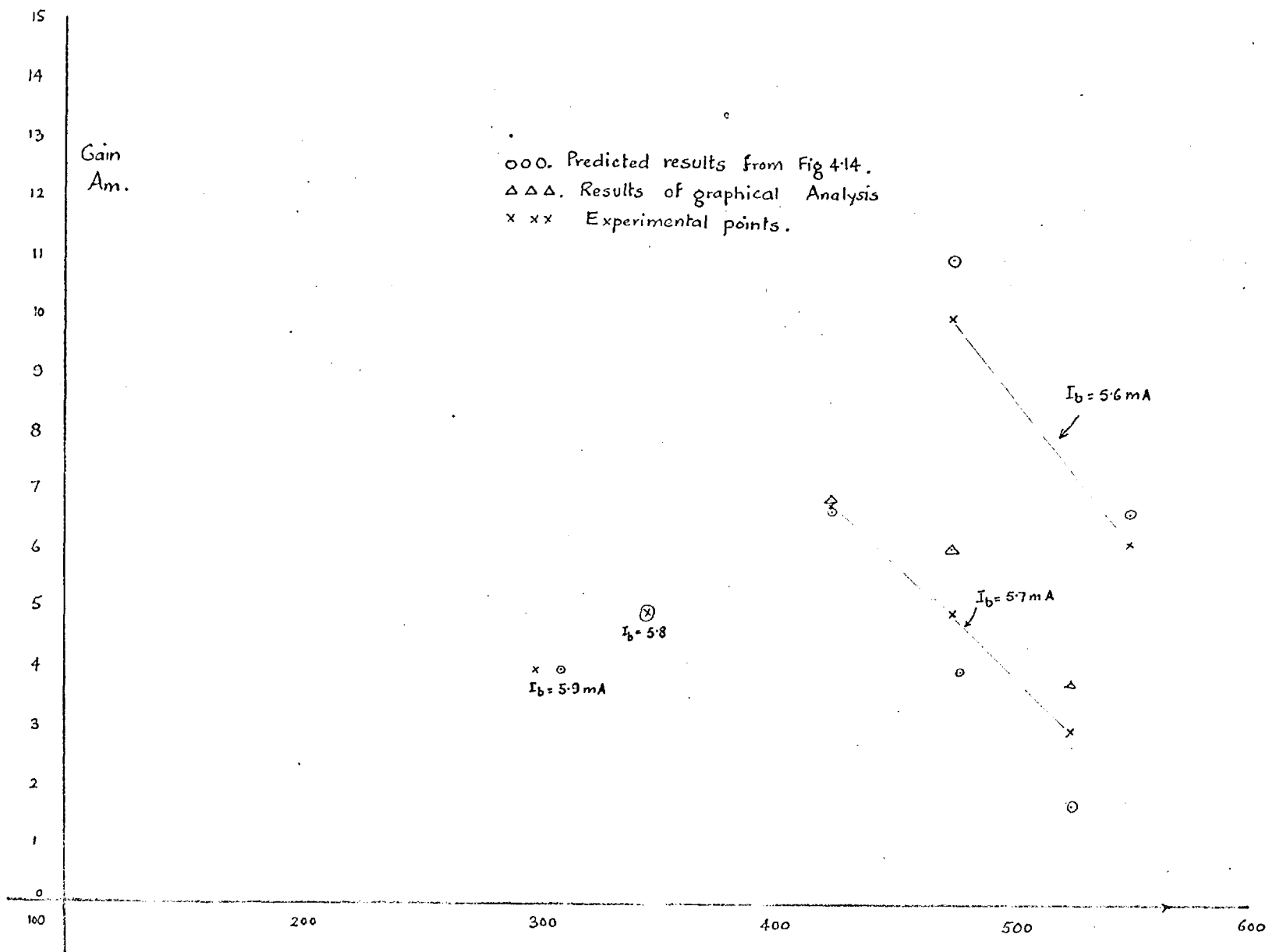


Fig. 4.25 Measured gains at low frequencies.

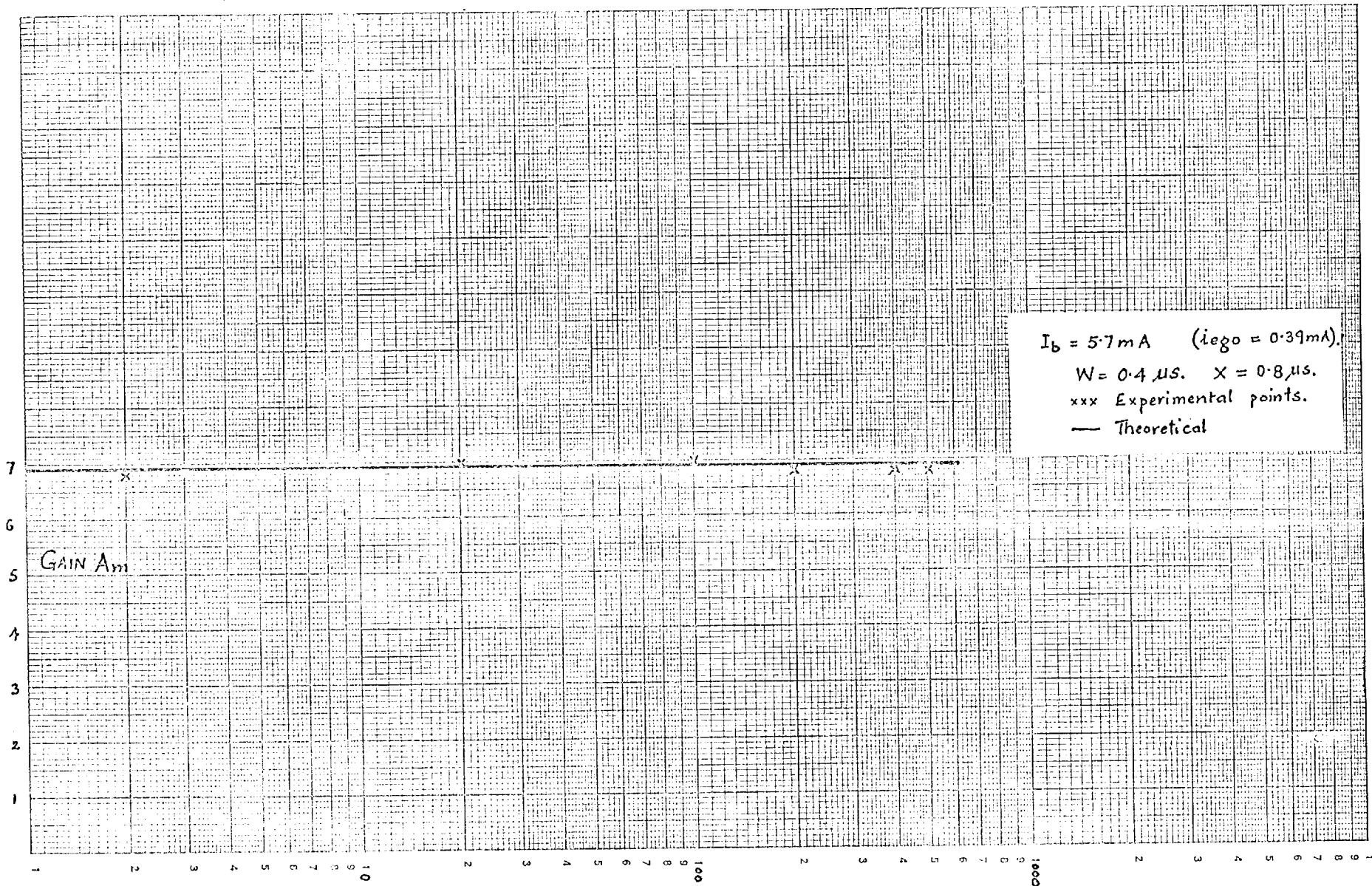


Fig. 4.26. Gain A_m against Signal Frequency.

Signal Frequency in Kc/s.

$$\begin{aligned} \text{then } R_t C &= 2.26 \times 10^{-10} \\ \text{and } L G_1 &= 1 \times 10^{-9} \times 0.035 \\ &= 3.5 \times 10^{-11} \end{aligned}$$

Therefore $R_t C > L G(v)$ and it is possible to achieve the practical operation of such an amplifier upto fairly high frequencies.

Fig. 4.23 is an oscillogram of the voltage transient across the tunnel diode due to the pump only.

Fig. 4.24 is an oscillogram of the peaks of the voltage transients in the presence of the signal. This Fig. also shows the sine wave input signal current. The signal input was monitored by the help of a current probe. The ratio of signal modulation amplitude to the amplitude of the input gives us the gain A_m .

The experimental gain figures (A_m), in general, were found to be slightly lower than the calculated ones (Fig. 4.25), but are very close to the results predicted by the analytical and graphical means.

The period of the pump waveform was adjusted to $0.8 \mu \text{ sec}$. According to the section 4.11, the max frequency of amplification will then be

$$\begin{aligned} &= \frac{1}{2 \times 0.8 \times 10^{-6}} \text{ c/s.} \\ &= 625 \text{ k c/s .} \end{aligned}$$

Measurements were carried out over the whole of this frequency range. Fig. 4.26 shows the results.

CONCLUSIONS

It is possible to predict the performance of the regenerative amplifier by a few simple calculations and these are found to be in good accord with measurements.

The dependence of the gain and frequency response of the amplifier on the various circuit parameters has been studied. On the basis of these

investigations, the circuit elements can be optimized for gain.

It is shown that a more suitable tunnel diode should give much higher gains. Such a tunnel diode should have a minimum $\frac{I_p}{G_1}$. In practice the diodes commercially available have I_p / G_1 very nearly constant whatever their peak currents.

Very high gain figures are possible if the excess pump current i_{ego} is kept to a low value but the amplifier becomes very sensitive to any spurious variations in the circuit conditions. In practice, a transducer gain of about 10 db seems a good compromise for such an amplifier.

CHAPTER FIVE

5. REGENERATIVE AMPLIFIER WITH SINE WAVE PUMP

5.1 Introduction

We shall now examine the conductance function due to sinusoidal pump. Of all the pump waveforms, the sinusoidal pump has the greatest practical importance because of the ease with which it can be generated and applied.

The general approach to the determination of conductance functions due to sine wave pump is similar to that of the last Chapter. The fundamental differential equation 4.11. for the response of tunnel diode becomes more complicated because of the presence of the time dependent term due to the pump. This equation for sinusoidal pump can be solved by the Runge-Kutta method (Appendix A.4.) of step by step integration; this is inordinately tedious and therefore, a digital computer solution is necessary.

Conductance functions obtained by the action of sinusoidal pump, although essentially the same in shape as those due to square wave pump, are different in some aspects. It is possible, on the basis of these special characteristics of the conductance function due to sine wave pump, to make some very useful approximations.

Essential to the evaluation of the amplifier is the conductance slope, $G'(x_1)$. A method is developed for the approximate determination of this factor.

Further approximations and piece-wise linear analysis provide us with the value of the negative-conductance area a and the conductance slope $G'(x_2)$. The approximate analysis is considerably simpler than the step by step integration mentioned above.

A study of regenerative amplifier with square wave pump is comparatively simple; conductance slope $G'(x_1)$ can be determined directly once the magnitude of the pump current is specified and it is entirely independent of the width of the pump pulse^{*}. For sinusoidal pump, $G'(x_1)$ is dependent not

^{*}

except for the trivial case when the pump pulse width $W < x_1$.

only upon the amplitude but also on the frequency of the pump current; $G'(x_1)$ can have the same value for widely differing magnitudes of the pump current if the pump frequency is so adjusted. The area a is again dependent upon both these factors. In Chapter 4, we studied the behaviour of the amplifier in the presence of different magnitudes of square wave pump current and then the width and the frequency of the pump pulse could be controlled to give the required conditions of gain and the type of output desired. For sine wave pump, once again, it is not possible to separate the two factors of the pump magnitude and frequency. Because of this the gain of the regenerative amplifier with sinusoidal pump is studied for conditions of different pump amplitude and frequency.

5.2 Numerical Determination of Conductance Function

The differential equation for the circuit of Figure 4.6. for a sine wave pump is

$$C \dot{v} = I_b \sin \omega_p t - f(v) - G_t v \quad 5.1.$$

$$\begin{aligned} \text{If } \mu_p &= c\omega_p \\ \text{and } t &= cx \end{aligned}$$

$$\dot{v}(x) = I_b \sin \mu_p x - f(v) - G_t v \quad 5.2.$$

The solution of this equation for different values of I_b and μ_p are given in Fig. 5.1. These solutions were obtained by the digital computer programme of Appendix A.4. The tunnel diode assumed for these calculations has static characteristic of Fig. 4.8. and G_t is assumed to be 0.01 mhos.

Fig. 5.2. gives the conductance-time graphs for $I_b = 5.7$ ma for different values of pump frequency μ_p .

5.3 Approximate Methods

From an examination of the conductance-time graphs of Fig. 5.2, we note that the conductance-time graphs are very nearly linear in the region $x = 0$ to $x = x_1$. Therefore the conductance slope $G'(x_1)$ is given

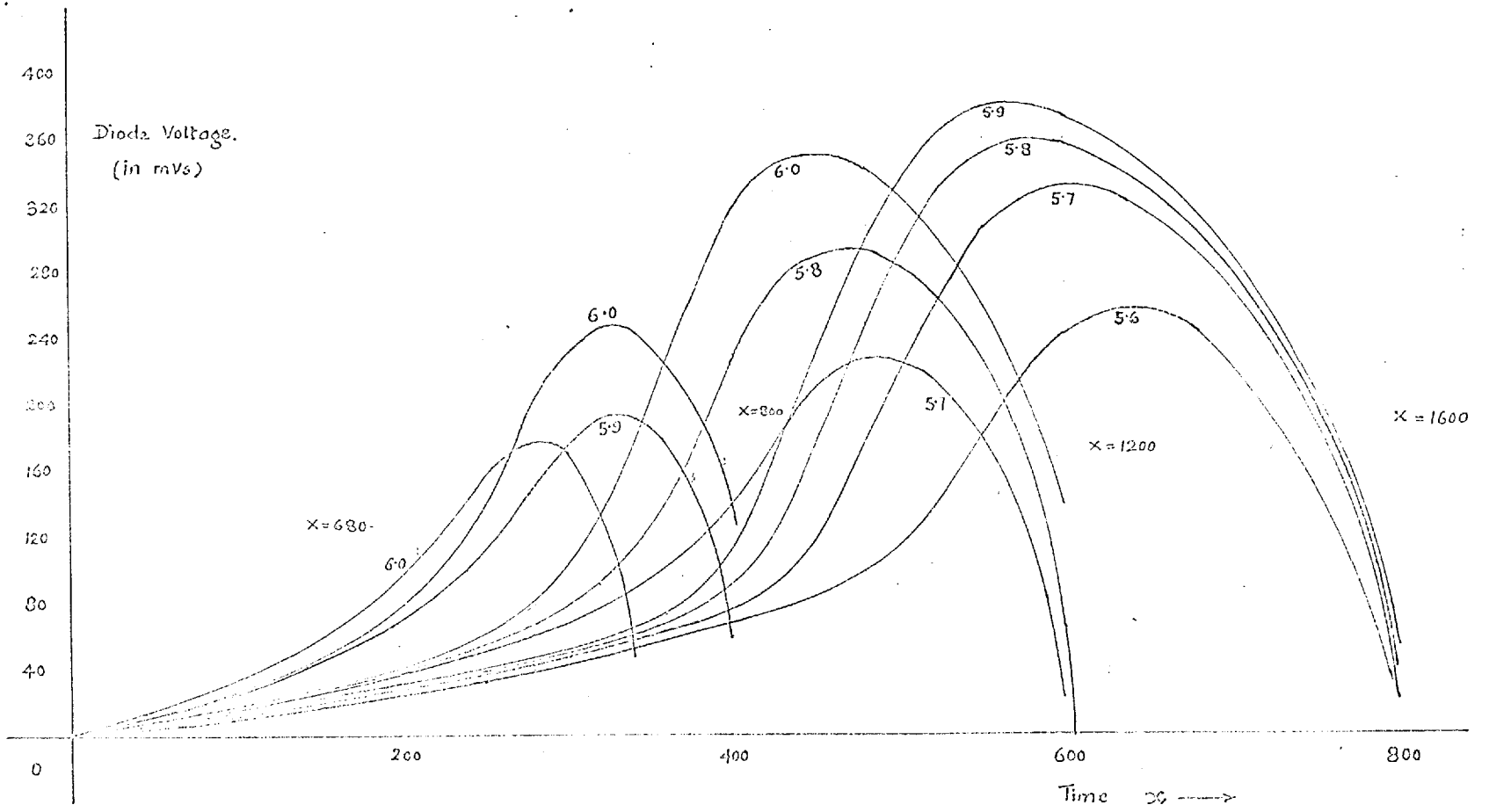
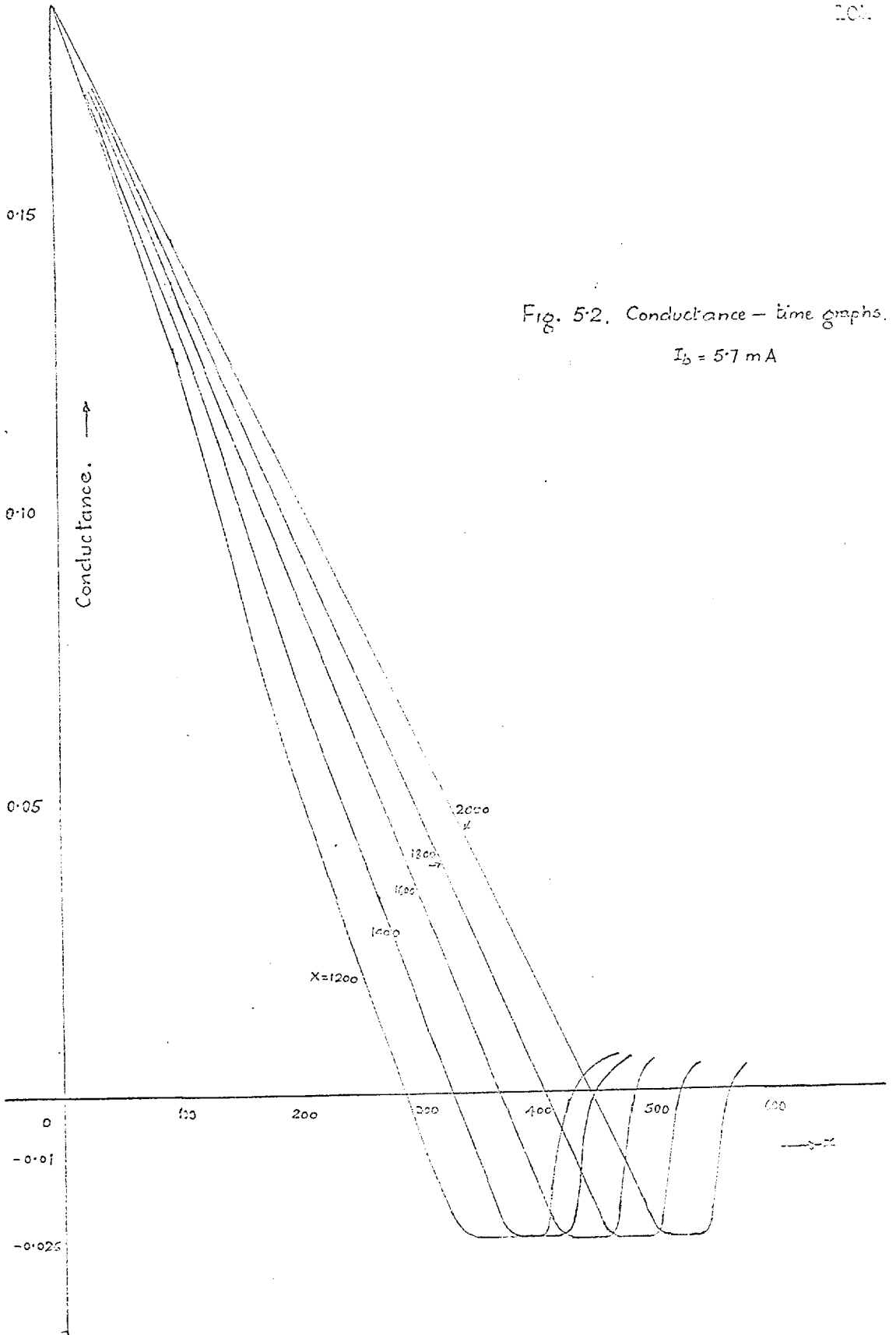


Fig 5.1.



approximately by

$$G'(x_1) \simeq \frac{G_0}{x_1} \quad 5.3.$$

where G_0 is the circuit conductance at $v = 0$,

$$\text{and } G'(x_1) = G'(v_{x_1}) \cdot \frac{dv}{dx} \Big|_{x_1} \quad 5.4.$$

From the equation 5.2, 5.3 and 5.4

$$\frac{G_0}{x_1} = G'(v_{x_1}) \left[I_b \sin \mu_p x_1 - f(v_{x_1}) - G_t v_{x_1} \right] \quad 5.5.$$

$$\text{or } \sin \mu_p x_1 = \frac{1}{I_b} \left[\frac{G_0}{x_1 G'(v_{x_1})} + f(v_{x_1}) + G_t v_{x_1} \right] \quad 5.6.$$

This is a transcendental equation in x_1 . G_0 , $f(v_{x_1})$, v_{x_1} and $G'(v_{x_1})$ are constants of the circuit. For a given value of G_t these can be determined from the tunnel diode characteristic.

Equation 5.6 can be solved by graphical means. In Fig. 5.3. the term $\sin \mu_p x$ is plotted for the range of interest for different values of μ_p . The right hand side of equation 5.6 is also plotted on the same graph for different values of I_b . x_1 , for a specified μ_p and I_b , is given by the intersection of the two graphs corresponding to the given μ_p and I_b .

In general there are three possibilities depending upon whether the graphs of specified μ_p and I_b

a) intersect in two points. The lower of the two values of x at the intersection points is x_1 and the higher value is a trivial solution;

b) intersect in one point; i.e. they are tangential to each other. The point of intersection gives x_1 . The value of x_1 in this case is always greater than $X/4$ because the graphs for different I_b are monotonically increasing functions of $\frac{1}{x}$ (Fig. 5.3);

c) do not intersect at all. No x_1 exists; the specified values of μ_p and I_b for such a case are incompatible for the transition of the circuit into the negative-conductance region and are therefore of no interest to us.

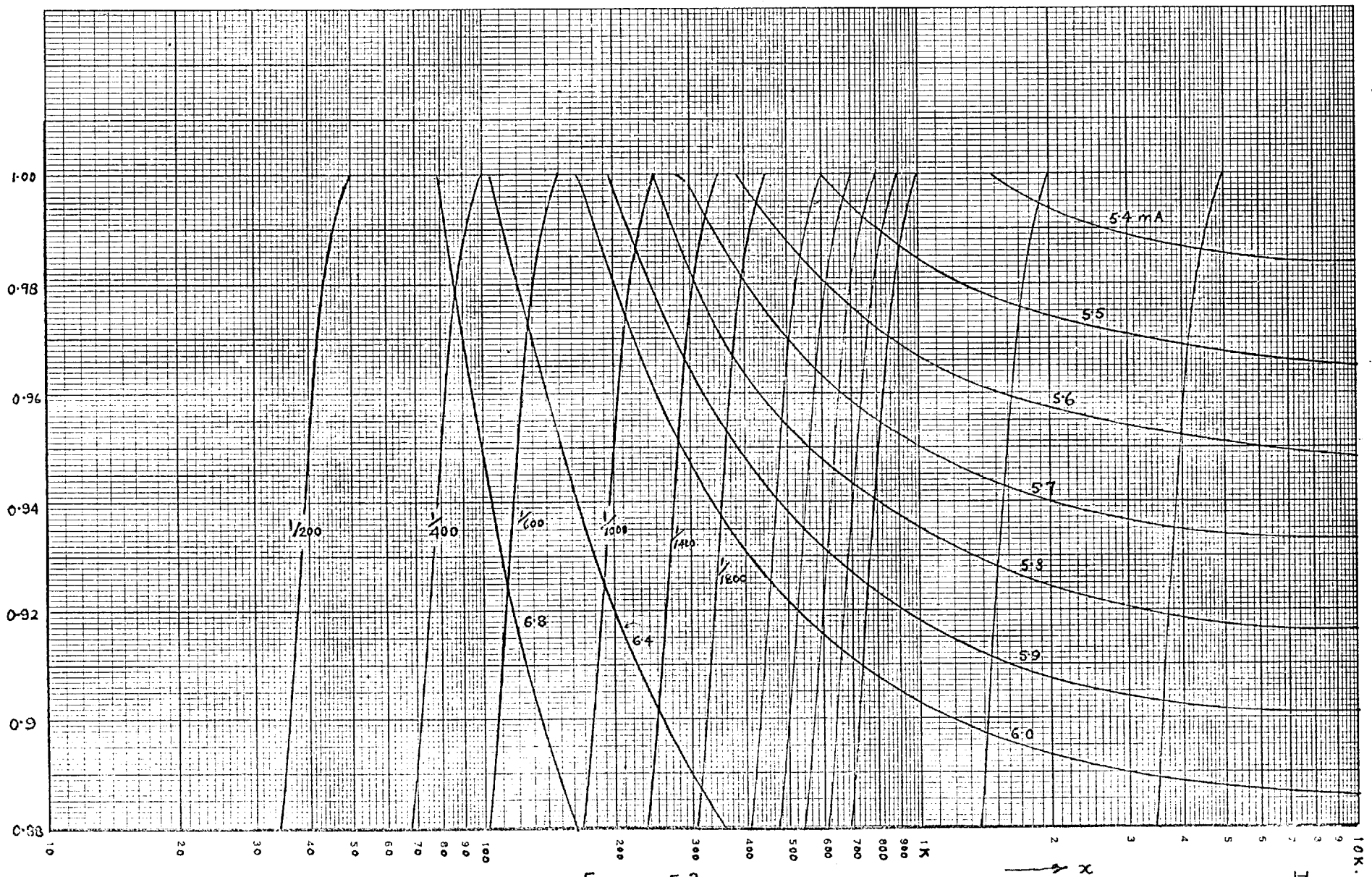


Figure. 5.3.

Fig. 5.4 shows the values of x_1 obtained by the computer as well as the approximate calculations. The error in the value of x_1 determined by the approximate method is less than ± 3 per cent for most of the range studied.

From the values of x_1 , the respective conductance slopes $G'(x_1)$ can be calculated by the means of equation 5.3 or equations 5.2 and 5.4,

The area a can be calculated by dividing the area into three regions as in Section 4.8, Fig. 4.11. $G'(x)$ is very nearly equal to $G'(x_1)$ over the voltage range v_{x_1} to v_y (Fig. 4.10). $G(v_{x_1}) = 0$ and $G(v_y) = G_t - G_1$ where $(-G_1)$ is the maximum negative conductance of the diode.

$$\text{Then the time } \delta x_1 = \frac{|G_t - G_1|}{G'(x_1)} \quad 5.7.$$

$$\begin{aligned} \text{and the triangular area } \delta a_1 &= \frac{\delta x_1}{2} |G_t - G_1| \\ &= \frac{|G_t - G_1|^2}{2G'(x_1)} \end{aligned} \quad 5.8.$$

$$\text{The rectangular area } \delta a_3 = \delta x_3 \cdot |G_t - G_1| \quad 5.9.$$

The time δx_3 is the time taken for the diode voltage to rise from the voltage v_y to v_z . Over this range the circuit conductance is approximately constant at $(G_t - G_1)$. An analytical solution of equation 5.1 is therefore possible for this region.

The complete solution of equation 5.2 for this region is

$$v = \frac{I_b}{\mu_p^2 + G_c^2} \left[G_c \sin \mu_p x - \mu_p \cos \mu_p x \right] + A \exp(-G_c x) + f(v_y) + G_c v_y \quad 5.10.$$

where $G_c = G_t - G_1$ and

A is an arbitrary constant which can be evaluated by inserting the initial conditions of the circuit into the equation 5.10. The initial conditions are at $x = x_1 + \delta x_1$,

$$v = v_y.$$

Equation 5.10. can be solved for the voltage range v_y to v_z and δx_3

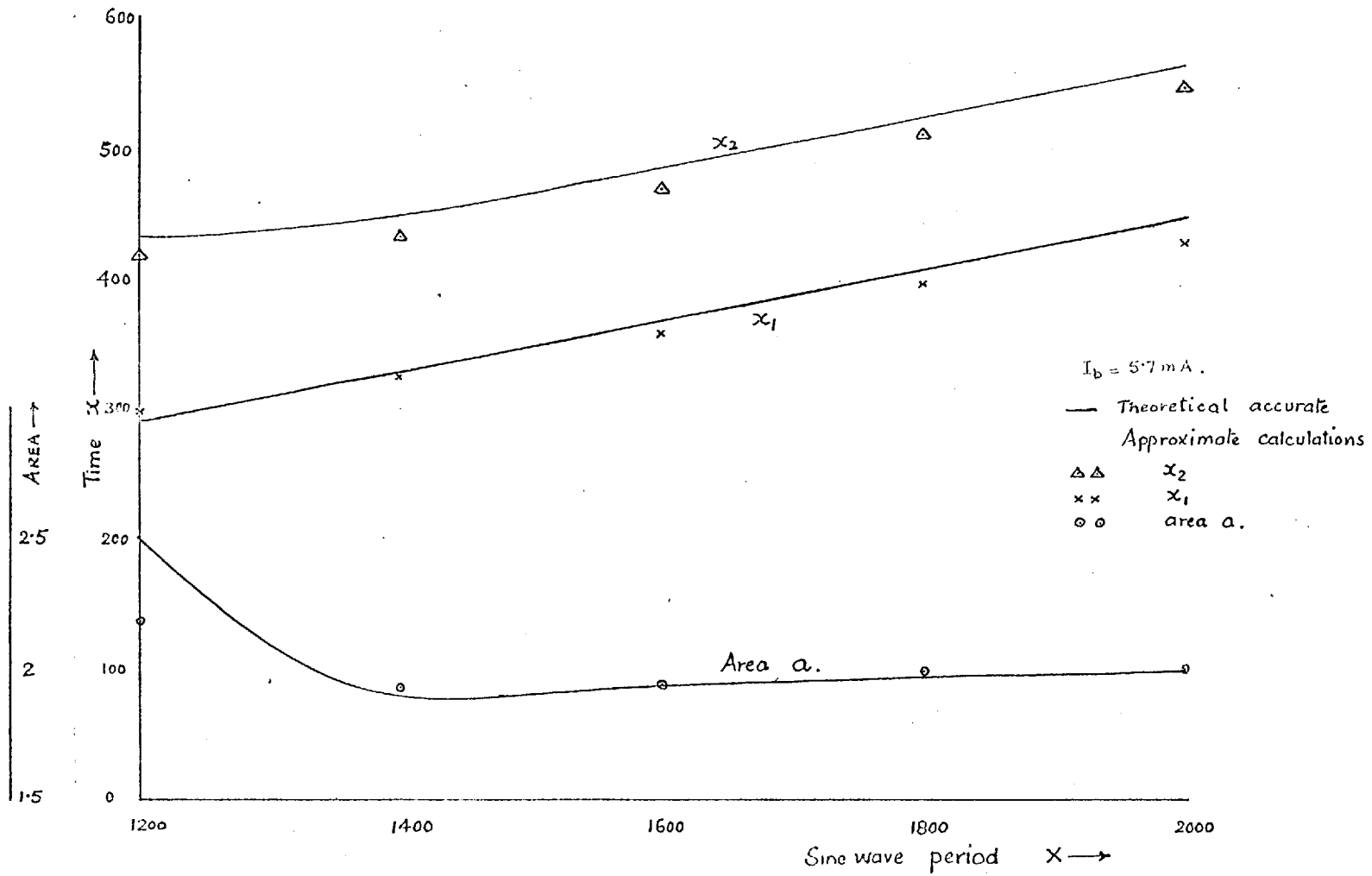


Figure. 5.4.

obtained.

The third part δa_2 of the negative conductance area can be determined approximately by noting the fact that $\frac{dv}{dt}$ remains nearly constant over the voltage range v_z to v_{x_2} (Fig. 5.1, v_z for the diode with static characteristics of Fig. 4.8 is at 150 mV and v_{x_2} at 190 mV)

$$\therefore \delta x_2 = (v_{x_2} - v_z) / \dot{v}]_z \quad 5.11.$$

$$\text{and } \delta a_3 = \frac{\delta x_2}{2} |G_t - G_1| \quad 5.12.$$

The total area $a = \delta a_1 + \delta a_2 + \delta a_3$ and can be obtained from the equations 5.8, 5.9 and 5.12.

The time x_2 is given by

$$x_2 = x_1 + \delta x_1 + \delta x_2 + \delta x_3$$

$G'(x_2)$ can now be easily evaluated.

$$G'(x_2) = G'(v_{x_2}) \cdot \dot{v}]_{x_2} \quad 5.13.$$

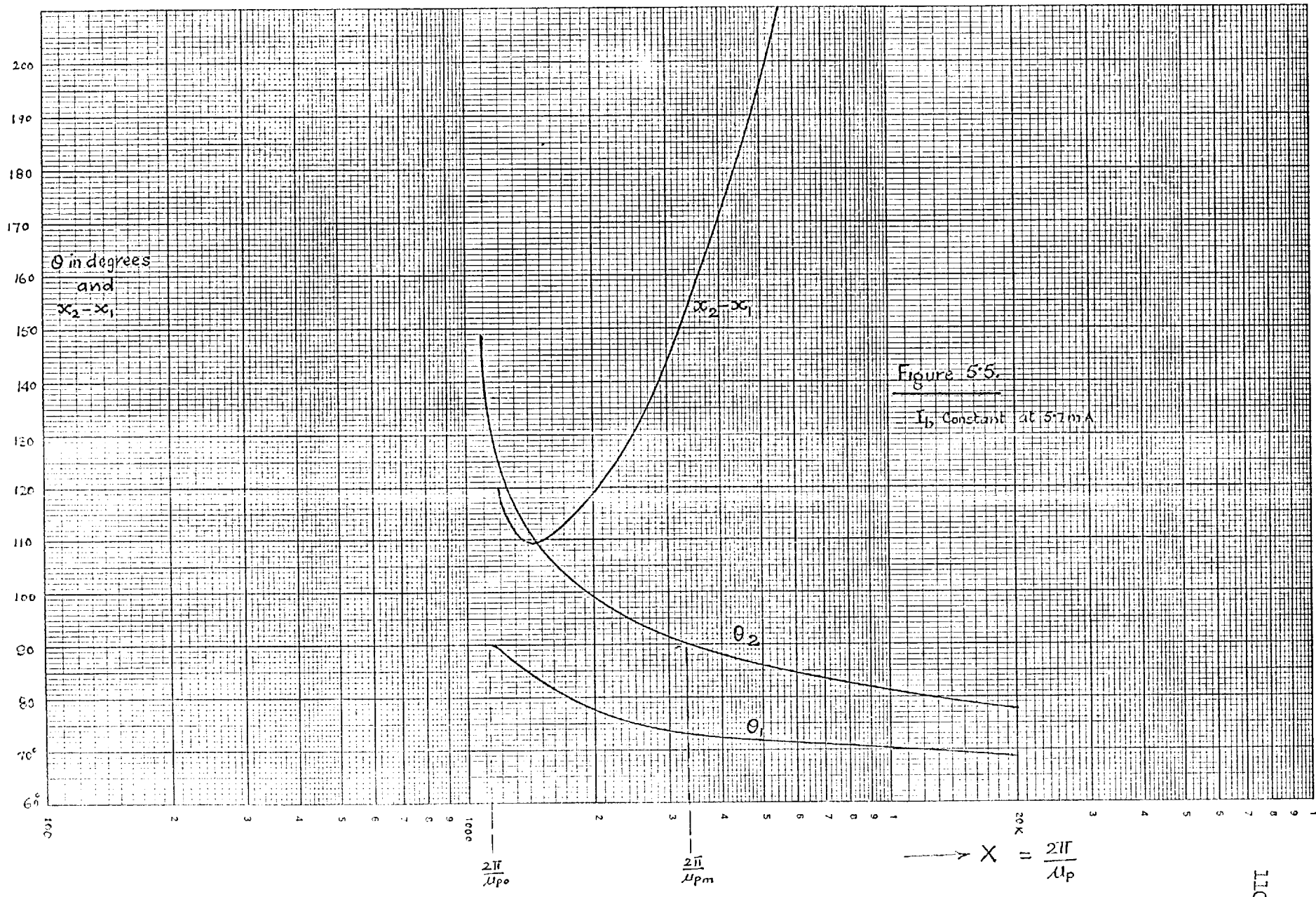
$$\text{and } \dot{v}]_{x_2} = I_b \sin \mu_p x_2 - f(v_{x_2}) - G_t v_{x_2} \quad 5.14.$$

Fig. 5.4. gives the approximate and accurate values of x_1 , x_2 and area a . The approximate calculations give results very close to the accurate ones.

5.4 Dependence of Gain on Pump Frequency

The transition of tunnel diode through any region of voltage depends upon the amount of excess pump current available at all the points in that region. The higher the excess pump current faster the transition. The excess pump current in any region depends not only upon the amplitude I_b of the sine wave pump but also upon the frequency of the pump.

If the amplitude I_b of sine wave pump is kept constant and the frequency $\frac{\mu_p}{2\pi} = \frac{1}{X}$ is varied, the conductance slopes $G'(x_1)$ and $G'(x_2)$, and negative-conductance area a vary with the frequency. To study the effect of pump frequency on the conductance slope $G'(x_1)$ we will study the



equations 5.2 and 5.4. From equation 5.2

$$\begin{aligned} G'(x_1) &= G'(v_{x_1}) \cdot \dot{v} \Big|_{x_1} \\ &= G'(v_{x_1}) \cdot i_{\text{ego}} \end{aligned}$$

$$\text{and } i_{\text{ego}} = I_b \sin \mu_p x_1 - f(v_{x_1}) - G_t v_{x_1}$$

The excess pump current i_{ego} at $x = x_1$ and hence $G'(x_1)$ depend upon the angle $\theta_1 = \mu_p x_1$. Fig. 5.3 gives the time x_1 for a given pump frequency μ_p and amplitude I_b . The value of θ_1 for different values of μ_p and a constant value of I_b are given in Fig. 5.5. The lower the frequency the further away the corresponding x_1 is from the peak of the sine wave (i.e. $\theta_1 < \frac{\pi}{2}$); i_{ego} and therefore $G'(x_1)$ both reduce with frequency (Fig. 5.6). The maximum value of $G'(x_1)$ is reached at a frequency μ_p when $\mu_p x_1 = \frac{\pi}{2}$.

If the pump frequency is increased further θ_1 becomes greater than $\frac{\pi}{2}$ and the conductance slope $G'(x_1)$ once again decreases.

The conductance slope $G'(x_2)$ is determined by the equations 5.13 and 5.14 and is dependent upon $\theta_2 = \mu_p x_2$. θ_2 is an increasing function of frequency (Fig. 5.5). $G'(x_2)$ will be a maximum at a frequency μ_{pm} such that $\mu_{\text{pm}} x_2 = \theta_2 = \frac{\pi}{2}$.

$$\text{The maximum value of } G'(x_2) = G'(v_{x_2}) \left[I_b - f(v_{x_2}) - G_t v_{x_2} \right] \quad 5.15.$$

As the frequency of pump reduces from this value, θ_2 reduces and $G'(x_2)$ is lower than the peak value given by the equation 5.15. (Fig. 5.6).

If $\mu_p > \mu_{\text{pm}}$, $\theta > \frac{\pi}{2}$ and $G'(x_2)$ decreases once again. At a frequency μ_{po} , $I_b \sin \mu_{\text{po}} x_2 = f(v_{x_2}) + G_t(v_{x_2})$ i.e. $G'(x_2)$ is zero. In this case, the peak of the transient due to the pump is arrested at the voltage v_{x_2} . This is the condition for maximum gain A_m at the peak of the transient as discussed in Section 4.3.

The area a depends upon the excess pump current available when the tunnel diode traverses the negative-conductance region. When θ_1 is less than but close to $\frac{\pi}{2}$, then as the tunnel diode goes into negative-conductance area, $i_b = I_b \sin \mu_p x$ is rising; i_b keeps rising till the peak is reached

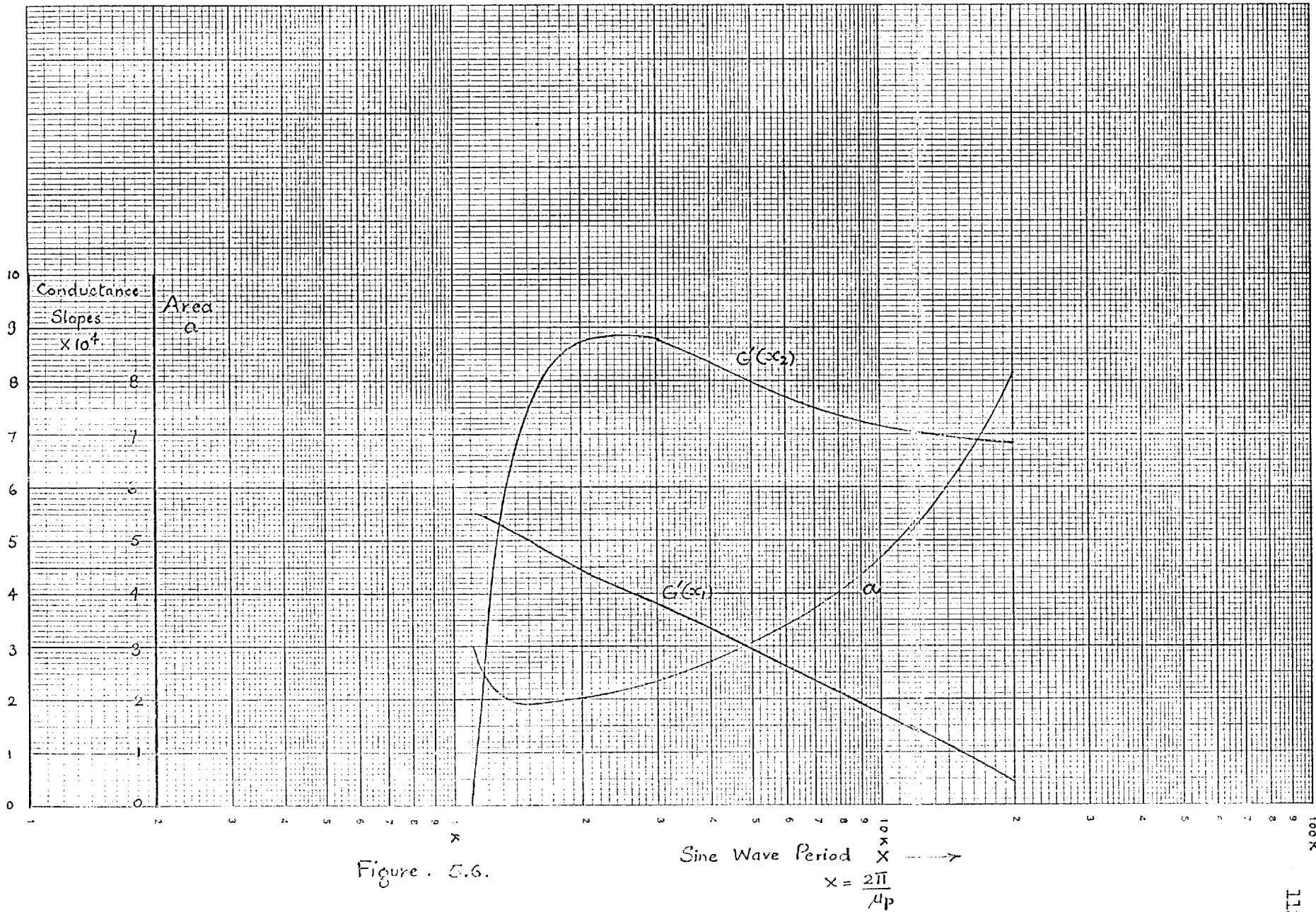
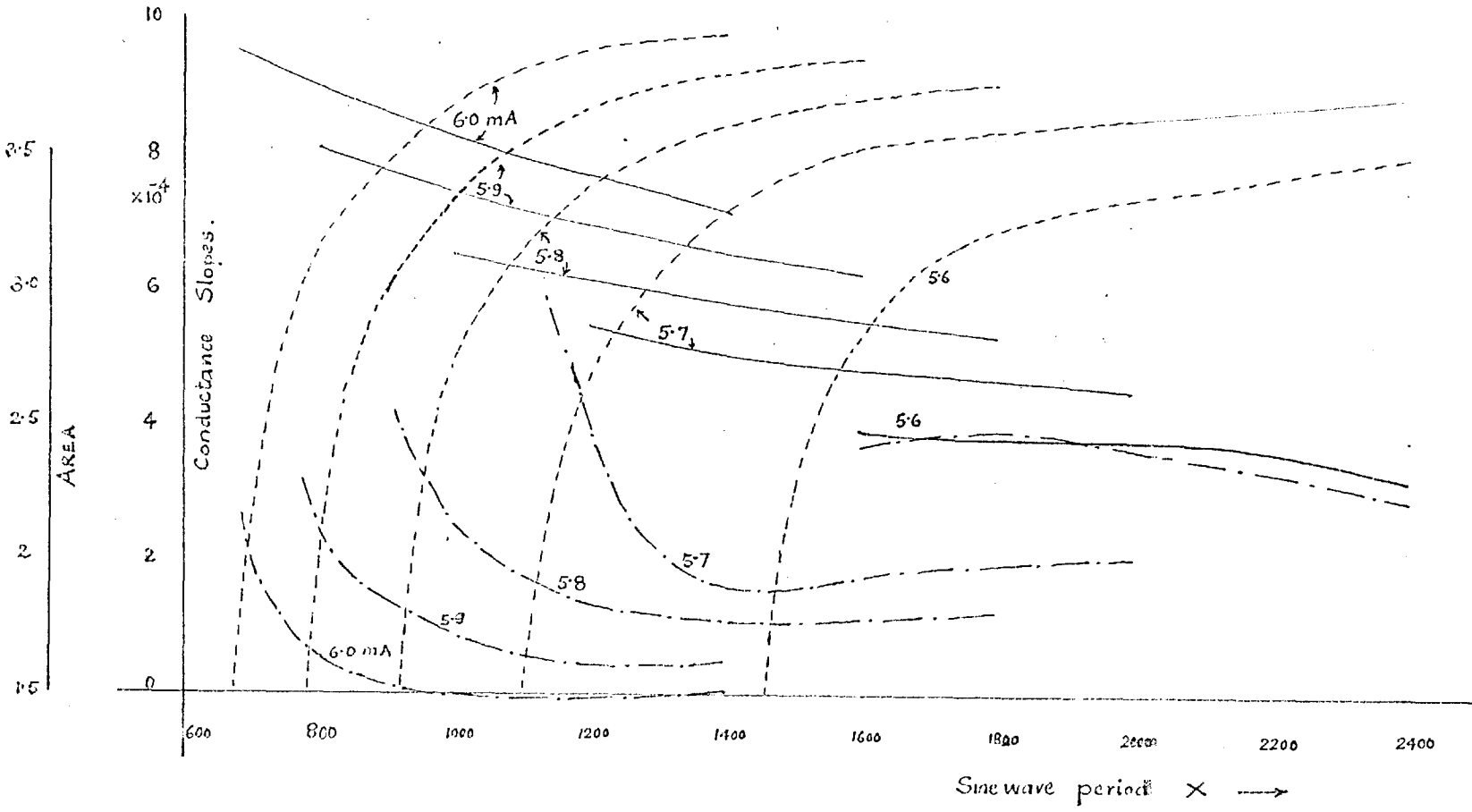
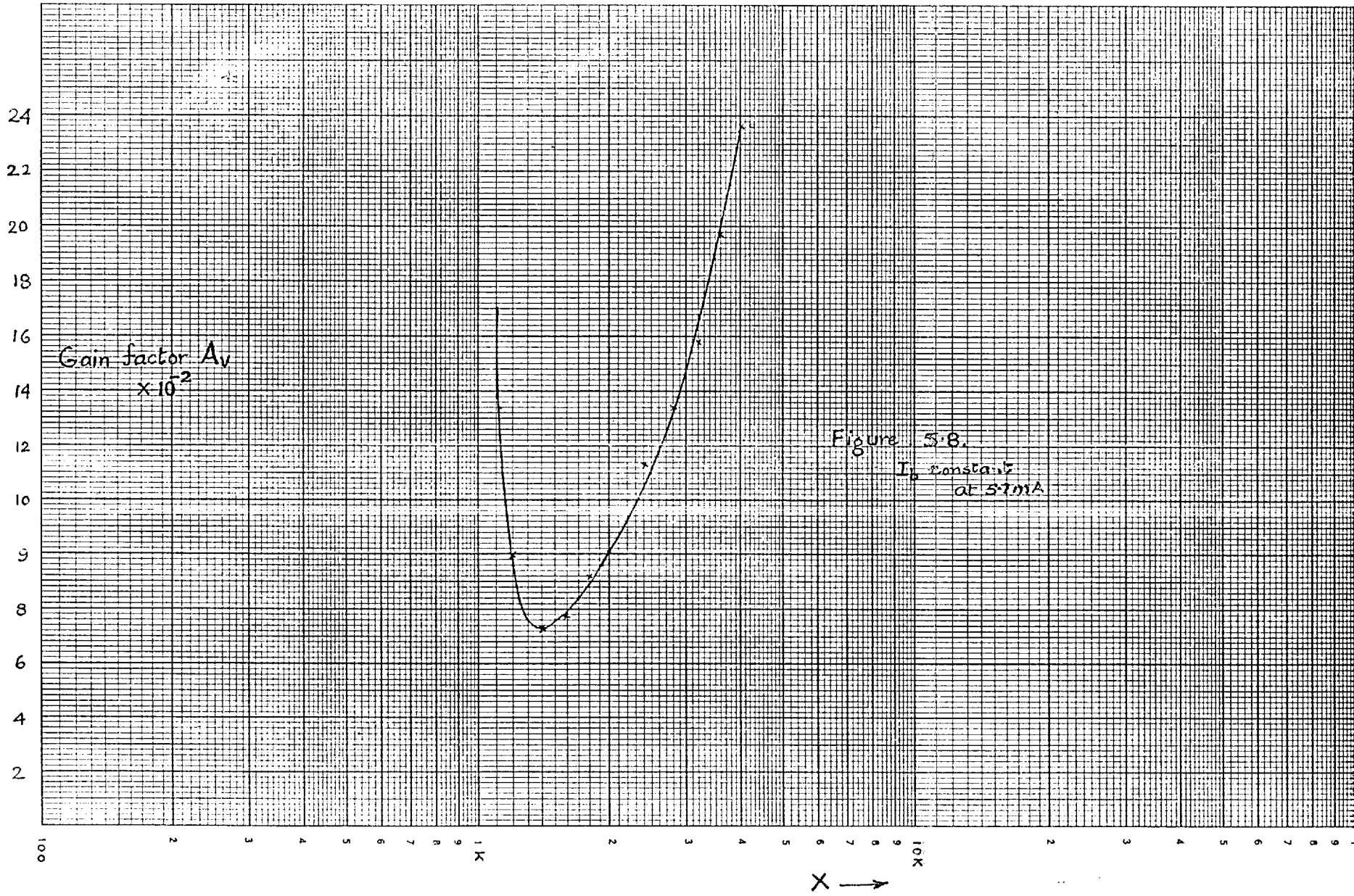


Figure. 5.6.

Figure 5.7.

--- $G'(x_2)$
 — $G'(x_1)$
 - - - area cu





at $\mu_p x = \frac{\pi}{2}$ and then i_b reduces. Negative-conductance area in this case is small. When $\theta_1 = \frac{\pi}{2}$, the area a is larger because in this case i_b keeps on reducing from the peak value. If θ_1 is very much smaller than $\frac{\pi}{2}$, the negative-conductance area once again is larger because i_b remains below the peak for most of the cycle and the transition through the negative-conductance region is slow. Fig. 5.5 shows the variation of period $(x_2 - x_1)$ with frequency. Fig. 5.6 shows the behaviour of all these parameters $G'(x_1)$, $G'(x_2)$ and area a when I_b is kept constant and pump frequency μ_p is varied. Fig. 5.7 gives graphs similar to Fig. 5.6 for a range of values of pump current I_b .

From the values of $G'(x_1)$, $G'(x_2)$ and area a , the gain factor A_v can be calculated. Fig. 5.8 gives A_v against pump frequency. $A_m = A_v G_t$ is fairly high at over 16 at a frequency of $\frac{1}{1100}$. At this frequency $G'(x_2) = 0$ i.e. $\mu_p = \mu_{po}$ and the peak of the signal transient appears at the peak of the diode voltage due to the pump current. In this region of frequency close to μ_{po} , A_v is very sensitive to small frequency changes in μ_p ; 10 per cent reduction in pump frequency can cause a gain reduction of nearly 50 per cent.

If the pump frequency is reduced from this value, A_v reduces very rapidly, goes through a minimum and increases slowly with a reduction in frequency. At lower frequencies i_{ego} is very small and is affected to a large extent by small changes in the value of I_b and the other circuit parameters like G_t and the tunnel diode characteristics.

Transducer gain, in addition to the parameters $G'(x_1)$, $G'(x_2)$ and area a is also dependent upon the period $X = \frac{2\pi}{\mu_p}$. Though the factor A_v goes through a minimum (Fig. 5.8) and then increases with a reduction in frequency, the period X increases more rapidly. Transducer gain, therefore, reduces with frequency (Fig. 5.9). Transducer gain rises rapidly near the frequency μ_{po} and is rather sensitive to pump frequency changes.

5.5 Dependence of Gain on Pump Amplitude

If the pump frequency μ_p is kept constant, the parameters $G'(x_1)$, $G'(x_2)$ and area a vary with pump amplitude as shown in Figs. 5.7 and 5.10.

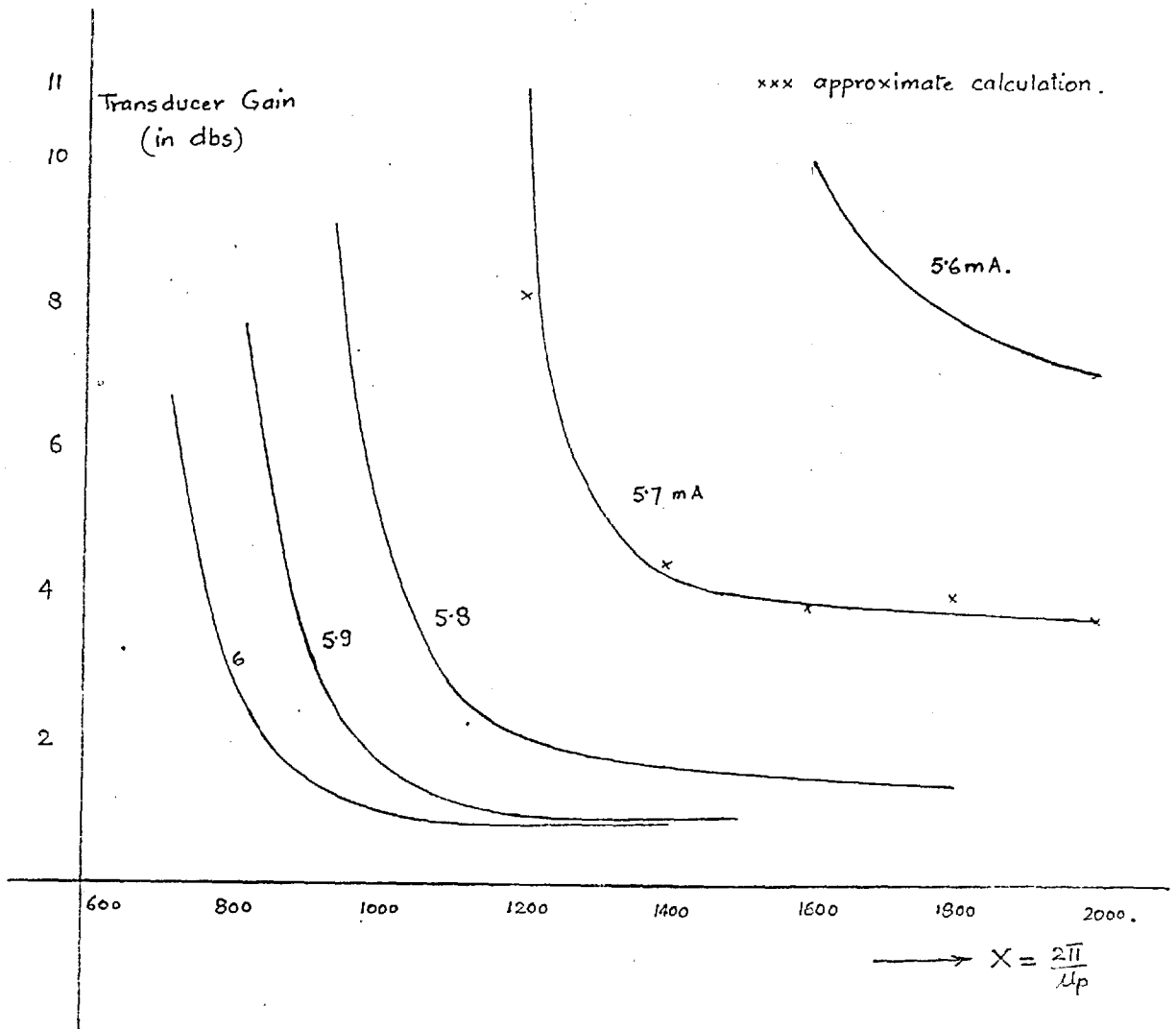


Fig. 5.9. Transducer gain against $\frac{2\pi}{\mu_p}$ (= X)

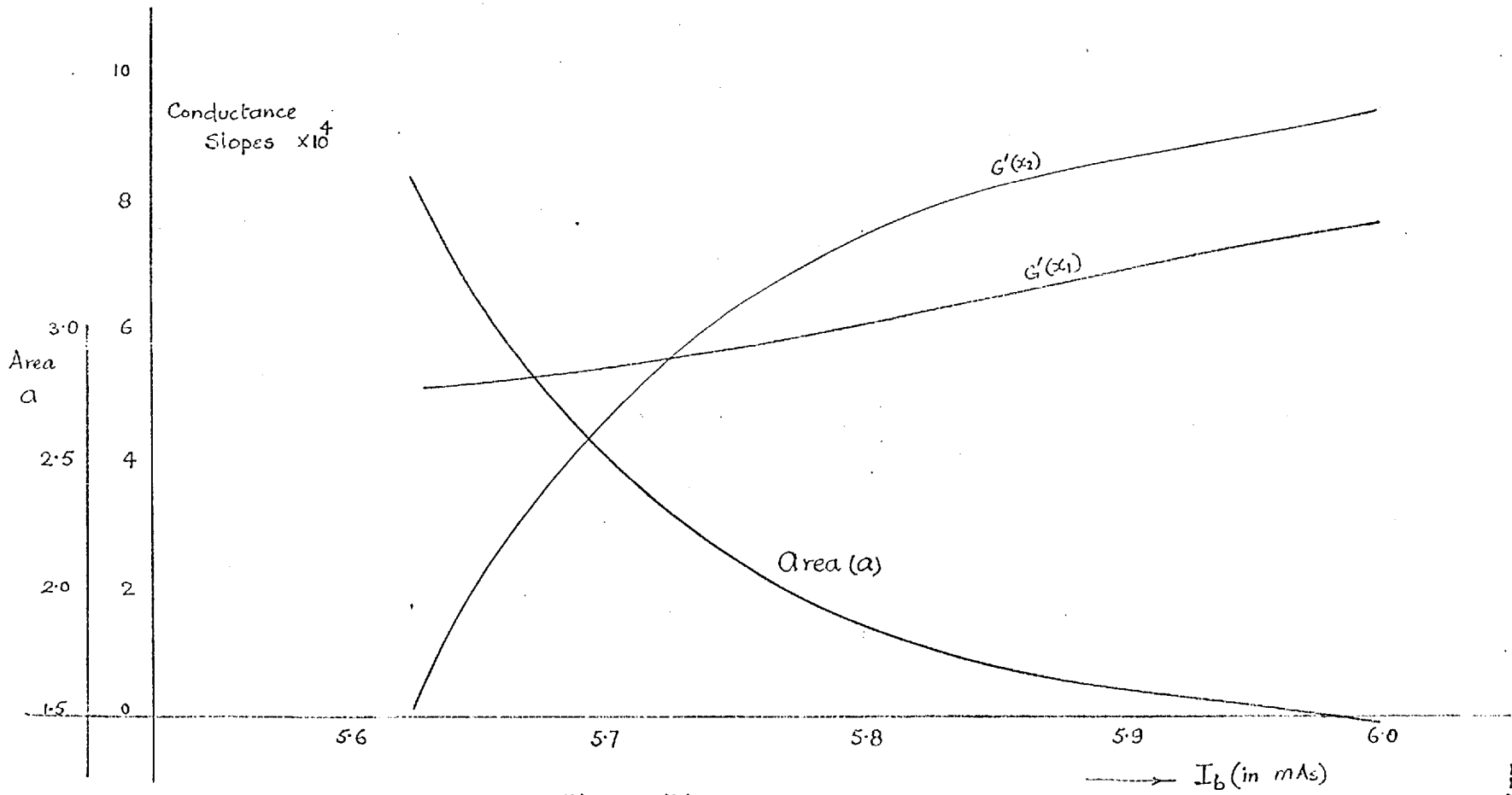


Figure 5.10

Period \times Constant at 1200

The lower the pump current the higher the area a and the lower the factors $G'(x_1)$ and $G'(x_2)$. The lower the pump current higher is the gain of the amplifier.

For each value of I_b there is a corresponding value of μ_{po} where $G'(x_2) = 0$. μ_{po} against I_b graph is drawn in Fig. 5.11. This figure also gives the values of A_m against the pump current I_b at the corresponding pump frequency μ_{po} . The frequency μ_{po} reduces with pump current I_b and the corresponding A_m increases with a reduction in the pump current.

Transducer gain against I_b for different pump frequencies is shown in Fig. 5.12. Transducer gain increases slowly with decrease in I_b for the regions of low transducer gain (of the order of 1db or so). Near the value of I_b for which the frequency μ_p is very close to μ_{po} , gain rises quite rapidly. As discussed earlier this region of operation is very sensitive to any small spurious variations in pump frequency and amplitude.

It should be noted that the transducer gain, at frequencies $\mu_p \ll \mu_{po}$, is higher for lower I_b . But if I_b is made very small, any small change in I_b will modify the amplifier gain by a large amount. For example at a frequency of $\frac{1}{1700}$, an increase of I_b from 5.6 mA to 5.7 mA reduces the gain by 5db, whereas an increase of I_b from 5.7 mA to 5.8 mA reduces the gain by only 2db.

Thus there are two limits between which regenerative amplifier with sine wave pump can work;

1) The transducer gain is very high near the pump frequency μ_{po} corresponding to a given I_b but it is very sensitive to small changes in frequency.

2) The transducer gain can be made very large at frequencies away from μ_{po} by reducing I_b but in this case the gain becomes very sensitive to small spurious variations in I_b .

Fig. 5.13. shows a three dimensional representation of the gain dependence on the pump frequency and amplitude. It will be noted that as I_b is reduced to obtain high gains frequency has to be reduced too. The

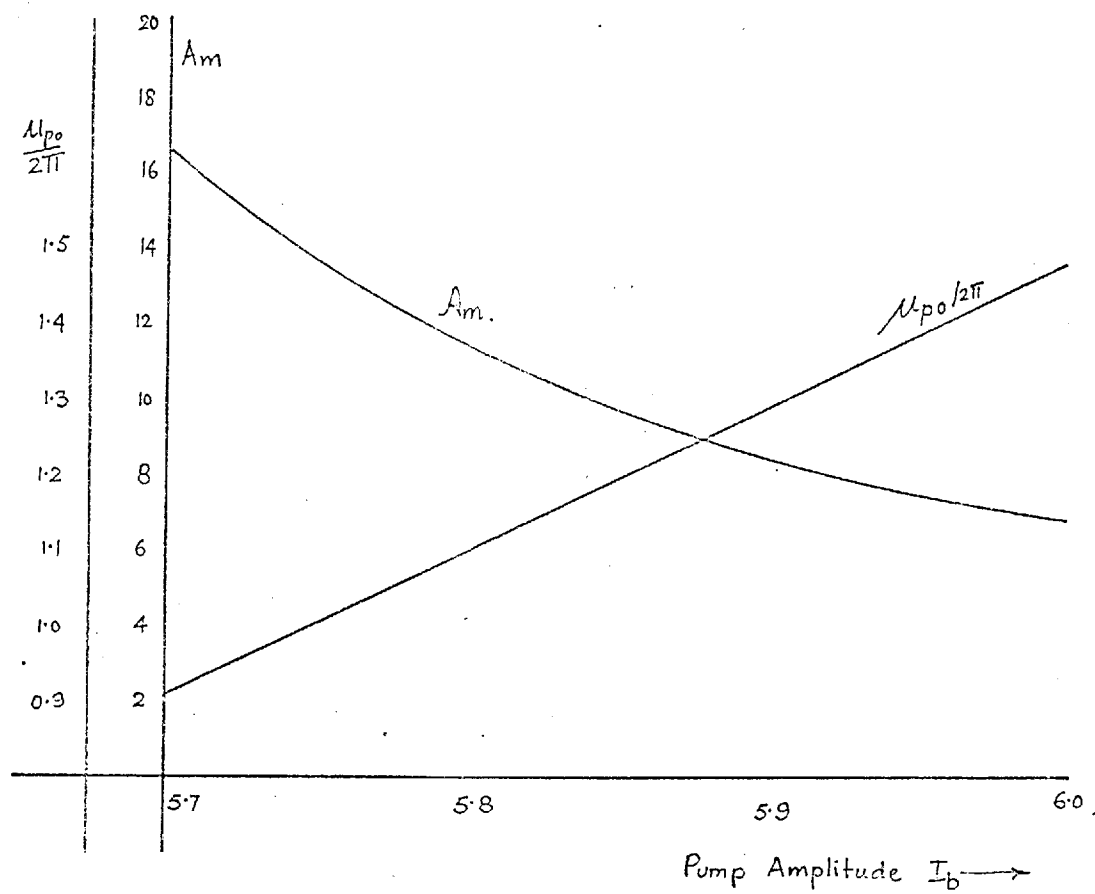


Figure 5-11.

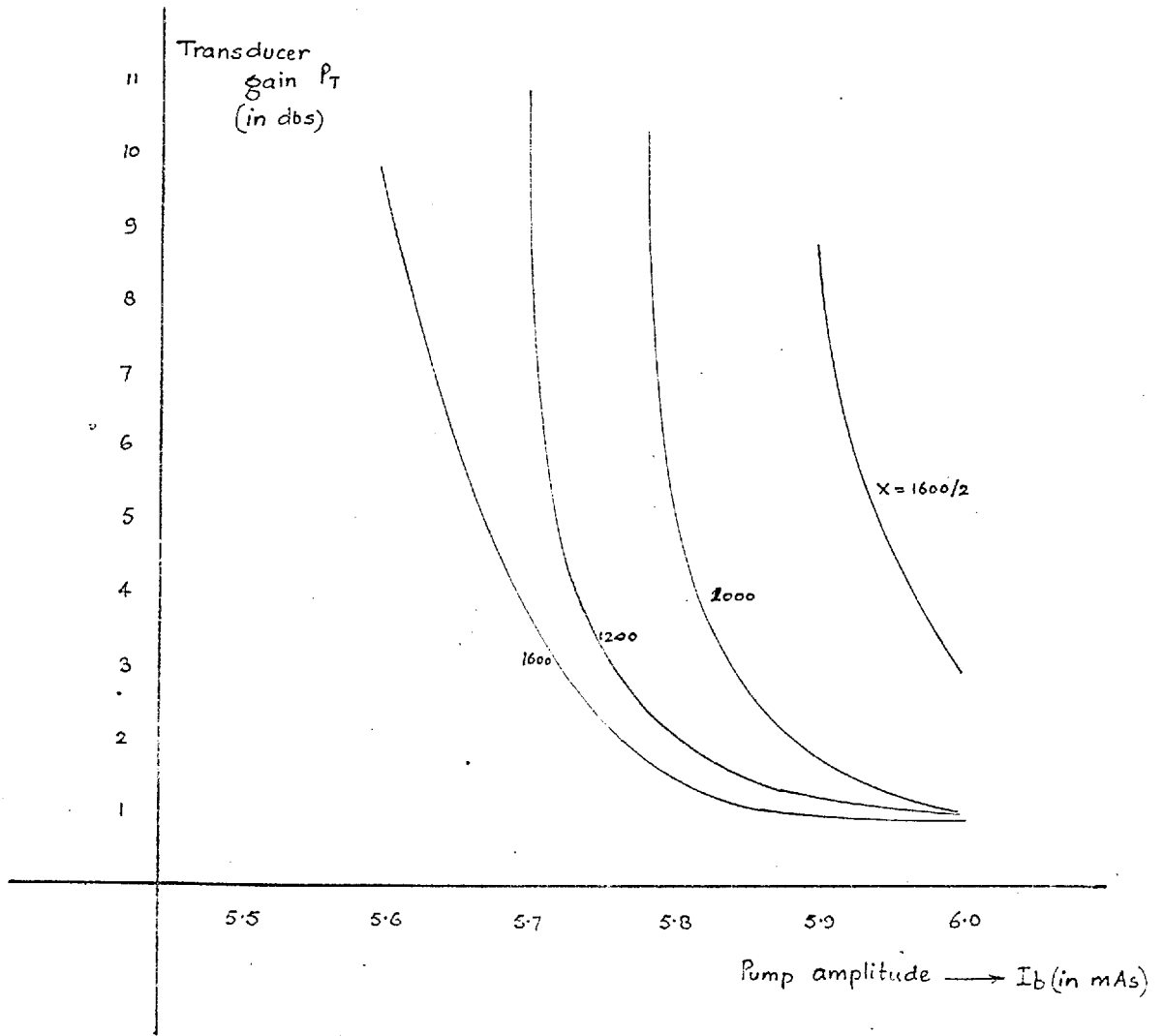


Fig. 5.12.

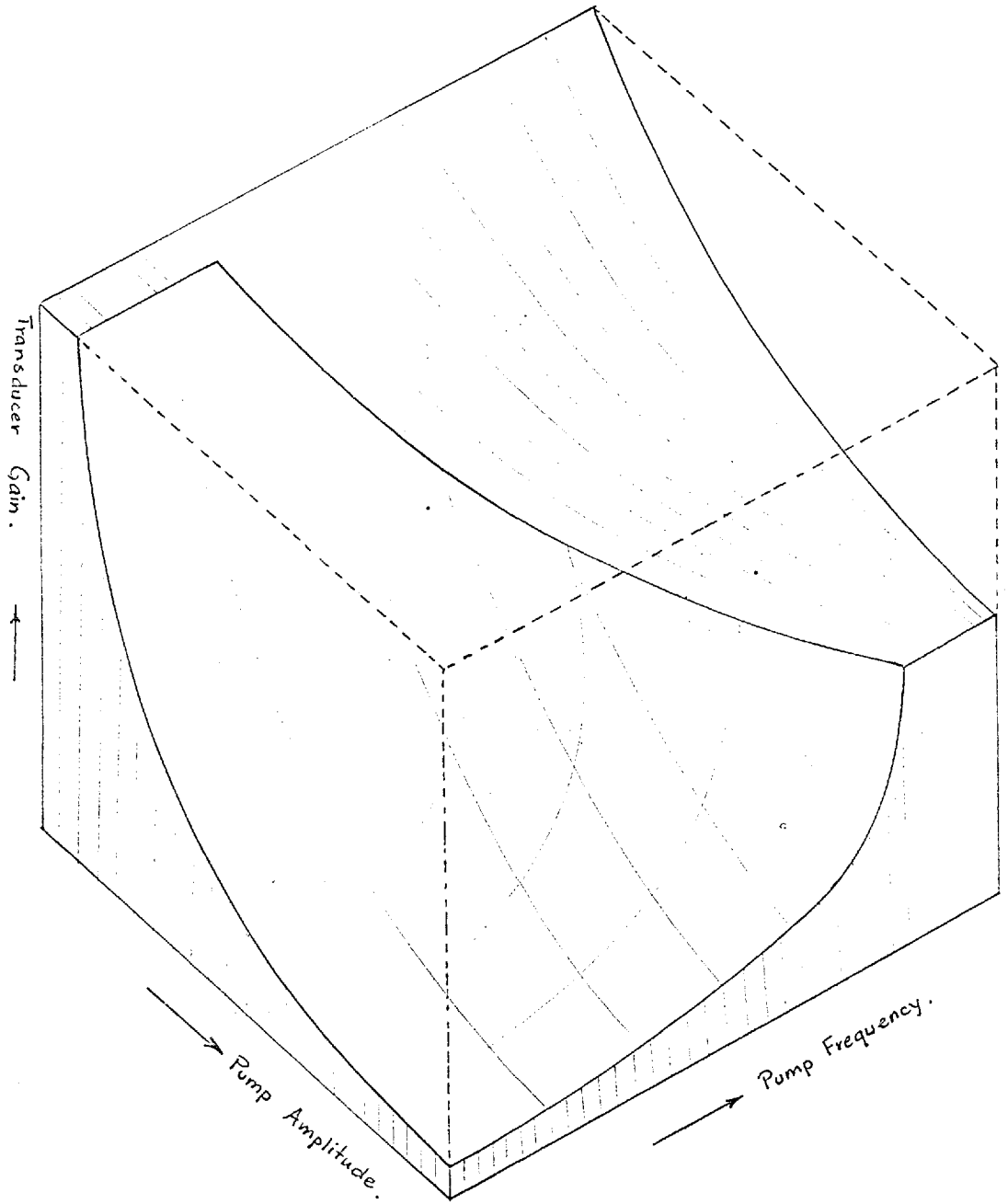


Figure 5-13

limit to this process takes place when I_b is such that the excess pump current i_{ego} tends to zero, in which case gain tends to infinity at a pump frequency very nearly equal to zero,

5.6 Experimental Investigations

5.6.1 Method of measurement

Transducer gain measurements were carried out at low frequencies as well as at the maximum frequency range possible for the diodes available.

The transducer gain in the circuit of Fig. 5.14, can be determined readily by the measurement of voltage gain.

If $G_b \ll G_s + G_L$, we can neglect G_b .

Power delivered to the load $P_o = v_1^2 G_L$

where v_1 is the voltage across the load.

Now Power available from the generator

$$P_{avs} = \frac{I_s^2}{4G_s}$$

If v_s is the voltage across the conductances G_s and G_L in parallel, with tunnel diode out of circuit,

$$P_{avs} = \frac{v_s^2}{4G_s} (G_s + G_L)^2$$

$$\text{Therefore transducer gain } P_T = \frac{v_1^2 4G_s G_L}{v_s^2 (G_s + G_L)^2}$$

$$\text{For } G_s = G_L$$

$$P_T = \frac{v_1^2}{v_s^2}$$

Thus transducer gain in decibels equals voltage gain in decibels.

The voltage input v_s is measured by removing the tunnel diode out of the circuit. Then the tunnel diode is inserted and the pump current and

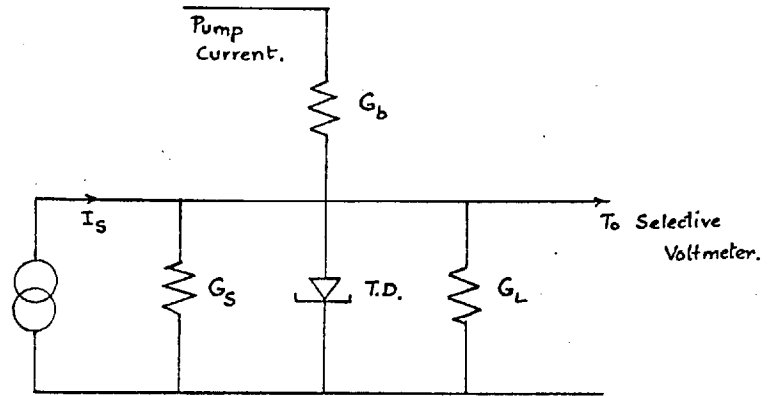


Figure 5.14.

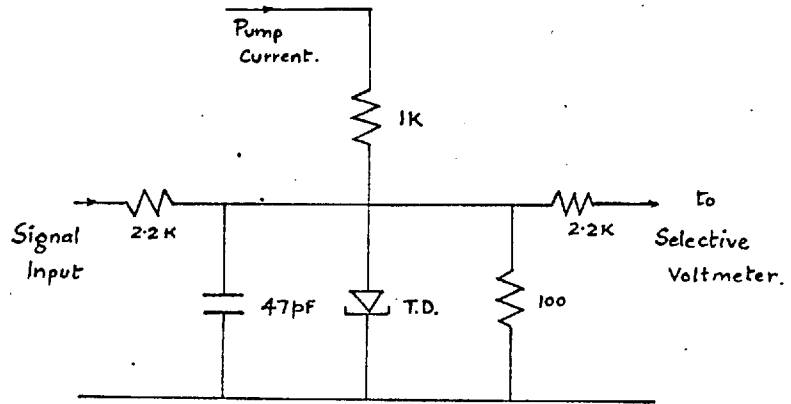


Figure 5.15.

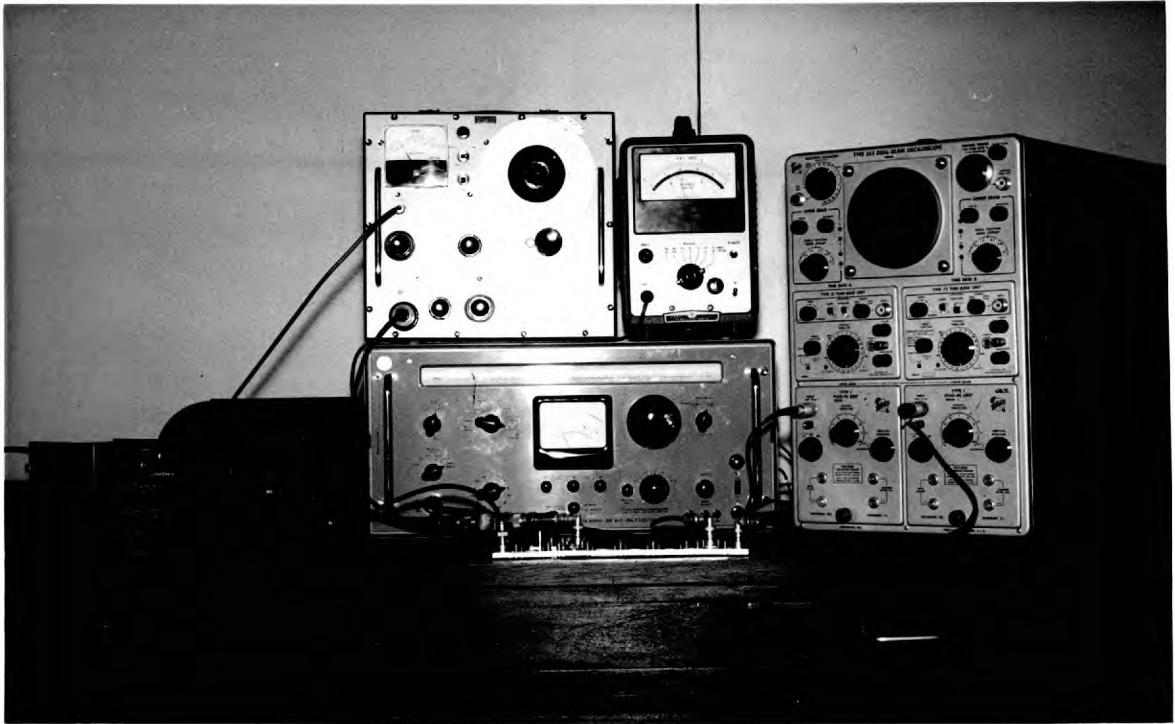


Fig. 5.16 : Experimental Set up for Measurement of Transducer Gain.

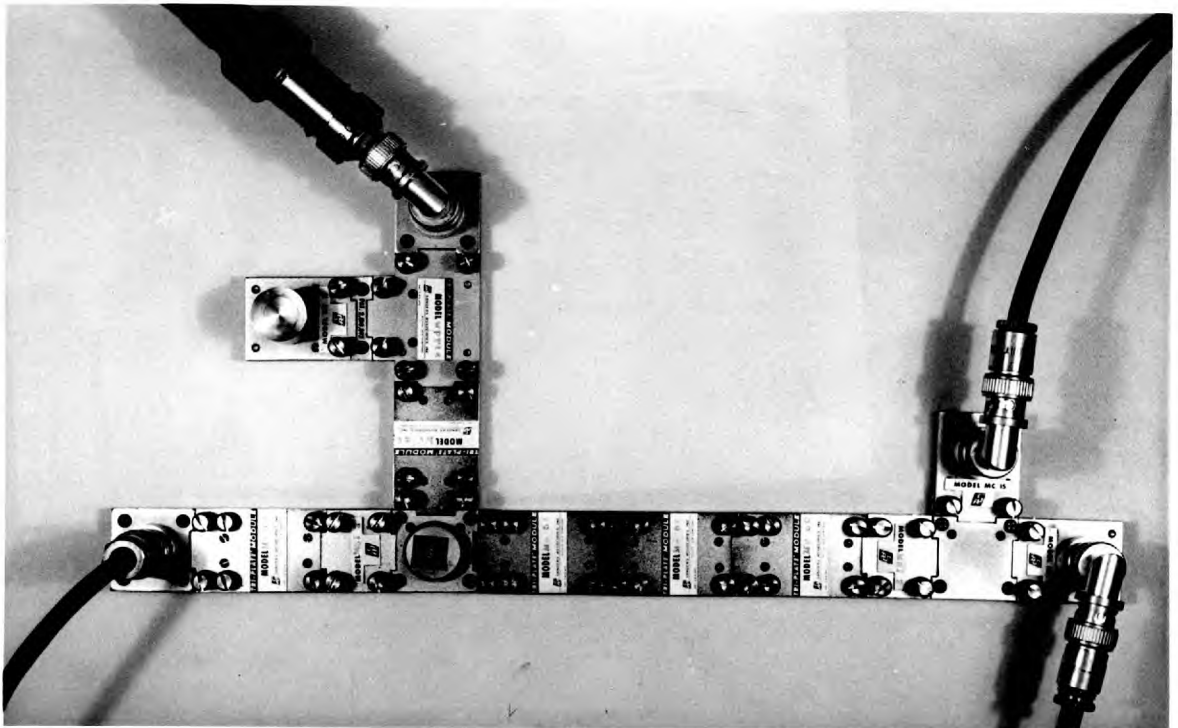


Fig. 5.17 : Strip Line Amplifier used for the Measurements.

frequency adjusted to the specified values. The voltage v_1 can now be measured and transducer gain obtained.

5.6.2 Low frequency measurements

The circuit employed for low frequency measurements was that of Fig. 5.15. Fig. 5.16 gives a pictorial view of the experimental set up. Strip line components were used to construct the amplifier (Fig. 5.17). These components are in the forms of mounts for resistors, capacitors and tunnel diodes. The strip line components were used to keep the lead inductances to a minimum. A regenerative amplifier can be manufactured as a very small integrated unit but in our experimental set up the size of the amplifier is comparably very large due to modular construction.

It is not necessary to use strip line components for the low frequency measurements but they were used for the sake of convenience. The tunnel diode used has a self capacitance of nearly 3pF. and is of a pill type construction. An extra capacitance of 47 pF. was added across the tunnel diode.

$$\text{For } X = 1200$$

$$\begin{aligned} T &= XC = 1200 \times 50 \times 10^{-12} \\ &= 0.06 \times 10^{-6} \text{ secs.} \end{aligned}$$

$$\text{or the pump frequency } f_p = 16.67 \text{ mc/s.}$$

The circuit parameters for this experiment are given in table 5.1. If the performance predicted by theory is to be obtained then the circuit elements must satisfy the condition derived in section 4.5. i.e. $LG(v) \ll R_t C$.

$$\text{Now } L = l_n H \text{ (estimated value).}$$

$$R_t = 100 \text{ ohm.}$$

$$C = 50 \times 10^{-12}$$

$$\therefore R_t C = 100 \times 50 \times 10^{-12} = 5 \times 10^{-9}$$

$$\text{and } LG(v) = 1 \times 10^{-9} \times 0.185 = 0.185 \times 10^{-9}$$

$$\text{where } G(v) = 0.185 \text{ at } v = 0.$$

Table 5.1

$$I_b = 5.7 \text{ mA}$$

$$X = 1200$$

$$G'(x_1) = 5.45 \times 10^{-4}$$

$$G'(x_2) = 4.65 \times 10^{-4}$$

$$A_v = 9 \times 10^2 \text{ (obtained from approximate calculations)}$$

$$C = 50 \times 10^{-12} \text{ F.}$$

$$R_t = 100 \text{ ohms } \left(= \frac{1}{G_t} \right)$$

$$L = 1 \text{ nH}$$

$$G(v) = 0.185 \text{ mhos at } v = 0$$

$$G(v) = -0.035 \text{ mhos at } v = 90 \text{ mV.}$$

∴ this condition is more than satisfied.

If the frequency response of the amplifier is not to fall by more than 10% in the band of signal frequencies of $\frac{\mu_p}{4\pi}$ then the condition 3.29 must be met.

Condition 3.29 is

$$\begin{aligned}\mu_p^2 &< 0.84 G'(x_1), \\ \left(\frac{2\pi}{1200}\right)^2 &< 0.84 \times 5.45 \times 10^{-4} \\ 0.275 &< 4.58\end{aligned}$$

Finally the damping period must be adequate. For this we check the values of circuit parameter in condition 3.38

$$\exp \left[- \frac{G'(x_2)}{2} (dp)^2 \right] = \left[\frac{0.05}{4G_S G_L A_v^2} \right]^{\frac{1}{2}}$$

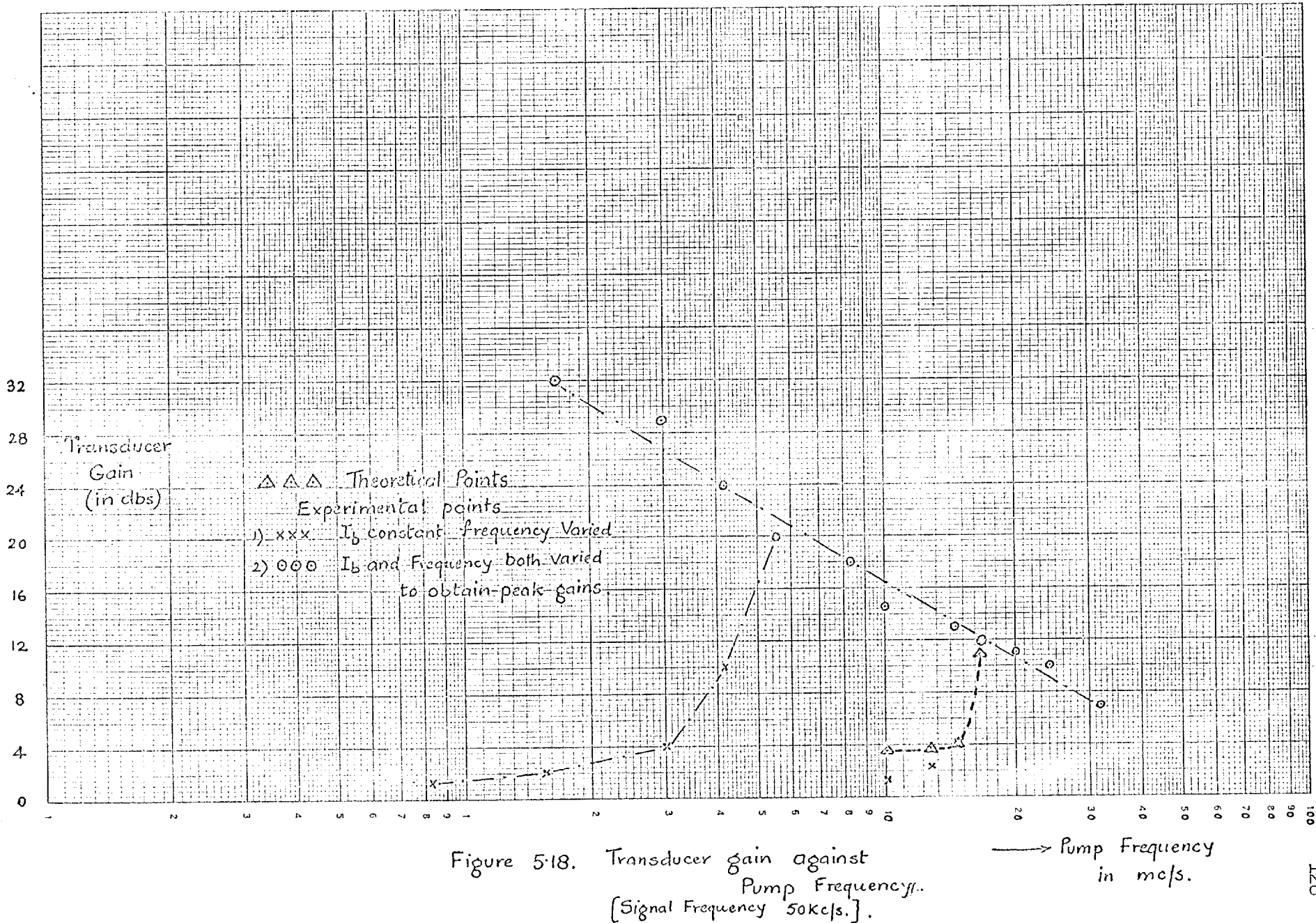
$$G'(x_2) = 4.65 \times 10^{-4}$$

$$G_S = G_L = 0.005$$

$$A_v = 9 \times 10^2$$

∴ $dp = 177$ which is adequately satisfied for the cycle period of 1200. Figs. 5.18. and 5.19. give some of the results obtained from the measurements carried out on the circuit of Fig. 5.15. Two sets of points in Fig. 5.18. for I_b constant are of the same shape as the graphs of Fig. 5.9. High gain points correspond very closely to the predicted results but gain seems to reduce rather more quickly than the predicted results. A likely explanation for this is that when the pump frequency is changed the amplitude changes slightly but this change, which may be as small as 2% of the intended pump current, cannot be easily measured with voltmeters used.

The points on the graph of Fig. 5.18. shown by small circles give the maximum transducer gain that could be measured at the corresponding frequencies when I_b was adjusted to give maximum gain. The trend is as



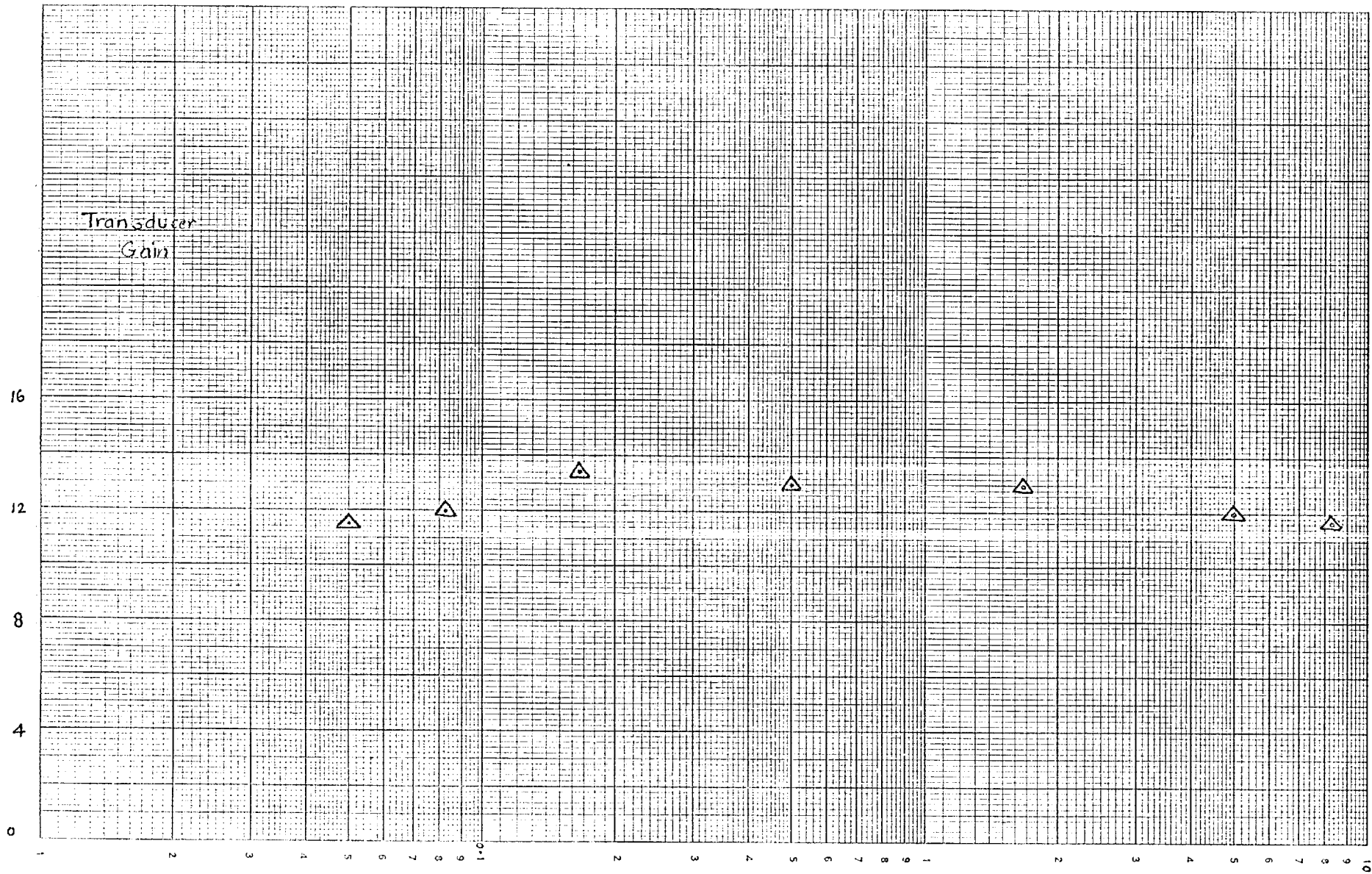


Fig. 5-19 Frequency Response Curve.

Pump frequency = 16.67 m/s.

$V_b = 3.75$ volts.

Signal Frequency in m/s →

predicted; the transducer gain increases if the pump frequency and amplitude are reduced simultaneously (discussed at the end of section 5.5).

Fig. 5.19. shows the frequency response curve. The difference between the maximum and minimum gain in the band is approximately 5 db. This can be caused very easily by very small drifts in pump amplitude and frequency and the measuring equipment and is considered insignificant.

5.6.3 High frequency measurements

The diode employed for measurements at high frequencies has a capacitance of 2.75 pF.

If $X = 1200$

$$\begin{aligned} \text{then pump frequency } f_p &= \frac{1}{1200 \times 2.75 \times 10^{-12}} \\ &= 306 \text{ mc/s.} \end{aligned}$$

The condition $L G(v) < CR_t$ is once against satisfied but not with the same margin as at lower frequencies. In this case $L G(v)$ is comparable with CR_t at $v = 0$ but an order of magnitude less in the negative-conductance area.

$$\begin{aligned} CR_t &= 2.75 \times 10^{-12} \times 100 = 2.75 \times 10^{-10} \\ L G(v) &= 1 \times 10^{-9} \times 0.035 = 3.5 \times 10^{-11} \end{aligned}$$

where $G(v) = -0.035$ and is the maximum negative conductance of the diode.

The experimental set up was similar to the one shown in Fig. 5.15. 47 pF capacitor was deleted and the high frequency measuring equipment was substituted for the low frequency instruments.

Transducer gains of 8-10 db were obtained at signal frequencies of 10, 100 and 150 mc/s.

5.7 Conclusions

Approximate methods of determining the transducer gain and other

circuit properties agree very closely with the accurate computer calculations. At higher transducer gains, the theoretical and measured results are in close agreement but at lower gains there is greater discrepancy between the results.

Very high gains of over 32 db can be obtained if pump current and pump frequency both are reduced. If pump current is reduced such that the excess pump current i_{ego} is very small, the gain of the amplifier is sensitive to the spurious variations of pump amplitude and other circuit elements. The frequency band of amplification is also decreased in direct proportion to the reduction in pump frequency.

Fairly high gains over 10 db can be obtained if the pump current is high and at the same time pump frequency is high but in this case, though the frequency band of amplification rises with the increase in pump frequency, the gain becomes very sensitive to pump frequency and amplitude.

As a compromise, it is possible to obtain gains of the order of 4-10 db without undue restrictions on the circuit tolerances.

A comparison of the performance of regenerative amplifiers with square and sine wave pumps can best be done by studying the following results.

From Fig. 4.15. for $I_b = 5.7$ mA i.e. $i_{\text{ego}} = 0.39$, transducer gain expected is 9 db at $\frac{\mu_p}{2\pi} = \frac{1}{354}$ (if we assume that $X = 2x_2$). If I_b increase ~~from~~ ^{to} 5.8 mA transducer gain reduces by one db. On the other hand if I_b reduces by 0.1 mA to 5.6 mA then transducer gain rises by 2 db.

Now for sine wave pump of amplitude $I_b = 5.7$ mA transducer gain is 11 db at a pump frequency $\frac{\mu_p}{2\pi} = \frac{1}{1200}$ (Fig. 5.9). A small change in frequency from $\frac{1}{1200}$ to $\frac{1}{1300}$ reduces the gain from 11 db to 5.3 db. Thus transducer gain is very sensitive to a change in frequency. Below a pump frequency of $\frac{1}{1400}$ transducer gain reduces very slowly with frequency but it is still very sensitive to a change in I_b . At a pump frequency of $\frac{1}{1700}$ where transducer gain is just under 4db, if pump amplitude I_b changes from 5.7 mA to 5.8 mA gain is reduced by 2 db. On the other hand if I_b is decreased by 0.1 mA to 5.6 mA, transducer gain rises by 5 db to 9 db.

We arrive at two important conclusions from the above discussion.

1) For a given pump current and circuit conditions the frequency band of amplification for sine wave pump is about $\frac{1}{4}$ of the frequency band for square wave pump. This is due to the fact that the time x_1 required for the conductance to reduce from G_0 to zero is considerably larger for sine wave. The time $x - x_2$ is again much larger and is determined by the sine wave period as against the square wave pump where this period can be controlled. The effect of these factors is to reduce the pump frequency for the sine wave pump even though the period $x_2 - x_1$ is the same as in the case of a square wave pump.

2) Under the same conditions of tolerances of the circuit the gain of a regenerative amplifier with sine wave pump is much lower than that with square wave pump.

As mentioned at the beginning of Chapter 4, at very high frequencies, square wave is not as practical a waveform as sine wave. At higher frequencies, square wave pump degenerates into a sine wave pump because of the fact that the rise time of square waves becomes comparable with the pulse width of the square wave. Further, if the square wave is to retain its shape, then it will have to be applied to the tunnel diode through a very large bandwidth network and this is either impractical or too expensive to achieve at very high frequencies. It is realised, therefore, that the maximum potentialities of the regenerative amplifier suggested in this thesis may not be achieved at very high frequencies. Nevertheless, transducer gains of the order of 4-10 db are possible in practice.

CHAPTER SIX6. REGENERATIVE AMPLIFIER STAGES IN CASCADE6.1 Introduction

We have seen in Chapters 4 and 5 that the higher the gain of a regenerative amplifier, the more sensitive it is to small variations in the pump amplitude, frequency, waveform and to small drifts in the circuit parameters. A drop in gain of 50 per cent may be caused by an increase in pump amplitude of 2 per cent. For higher gains, the frequency of pump also has to be reduced and therefore the frequency band of amplification is reduced. It seems likely and promising that by connecting regenerative amplifier stages in cascade, we may be able to increase the gain-bandwidth product of the amplifier without increasing the sensitivity of the amplifier to spurious variations in the circuit conditions.

Tunnel diode is a two terminal device and the amplifiers using tunnel diodes are bi-directional. Regenerative amplifier stages in cascade may be so designed that the first stage is in a quiescent condition when the second stage is in the process of regeneration and so on. This implies delay between stages and at higher frequencies these delays may be obtained by strip line techniques. It seems possible, thus, without any major complication, to achieve the property of unidirectional flow of signal, to increase the gain-bandwidth product over that of a single stage and at the same time preserve the simplicity of fabrication by cascading regenerative amplifier stages.

The analysis of a multi-stage regenerative amplifier multiplies in complexity; the current input to the second stage has a complex waveform which is a combination of the pump waveform and the output of the first stage. If the amplifier is not unidirectional then the effect of feedback must also be considered. The only feasible approach to obtaining an accurate assessment of the properties of a cascaded amplifier seems to be a digital computer solution of the problem. But we shall see in the following sections the number of factors on which the gain of a cascaded amplifier depends is considerable and these factors have conflicting influences. Thus, even

computer analysis would be very elaborate and laborious. It is possible, however, to form some intuitive understanding of a cascaded amplifier based on the knowledge of the regenerative processes in a single stage amplifier.

In this Chapter, we discuss the different types of simple cascading arrangements that seem possible and some practical results are presented to substantiate the general conclusions.

6.2 Considerations for a Cascaded Amplifier

In a manner similar to that for a single stage regenerative amplifier, the gain of a cascaded amplifier will depend upon the conductance slopes $G'(x_1)$ and $G'(x_2)$, and the negative-conductance areas traversed by the individual stages. An additional factor due to cascading is the influence of the coupling between stages. The coupling elements between the stages can be so designed as to fulfill the following functions -

- 1) The gain of the first stage should be as high as possible.
- 2) The signal input to the second stage should be a maximum and so arranged as to produce maximum gain from the stage.
- 3) The amplifier should be unilateralized or what is the same thing the feedback from any stage to the stage preceding it should be minimized.

We consider these three conditions in detail in the following sections.

6.2.1 Maximization of the first stage

The gain of the first stage depends upon the pump amplitude, frequency and waveform, tunnel diode parameters and the total conductance G_t as discussed in Chapter 4. Assuming the cascaded amplifier is unilateral the only parameter of the first stage that is affected by the second stage is G_t . For a maximum gain and a maximum current output from the first stage, the conditions derived in sections 3.9 and 4.12 should be satisfied. These conditions can best be fulfilled by a cascading arrangements such as Fig. 6.1. (Any arrangement with a shunt conductance would involve a loss of gain).

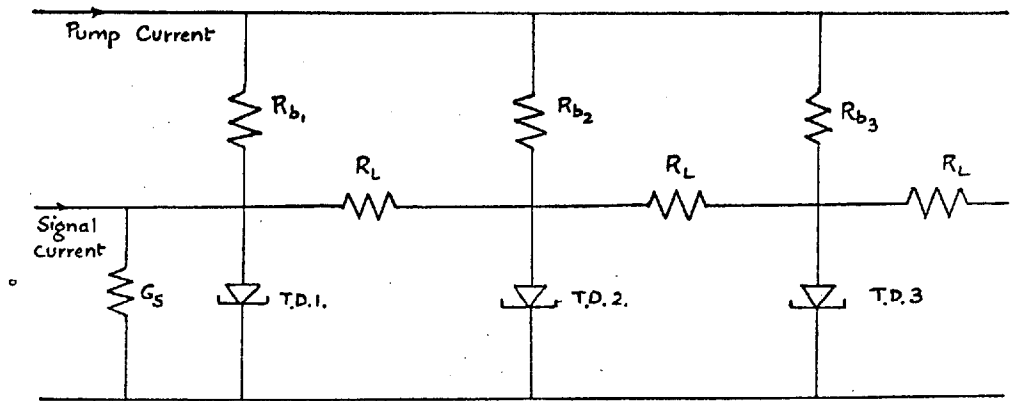


Fig. 6-1. Cascaded Amplifier Circuit

6.2.2 Optimum conditions for the second stage

As we have seen in section 3.5, the sensitivity of a regenerative amplifier to signal is represented by an error curve centered around the point $x = x_1$. The signal output voltage is an error curve with its maximum at the point $x = x_2$ (see section 3.7). These facts apply to all the stages in cascade. If the output from the first stage is impressed on the second stage without any delay between the stages then there is no likelihood of gain from the second stage; at the time $x = x_1$ for the second stage, the first stage signal output will be very low compared with later on in the cycle. Therefore, it is necessary to impress the signal from the first stage when it is at its maximum to the second stage when the second stage is at its most sensitive to the signal input.

Fig. 6.2a shows current output from first stage under the action of a square wave pump of width W . Fig. 6.2b shows current input to second stage due to the first stage and pump current. The pump input to the second stage is delayed. This delay is arranged such that the signal output current is a maximum (at the time x_2 for the first stage denoted by x_{21}) at the point where the second stage is at its most sensitive to signal (at the time x_1 for the second stage denoted by x_{12}).

The delay is, therefore,

$$D = x_{21} - x_{12} \quad 6.1.$$

so that input from the first stage arrives at the second stage a time D earlier than the pump. A schematic diagram of a cascaded amplifier with this delay incorporated in it is shown in Fig. 6.3.

If the two transients follow very nearly the same trajectory then

$$D \approx x_2 - x_1 \quad 6.2.$$

But, unfortunately, this is not the only criterion for the adjustment of the temporal relationship between the cycle of operation of two consecutive stages. Along with signal input to the second stage and its own pump input, there is a current input to the second stage due to the voltage transient of the first stage. The current input to the second stage due to this voltage transient at any time depends on the magnitude of the load

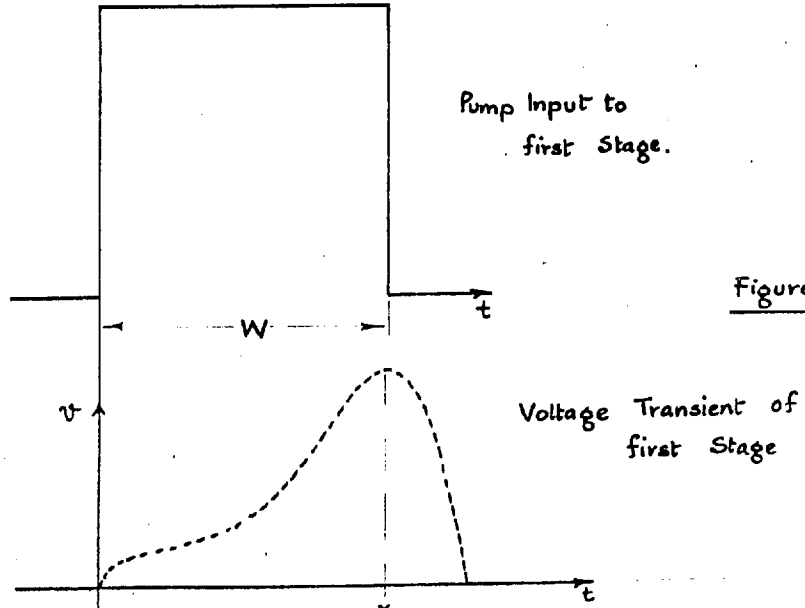


Figure. 6.2 a.

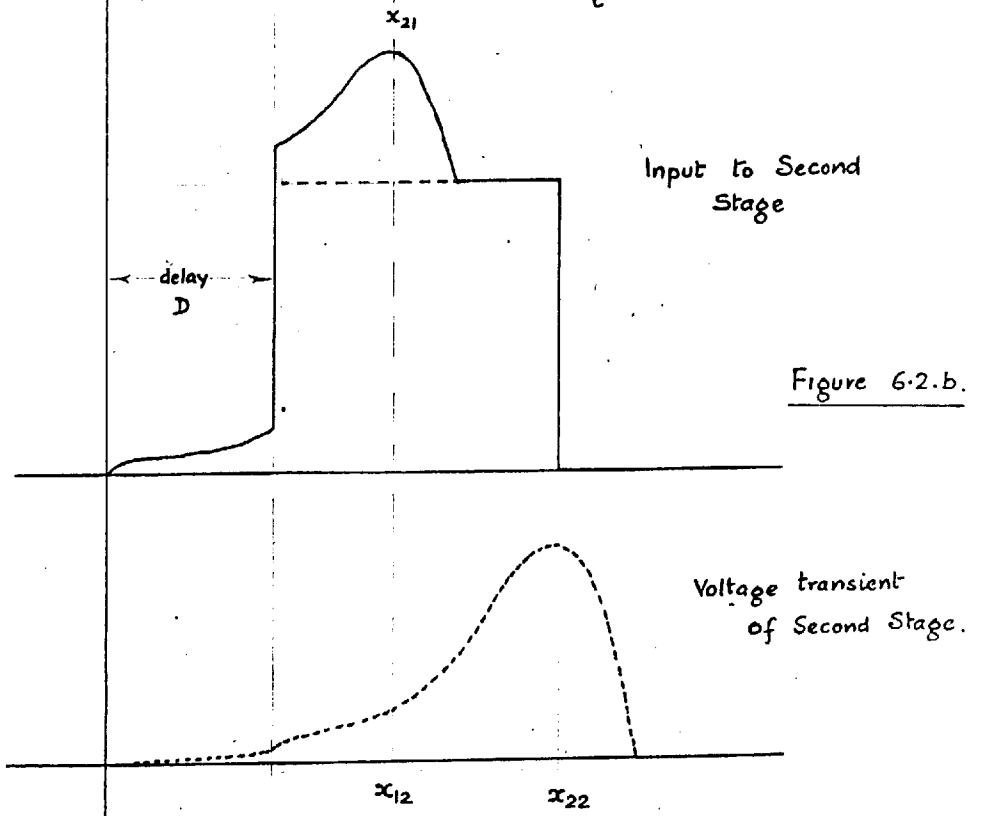


Figure 6.2.b.

$$\text{Delay} = x_{21} - x_{12}$$

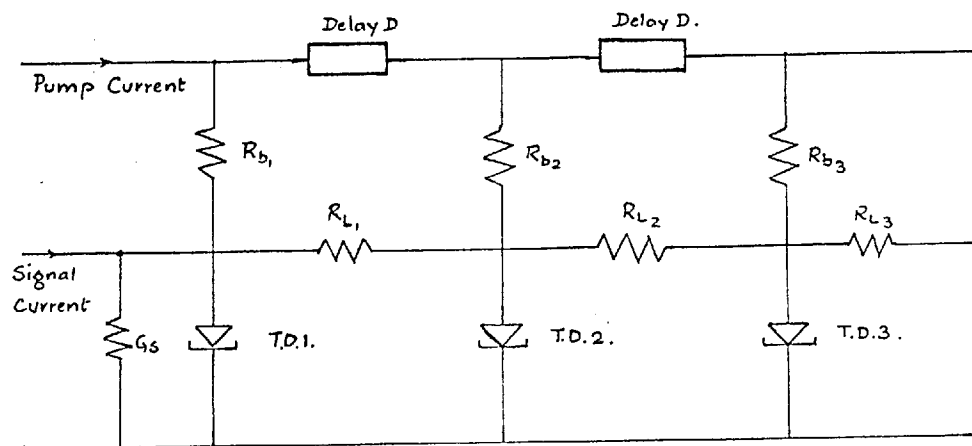


Figure 6.3. Cascaded Amplifier with delay in the pump circuit

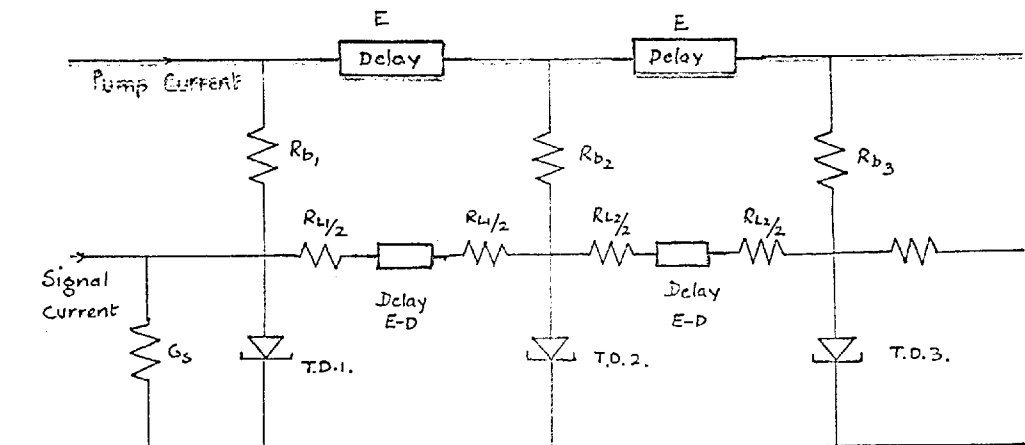


Figure .G.4. Cascaded Amplifier with delay
in the pump and signal circuits.

resistor R_{L1} and the position in time of this transient with respect to the cycle of operations of the second stage. The magnitude of this current can and does modify the voltage transient of the second stage considerably. Therefore the conductance slopes $G'(x_1)$, $G'(x_2)$ and negative conductance area a for a stage after the first are determined by the pump input to it and the input current due to the transient of the preceding stage. In this way it may be that the point of maximum signal output from the first stage has been positioned to coincide with the most sensitive period of the second stage but this may not result in an optimum gain condition because the current input due to the transient of the first stage causes the second stage to switch off very quickly; in such a case the negative-conductance area for the second stage may be very small etc. Hence it is necessary to determine the optimum delay between stages for a maximum gain from an amplifier in cascade. The signal delay D given by equation 6.1 is not the optimum but is expected to be close to it.

The gain of a regenerative amplifier depends upon the excess pump current available at x_1 , during the transition through the negative-conductance area and at x_2 . The excess pump current for the first stage can be controlled to give the performance required from the stage but the excess pump current for the second stage is determined by the magnitude of the input from the first stage and its own pump current input.

If different stages in a cascaded amplifier are to have a degree of insensitivity, above a certain minimum to the spurious variation of the circuit conditions, all the stages in cascade must have their respective excess pump currents during any time in the regenerative period above a certain minimum.

6.2.3 Unilateralization of cascaded stages

There are a number of possibilities in the way tunnel diode regenerative amplifier stages can be cascaded. The most obvious arrangement is to connect identical stages together as in Fig. 6.1. Such a system as discussed in section 6.2.2, is not an optimum one with respect to the gain of the amplifier. Such an amplifier is not unidirectional each stage interacts with every other.

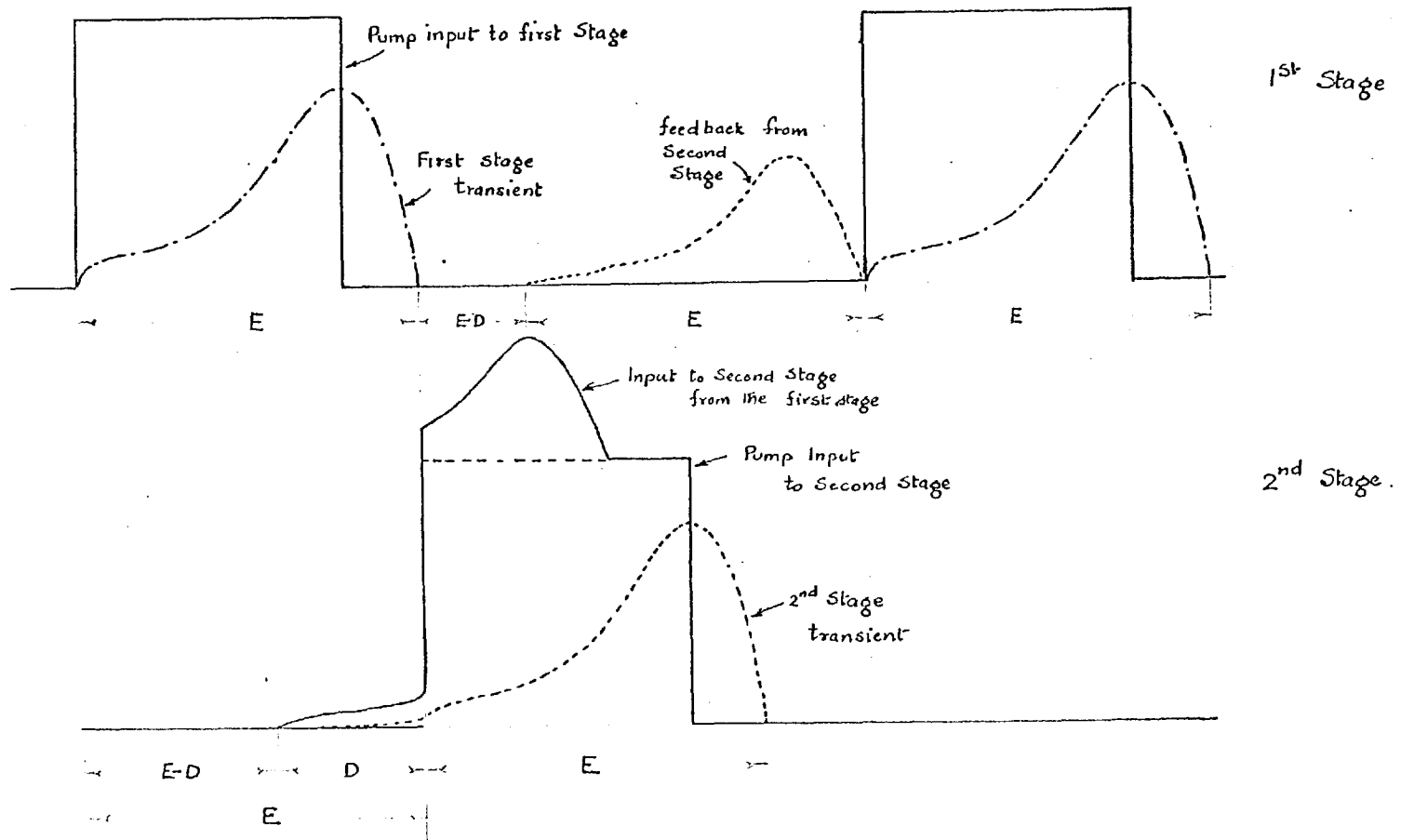


Figure 6.5.

It is necessary, as discussed in section 6.2.2. to introduce a delay between pump current input to different stages to ensure optimum gain conditions. If the delay can also be adjusted such that for any two consecutive stages the first stage is regenerative while the second is not and vice versa then signal flow through the amplifier will be unidirectional. An amplifier which satisfies the condition of optimum delay of section 6.2.2. and is unidirectional, is that of Fig. 6.4. In this circuit there are delay elements in the pump as well as signal paths. The diagram of Fig. 6.5 shows the relative delays in the two paths and their effect on the pump and voltage transients. The second stage pump is applied after a delay E such that first stage has reached the quiescent state. The current input from the first stage is applied to the second stage time D (Equation 6.1) in advance. This figure also shows the part of second stage current that is fed back to the first stage. To ensure that this is ineffective it is necessary that the mark to space ratio of the pump must at least be $\frac{E}{E+E-D}$. Thus we find that to make a unilateralized cascaded amplifier possible we have to increase the period X of the pump pulse. This increase in the period X will give rise to a reduction in the frequency band of amplification and the transducer gain.

6.3 Grading of Diodes in Cascaded Amplifiers

The pump and signal delays have been arranged to make the feedback ineffective; nevertheless, the feedback is present and a significant part of the amplified signal is lost if R_{L1} is comparable with R_{L2} and so on (Fig. 6.4). It seems desirable thus to have $R_{L1} \gg R_{L2}$ and so on. This can be accomplished by grading the diodes, e.g., T.D.1. has $I_p = 1\text{mA}$, T.D.2. has $I_p = 5\text{ mA}$ and T.D.3. with an $I_p = 22\text{ mA}$. As shown in section 4.6, the optimum load resistors in this case will bear an inverse relationship to that of the respective peak currents and if the diode capacitances are in the direct ratio of the peak currents, the pump pulse width required for these stages will be the same.

A further advantage of grading the tunnel diodes in a cascaded amplifier is to increase the signal handling capacity at each successive stage as the signal grows in amplitude.

While grading of diodes in a cascaded amplifier maximises the current gain A_i (see Section 3.9), it is not an optimum system for obtaining a maximum transducer gain. For a maximum transducer gain $R_{L1} = R_{L2} = R_{L3}$ etc. i.e. identical stages in cascade should be used.

6.4 Experimental Investigations

Measurements of gain A_m were carried out to investigate the gain capabilities of regenerative amplifier stages in cascade. The method of measurement was the same as that of section 4.15, i.e. the signal input current was monitored by a Tektronix current probe and the signal output was observed on an oscilloscope as modulation envelope on top of the voltage transients across the load.

6.4.1 Measurements on cascaded amplifier with square wave pump

Going back to the design of section 4.15 for a single stage amplifier, for $I_b = 5.7$ mA $x_2 = 177$. These values are for a tunnel diode with $I_p = 4.7$ mA and $G_t = 0.01$ mhos and therefore for a pump pulse width of 0.4 μ secs

$$C = \frac{0.4 \times 10^{-6}}{177} = 2260 \text{ pF}$$

We use a three stage amplifier with graded diodes. These have peak currents of 1 mA, 4.7 mA and 22 mA. The capacitance values for the diodes and their respective loads can now be calculated (sections 6.3 and 4.6).

For a diode with $I_p = 1$ mA

$$C = \frac{2260}{4.7} = 470 \text{ pF approximately (Section 4.6)}$$

and for a diode with $I_p = 22$ ma

$$C = 2260 \times 4.7 \\ = 0.01 \mu\text{F}$$

The loads will be in the inverse ratios of the peak currents i.e. if R_L for 4.7 mA diode = 100 ohms

$$\text{then for 1 mA diode } R_L = 100 \times 4.7 \\ = 470 \text{ ohms.}$$

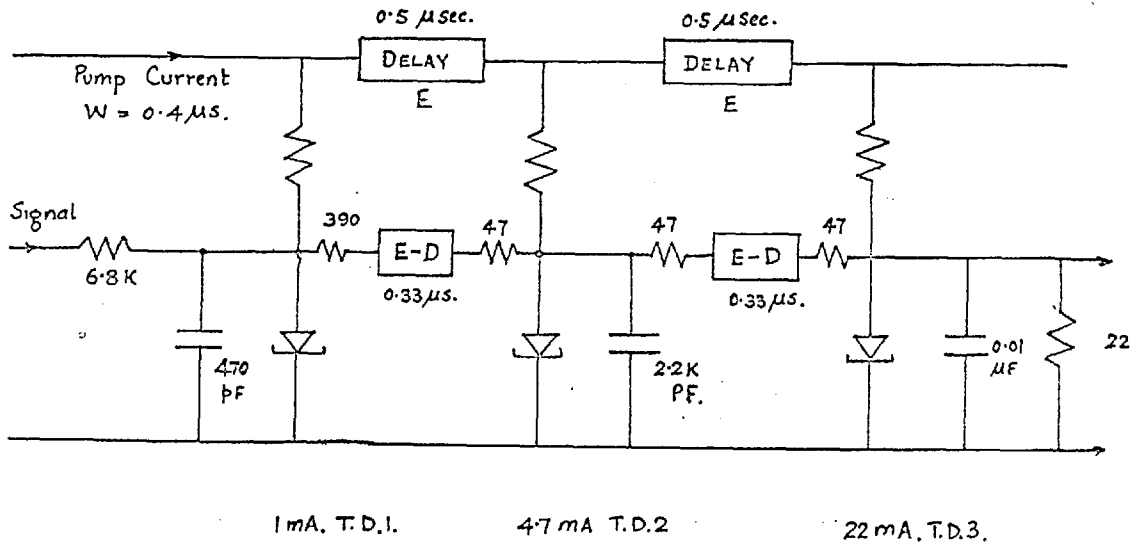


Fig. 6.6: Circuit of Cascaded Regenerative Amplifier.

for 22 mA diode $R_L = \frac{100}{4.7} = 22$ ohms (approximately)

Amplifier was connected together as in Fig. 6.6. The delay $E = 0.5$ μ sec.

$$\text{Delay } D = x_2 - x_1$$

$$\text{Now } x_2 = 177$$

$$\text{and } x_1 = 82 \text{ from Fig. 4.7 for } I_b = 5.7 \text{ mA}$$

$$\therefore D = 95$$

$$\text{or } D = 0.215 \text{ } \mu\text{sec. for } C = 2200 \text{ pF}$$

Delay in the signal path for a maximum gain is expected to be close to it. Optimum delay was found by the following procedure. Delay was adjusted close to the value $(E - D)$ in the signal path and E in the pump path. The pump input to the second stage was adjusted to arrest its voltage transient at voltage v_{x_2} . Then the modulation of the peaks of the transients was measured and compared with the modulation of the peaks of the first stage output.

Delay $(E - D)$ was changed in steps of 0.01 μ sec. till maximum gain was obtained. It was found that the optimum value of the delay in the signal path was very close to the value $E - D$.

Now $E = 0.5$ μ sec. Measured value of optimum $E - D$ was 0.33 μ sec.

$$\therefore \text{Optimum } D = 0.17 \text{ } \mu\text{sec.}$$

which is about 21 per cent lower than the calculated value above.

Once delays have been optimized, the stage gains can be measured. Following were the measured value of stage gains.

Total gain over three stages = 28

First stage gain = 6.34

Second stage gain = 2.5

Third stage gain = 1.8.

6.4.2 Measurements on cascaded amplifier with sine wave pump

A two stage amplifier shown in Fig. 6.7 was used. If $X = 1200$ then

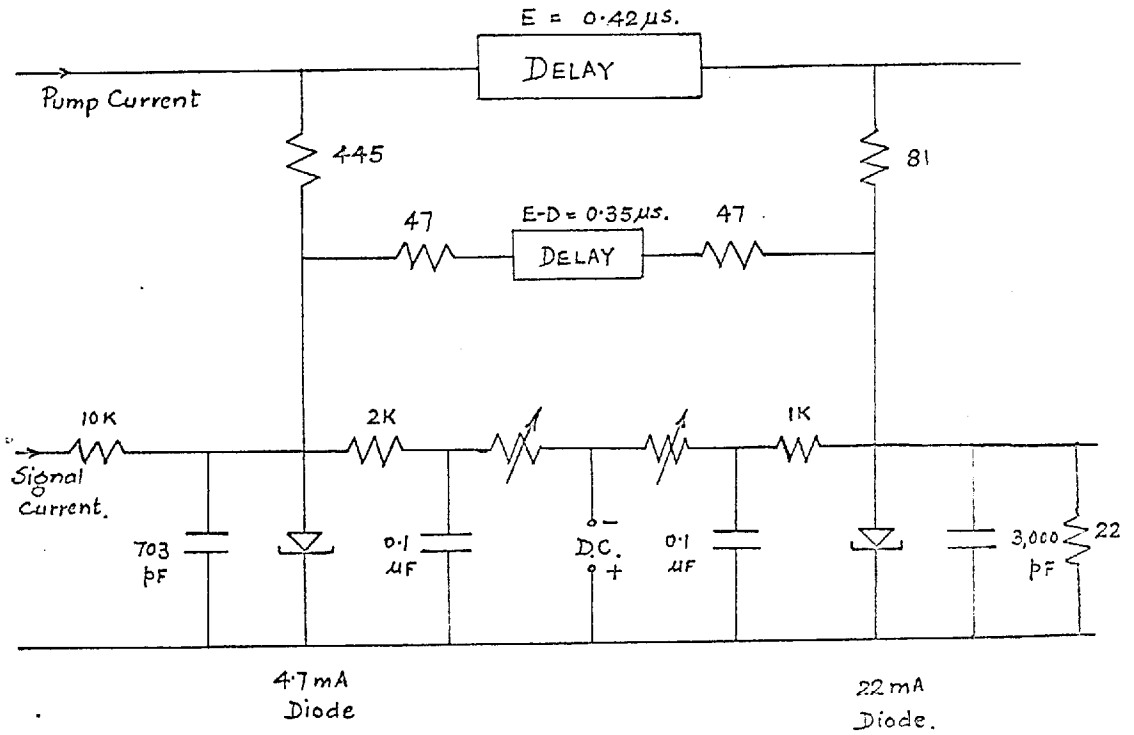


Fig. 6.7: Two stage Regenerative Amplifier
With Sine Wave Pump.

to give isolation between the two stages a mark to space ratio of $\frac{E}{2E-D}$ is required. We assumed D to be small and therefore a mark to space ratio of 0.5 was required.

To achieve this a direct current bias was applied to the tunnel diode so that it would be conducting in the forward direction for only $\frac{2}{3}$ of the period $\frac{X}{2}$.

$$\therefore \text{Sine Wave period} = 1800$$

$$\begin{aligned} \text{or Sine Wave period} &= 1800 \times 700 \times 10^{-12} \\ &= 1.26 \times 10^{-6} \text{ secs} \end{aligned}$$

if C = 700 pF is the capacitance across the circuit conductance;

$$\text{or the frequency of the sine wave} = 873 \text{ kc/s.}$$

Thus delay E is approximately 0.42 μ secs.

$$\text{Now } x_2 = 426 \text{ and } x_1 = 293 \text{ obtained from}$$

$$\begin{aligned} \text{Fig. 5.1. for } I_b &= 5.7 \text{ ma} \\ \text{and } X &= 1200 \end{aligned}$$

$$\begin{aligned} \text{therefore } D &= x_2 - x_1 = 133 \\ &= 0.0935 \times 10^{-6} \text{ secs.} \end{aligned}$$

The delay E - D required in the signal path for maximum gain was found to be 0.35. The optimum value of D is about 25 per cent lower than D given by the equation 6.1.

The following gain figures were measured

$$\begin{aligned} \text{Total gain} &= 10 \\ \text{First stage gain} &= 4 \\ \text{Second stage gain} &= 2.5 \end{aligned}$$

Efforts were made to get higher gains by adding a third stage but gain obtained from the third stage was very nearly unity.

6.5 Conclusions.

The gain contribution of each new stage that is connected in cascade to a single stage regenerative amplifier adds less and less gain as the number of stages increase. Measurements have shown that if significant contribution in gain is to be obtained from each stage in a cascaded amplifier, maximum number of stages in cascade is limited to two or at the most three (with square wave pump only).

The reason for this drop in gain of the later stages compared with the first is easy to see. For the sake of discussion, we assume that identical stages are connected in cascade and the pump waveform is square wave. If gain stability of all the stages with respect to the circuit tolerances is to be maintained constant, current input to each stage at its corresponding time x_1 should be the same. As we have shown by measurements, at the time x_1 for a second stage, the current input from the first stage is a little below its peak value. Thus the current input to the second stage after time x_1 (i.e. in the negative-conductance region) is a rising one (Fig. 6.5). The transition of the second stage through the negative-conductance region is faster than that of the first stage. The negative-conductance area a and hence the gain of the second stage is, therefore, reduced to below that of the first stage.

Similar explanation applies to later stages in the chain but the later stages receive progressively faster rising current input from their respective preceding stages and gain of successive amplifier stages in cascade progressively reduces.

Because of increase in cycle period X required to accommodate the period $2E - D$ between each period E , the frequency band of amplification and the transducer gain for each one of the stages in cascade is reduced approximately to $2/3$ the figure they will produce if each stage was used as a single stage amplifier (i.e. with Mark to space ratio of unity).

CHAPTER SEVEN7. NOISE IN TUNNEL DIODE REGENERATIVE AMPLIFIERS7.1 Introduction

The tunnel diode exhibits shot noise^{11,14,19} in the bias region where the diode static characteristic displays negative-conductance and for diode voltages less than the peak voltage v_p . in the forward conduction region for voltages greater than V_v there is a noise component due to diffusion current²⁴. At very much higher voltages, noise is due entirely to the diffusion component. At very low frequencies the tunnel diode also exhibits $1/f$ noise.

The tunnel diode series resistance R_s contributes thermal noise. The magnitude of this resistance is very small and the noise due to the series resistance does not become important till operation close to the cut off frequency f_r is desired.²⁵

In this work, shot noise is of main interest to us. The tunnel diode voltage transient, for regenerative amplifiers, is restricted to below the valley voltage V_v ; if the transient proceeds to voltages greater than V_v , the transducer gain and the frequency response of the amplifier both deteriorate. Thermal noise due to R_s is again not important because the regenerative amplifier with useful performance must operate at a fraction of the cut off frequency f_r .

In the regenerative amplifier, signal is sampled at the point $x = x_1$ where circuit conductance becomes zero. The signal current present in the circuit at this instant plays the greatest part in the determination of the amplitude to which signal is going to build up before being quenched. It is expected that noise current due to the diode must have the maximum effect at the same instant $x = x_1$.

The signal in a sampling system appears in discrete lines at the sampling frequency and its harmonics (including zero frequency) and the signal modulation appears as side-bands on these lines. The noise energy is distributed throughout the whole spectrum. The highest modulation side-band

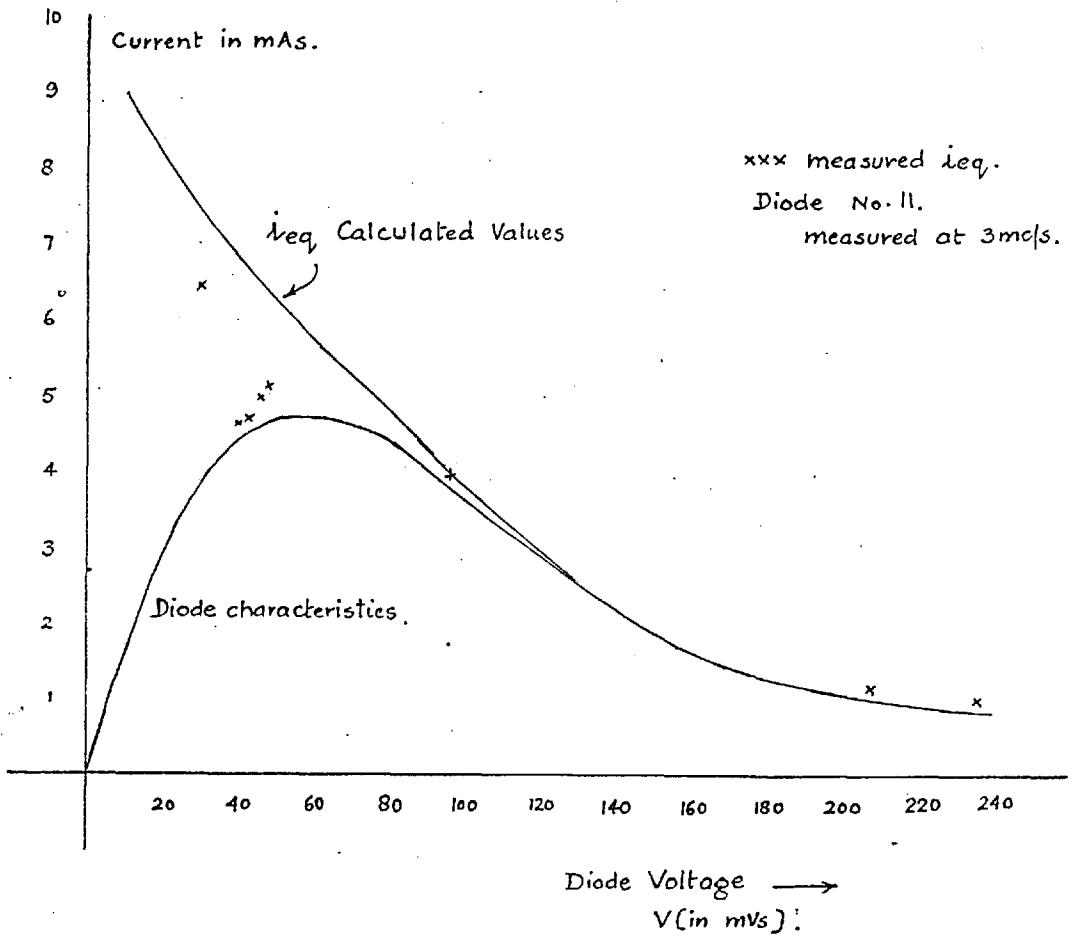


Figure 7.1.

that can be distinguished has a frequency equal to half the pump frequency. It is therefore necessary to restrict the amplifier bandwidth, by means of a suitable filter, so that only the side-bands of a single line are accepted. A low pass filter with bandwidth slightly less than half the pump frequency is thus necessary to avoid any interference from the lower side-bands of the line at the pump frequency. It is assumed in our analysis that this restriction can be implemented and that the output noise bears a linear relationship with the noise around the point $x = x_1$.

A complete and rigorous analysis of the noise in regenerative amplifiers is beyond the scope of this work. As we shall see, the analysis based on the above assumptions gives a very good prediction of results to be expected in practice.

7.2 Shot Noise in Tunnel Diodes

At frequencies much lower than the cut off frequency (the frequency at which the diode's terminal impedance no longer exhibits a negative real part. see Sec. 2.3) the shot noise is the main contributor.

As discussed in Sec. 2.2, following Esaki¹¹, we can assume that there are two current streams flowing across the junction in opposite directions. The net electron current flowing across the junction is the difference between these two current streams (equation 2.3).

For calculation of mean square noise current, we assume that both current streams are uncorrelated. Both of these current stream will then contribute full shot noise and the equivalent saturated diode current for the tunnel diode is the sum of I_Z and I_E (see Sec. 2.2).

If i_{eq} is the equivalent saturated diode current at a diode voltage v and the two opposing current streams are i_Z and i_E at that voltage then

$$i_{eq} = i_Z + i_E \quad 7.1.$$

i_Z and i_E can be determined at a given voltage by the equations 2.4 and 2.5. Therefore

$$i_{eq} \approx i_d \frac{1 + \exp \frac{-qv}{kT}}{1 - \exp \frac{-qv}{kT}}$$

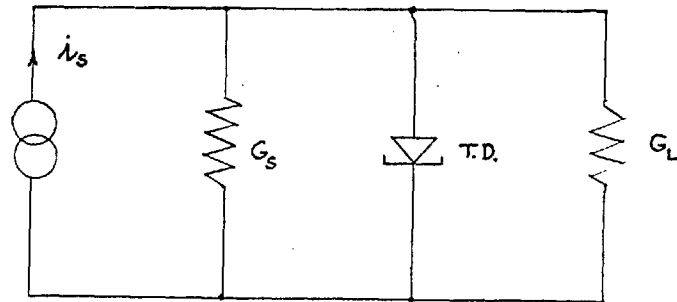


Fig 7.2. Amplifier Circuit

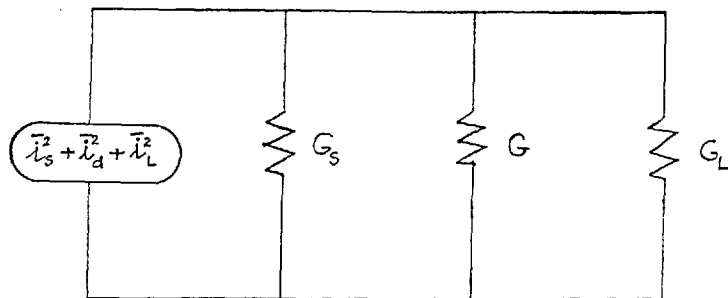


Fig. 7.3. Noise Equivalent Circuit.

where i_d is the diode current obtained from the diode current-voltage characteristics.

This is calculated for the diode characteristics of Fig. 7.1. Fig. 7.1 also gives the graph of i_{eq} against the diode voltage. i_d and i_{eq} approach each other when more than a few times $\frac{kT}{q}$ of bias is applied but $i_{eq} > i_d$ for diode voltage comparable with $\frac{kT}{q}$. i_{eq} was measured by the method outlined in Appendix A.5. The calculated and measured values for i_{eq} agree very well in the negative-conductance region (Fig. 7.1). For diode voltage less than its peak voltage V_p the error is much greater.

7.3 The Noise Figure of Regenerative Amplifier

For a linear negative-resistance amplifier a simple equivalent²⁶ circuit would be that of Fig. 7.2. This circuit is essentially the same as the one for a regenerative amplifier. Fig. 7.3 gives the noise equivalent circuit for the circuit of Fig. 7.2.

The current generators in the equivalent circuit represent the Johnson noise in the conductances and the shot noise in the diode and are given by

$$\overline{i_s^2} = 4 k T_s G_s B \quad 7.2.$$

$$\overline{i_d^2} = 2q i_{eq} B \quad 7.3.$$

$$\overline{i_L^2} = 4 k T_L G_L B \quad 7.4.$$

where T_s and T_L are the absolute temperatures of the source and the load conductances respectively. i_{eq} in equation 7.3 is the i_{eq} at the bias point. B is the bandwidth and k is the Boltzman Constant.

Since all the noise sources are in parallel we arrive at the noise figure simply by taking the ratio of the total mean square noise current to that contributed by source alone.

$$\text{Therefore, } F = \frac{\overline{i_s^2} + \overline{i_d^2} + \overline{i_L^2}}{\overline{i_s^2}} \quad 7.5.$$

where F is the noise factor.

Substituting from equations 7.2, 7.3 and 7.4

$$F = 1 + \frac{T_L G_L}{T_S G_S} + \frac{q i_{eq}}{2k T_S G_S} \quad 7.6.$$

Assuming $T_L = T_S = 290^\circ K.$

$$\text{and hence } \frac{q}{2k T_S} = 20$$

$$\text{Then, } F = 1 + \frac{G_L}{G_S} + 20 \frac{i_{eq}}{G_S} \quad 7.7.$$

This is the expression for the noise figure of a linear negative-resistance small signal amplifier.

In a regenerative amplifier i_{eq} is a function of time defined by the sequence of operation of the bias current of the diode. It is not possible by any simple means other than complicated digital computer calculations to study the transients in a regenerative amplifier in the presence of noise.

To obtain a simple guide to the noise figure of the regenerative amplifier, it is necessary to study the nature of i_{eq} through a cycle of operations. As explained in section 3.5 an input arriving at the point $x = x_1$ has the maximum effect on the circuit transient. The regenerative amplifier is less sensitive to an element of input arriving before or after $x = x_1$. This implies that the noise present at the point $x = x_1$ and hence i_{eq} at $x = x_1$ will determine to a very large extent the noise at the output of the amplifier. Furthermore, i_{eq} against time x (which can be obtained from the voltage against time and i_{eq} against voltage graphs for the circuit) around $x = x_1$ is very nearly linear and a time average of i_{eq} around $x = x_1$ will be equal to i_{eq} at $x = x_1$.

If the input noise is band limited to half the pump frequency then no band overlap or 'aliasing' effects should take place; the input noise at any frequency contributes to output noise at the same frequency and no other. In such a case, there should be a linear relationship between the noise power at the output and the noise power at the input.

If the above conditions are assumed to exist then noise figure of a

regenerative amplifier will be given by the expression 7.7 with the proviso that i_{eq} in this case is that at the point $x = x_1$ (at the voltage v_{x_1}),

$$\text{i.e. } F = 1 + \frac{G_L}{G_S} + \frac{20 i_{eq}(v_{x_1})}{G_S} \quad 7.8.$$

For low noise figures G_S should be as large as possible and G_L as low as possible but these conditions are not compatible with high gain conditions. For $G_t = G_S + G_L$ to be as large as possible and still have a large gain from the amplifier the tunnel diode negative conductance ($-G$) should be as high as possible. At the same time to keep i_{eq} at a minimum the diode should be a low peak current diode. Thus $I_p / |-G|$ should be minimized for the diode to be used in a low noise regenerative amplifier. This is the same condition as derived in section 4.13 for a diode most suitable for high gain amplifiers.

7.4 Measurements of Amplifier Noise Figure

Measurements of noise figure were carried out by two methods:

7.4.1 Noise generator method

The schematic diagram of the circuit is shown in Fig. 7.4. Fig. 7.5 gives the circuit of the amplifier used.

The noise output of the amplifier was noted on the R.M.S. voltmeter. Then noise generator input to the amplifier was increased and the rise in the voltmeter reading noted. If the noise power due to the tunnel diode amplifier can be doubled by the extra noise input from the noise generator then the noise figure of the amplifier is given directly by the noise figure reading of the noise generator. But this was not possible as the source resistance of the noise generator was 50 ohms and this was increased by connecting a resistance of 150 ohms in series to give the required source conductance of 0.005 mhos for the amplifier.

In this case if F_n is the reading on the noise generator then the noise figure of the amplifier will be

$$F = F_n \cdot \frac{\text{Noise generator source resistance}}{\text{Source resistance seen by the amplifier.}}$$

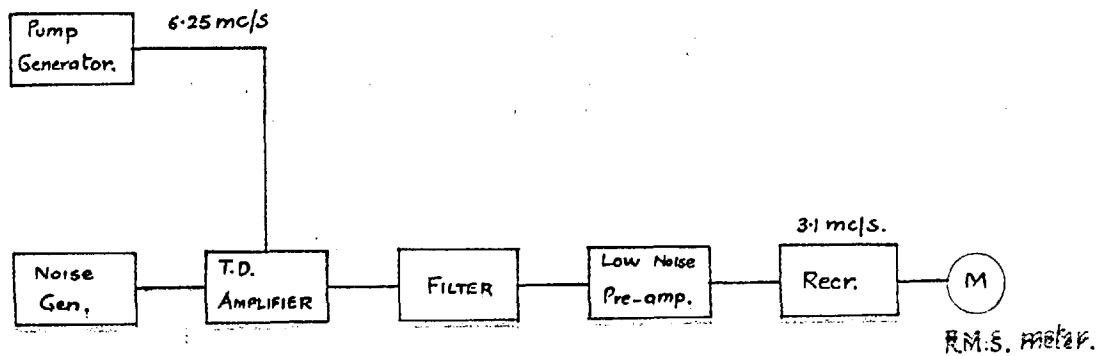


Figure. 7.4

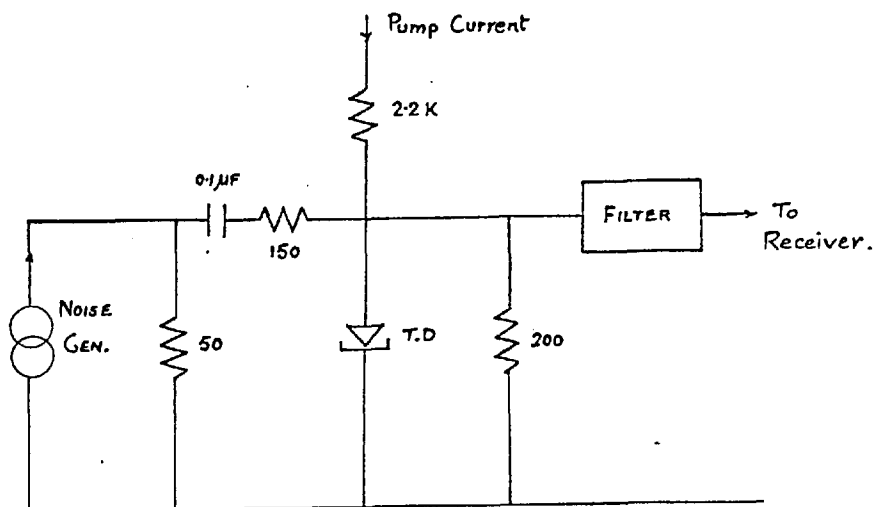


Figure 7.5.

$$= F_n \cdot \frac{50}{200}$$

$$= \frac{F_n}{4}$$

As the amount of noise power from the noise generator used (Rohde and Schwarz) is limited to a noise factor of 33, it was possible to increase the noise power due to the tunnel diode amplifier by only a small fraction.

If M_1 is the reading of the R.M.S. meter due to amplifier noise alone and M_2 is the reading of R.M.S. meter due to the noise of the amplifier and the noise generator then

$$\frac{\text{excess power due to noise generator}}{\text{noise power due to regenerative amplifier}} = P_n = \left(\frac{M_2}{M_1} \right)^2 - 1$$

$$\begin{aligned} \text{Noise factor of the amplifier} &= \frac{F}{P_n} \\ &= \frac{F_n}{4P_n} \end{aligned}$$

For the circuit of Fig. 7.5 following results were obtained

$$\begin{aligned} F_n &= 14.5 & M_1 &= 90 \\ & & M_2 &= 96 \end{aligned}$$

$$\therefore P_n = 0.1377$$

$$\begin{aligned} \therefore \text{Noise factor of the amplifier} &= \frac{14.5}{4 \times 0.1377} \\ &= 26.2 \end{aligned}$$

From the expression 7.7

$$\begin{aligned} F &= 1 + \frac{0.005}{0.005} + \frac{20 \times 5.5 \times 10^{-3}}{0.005} \\ &= 1 + 1 + 22 \\ &= 24 \end{aligned}$$

where $G_s = 0.005$ mhos and $i_{eq} = 5.5$ mA at $v_{x_1} = 64$ mV.
 $G_L = 0.005$ mhos

The measured result is 9.2 per cent higher than the predicted one.

Similar measurements on other amplifiers with different source and load resistances gave results + 10% of the calculated values.

7.4.2 C.W. method²⁷

The noise figure F of a network is defined as the ratio of the available signal to noise ratio at the signal generator terminals to the available signal to noise ratio at its output terminals.

If P_g = Available power from generator.

S = Available signal power at the output.

N = Available noise power at the output.

B = Noise bandwidth of the network.

$$\text{then } F = \frac{P_g}{kTB} (S/N) \quad 7.9.$$

The circuit of Fig. 7.6 was used to carry out the measurements. If the signal input is adjusted to double the noise power at the output then $S = N$.

If A = attenuation

R = source resistance of the signal generator

v = voltage output of the signal generator at the input to the attenuator.

Then substituting the values of P_g , k , T , S and N

$$F = \frac{v^2}{4R AB \times 10^{-21}} \quad 7.10.$$

The tunnel diode amplifier was excluded out of the circuit of Fig. 7.6 and the voltage v_1 required from the signal generator at the input of the filter to show a S/N ratio of unity was determined. Noise figure F_1 of the receiver with the low noise pre-amplifier and filter was then measured by

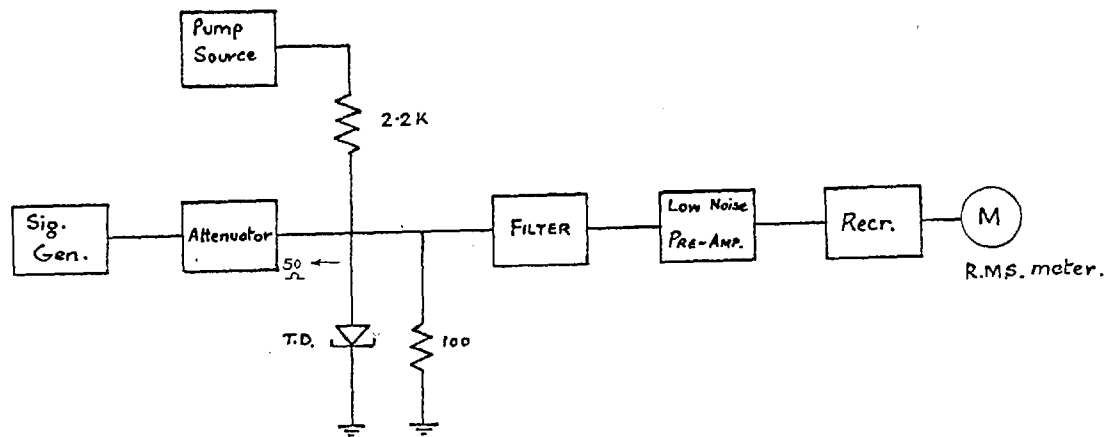


Figure 7.6.

the noise generator method of Sec. 7.4.1.

The tunnel diode amplifier was connected back as shown in Fig. 7.6 and the voltage v_2 required from the signal generator to show a S/N ratio of unity was measured. If F_2 is the noise figure of the tunnel diode amplifier

$$\frac{F_2}{F_1} = \frac{v_2^2}{v_1^2} \quad (\text{From equation 7.10})$$

$$v_1 = 6.8 \text{ mV} \quad F_1 = 2.2$$

$$v_2 = 13.0 \text{ mV}$$

$$\begin{aligned} \text{then } F_2 &= \left(\frac{13.0}{6.8}\right)^2 \times 2.2 \\ &= 8.04 \end{aligned}$$

Noise factor from equation 7.8

$$\text{for } G_s = 0.02 \quad G_L = 0.01$$

$$\text{and } i_{eq} = 5.5 \text{ ma at } v = v_{x1} = 64 \text{ mV (Fig. 7.1).}$$

$$\begin{aligned} \therefore F &= 1 + \frac{0.01}{0.02} + \frac{20 \times 5.5 \times 10^{-3}}{0.02} \\ &= 7.0 \end{aligned}$$

which is about 15% below the measured results.

7.5 Conclusions

An approximate expression for the noise figure of a regenerative amplifier has been suggested. Measurements carried out by the noise generator method of section 7.4.1. give results within 10% of the predicted results. But the C.W. method of Section 7.4.2 shows somewhat greater discrepancy between the measured and predicted results. Nevertheless, the approximation expression 7.8 gives a very good guide to the noise performance of the amplifier.

Noise performance obtained from regenerative amplifier is considerably worse than the typical response of a conventional negative-resistance

amplifier. The noise current which determines the noise performance of a regenerative amplifier is near the peak of the diode current-voltage characteristics whereas conventional amplifier is usually biased to the middle of the negative-resistance region where noise current is less than half that at the peak.

As shown in Section 4.12 transducer gain does not drop very much when G_t is changed from 0.01 to 0.02 mhos. But the noise figure reduces from a predicted value of 24 to 13 (these figures are calculated on the assumption that $G_s = G_L = G_t/2$) if G_t is increased from 0.01 to 0.02 mhos.

Noise figure of a regenerative amplifier can be further reduced by increasing the maximum negative conductance of the tunnel diode and reducing the diode peak current.

No measurements on the noise figures of cascaded amplifiers have been carried out. As discussed in sections 6.4 and 6.5, the first stage of cascaded amplifier gives gains of the order of gain expected from a single stage but the gain of a second stage is reduced to less than half the value of the gain of the first stage. A third stage gives a gain less than the second and so on.

Noise figure for two stages in cascade is given by

$$F_{12} = F_1 + \frac{F_2 - 1}{A_1}$$

where F_{12} is the noise figure of the cascaded amplifier

F_1 and F_2 are the noise figures of the first stage and second stage respectively

and A_1 is the gain of the first stage.

Thus unless the gain of the first stage is very high and the noise figure of the second stage very low, overall noise figure F_{12} will be much higher than F_1 . As we have seen these conditions are difficult to meet because the gain of the first stage is not particularly high and the later stages are going to contribute a noise power comparable with the first stage noise.

For a typical calculation with $G_S = G_L = 0.01$

$$F_1 = 14 \qquad F_2 = 14$$

$$A_1 = 2 \quad (\text{or } 3 \text{ db})$$

$$\begin{aligned} \therefore F_{12} &= 14 + \frac{13}{2} \\ &= 20.5 \end{aligned}$$

Thus the noise factor is considerably worsened by cascading.

The actual situation is not so simple as this because unless the signal input to the second stage is band limited to half the pump frequency there will also be noise due to conversion products of the side bands of the lines at higher harmonics of the pump frequency which will fall into the frequency band of amplification.

CONCLUSIONS

A new mode of regenerative amplification has been proposed and it has been shown to be feasible in practice. A general and detailed analysis has been carried out for such an amplifier. The analysis is not restricted to any one particular active device; the requirement of such an amplifier is that a conductance function of the type assumed in Chapter 3 should be seen by the signal to be amplified.

The simple and general mathematical expressions obtained are then applied to regenerative amplifiers using tunnel diodes as active devices. The performance of tunnel diode regenerative amplifiers is studied for practical pump waveforms like square and sine waves. Some approximate methods for the evaluation of conductance functions, due to these pump waveforms, have been suggested. These methods are shown to give results which are in close agreement with the accurate calculations and the measurements carried out on amplifiers.

Gain and frequency response characteristics of such amplifiers using tunnel diodes are dependent on the various circuit parameters like load conductance, tunnel diode characteristics, pump waveform, frequency and magnitude. From the detailed consideration of these factors, we arrive at the following conclusions regarding the circuit parameters.

1. Load and Source Conductances. To obtain a maximum gain from regenerative amplifier there is an optimum value for the sum of these conductances. If maximum transducer gain is desired then the load conductance should be equal to the source conductance. If maximum current gain is desired then source conductance should be zero and load conductance equal to the optimum value mentioned above for the sum of source and load conductances.

2. Tunnel Diode Characteristics. An ideal tunnel diode would, for maximum gain, have a current-voltage characteristic with a broad peak region. Its negative conductance should be as high as possible for a

given peak current; i.e. the factor $\frac{I_p}{|G|}$ should be a minimum. While the former could reduce the frequency band of amplification the latter has very little effect on frequency response and is, therefore, more useful parameter to maximize.

3. The Pump Current. It is shown that lower the pump current, (as long as excess pump current is greater than zero) the higher is the gain of regenerative amplifier and at the same time lower is the frequency band of amplification.

We find that there are rather serious limits placed on the maximum gain that can be obtained in practice, due to the considerations of circuit tolerances.

It has been demonstrated that regenerative amplifier with square wave pump has considerable advantages over that with sine wave pump. The period required to complete a full cycle of regeneration and damping is shorter because less time is needed to traverse positive conductance regions. The closer the positive - conductance areas of the conductance - time graph balance the negative-conductance area (and at the same time satisfy the conditions 3.20 for period t_1 and the condition 3.38 for damping period) the higher is the transducer gain that can be expected from the amplifier. Under the same conditions of gain stability with respect to circuit tolerances, tunnel diode regenerative amplifier with square wave pump gives higher gains than regenerative amplifier with sine wave pump.

As the time required to complete a cycle of regeneration with square wave pump is about a third or a quarter of that with sine wave pump, regenerative amplifier with square wave pump makes a better use of the high frequency capabilities of tunnel diodes. The maximum frequency of amplification with sine wave pump using the presently available diodes seems to be of the order of 250 to 300 mc/s. The same diode can be operated up to over 1 kmc/s for square wave pump and up to 10 kmc/s for linear negative-resistance amplifiers.

Unfortunately square wave pump is neither easy to generate nor to apply at higher frequencies and the maximum potentialities of regenerative

amplifier may not, therefore, be realized in practice.

Other main restriction on the maximum frequency of pump current and hence the maximum frequency of amplification is due to the diode capacitance. But a reduction in diode capacitance does not produce an improvement in the performance of regenerative amplifier relative to the performance of non-regenerative negative-resistance amplifier.

If it is possible only to minimize the diode capacitance and the diode negative conductance can not be increased at the same time, the extended frequency capabilities of the diode may be of little use for the condition $LG < R_t C$ may not be satisfied. There is a limit to the minimum value of L than can be achieved by conventional means and it may be necessary to resort to solid state circuit techniques. With the conventional techniques the condition $LG < R_t C$ may be satisfied with some effort for regenerative amplifiers with pump frequency of around one kcm/s. Nevertheless, useful performance, even though not as promising as at lower frequencies, may still be obtained at frequencies above 1 kcm/s.

Noise performance of the regenerative amplifier is considerably worse than non-regenerative negative-resistance amplifiers; noise figures of the order of 10 db are obtainable for regenerative amplifiers compared with 6 db or better from negative-resistance amplifiers. The noise current for the regenerative amplifier is that near the peak of the current voltage characteristic whereas the non-regenerative amplifier is usually biased to the middle of the negative-resistance region where noise current is less than half that at the peak.

Noise figure of the regenerative amplifier can be reduced substantially if the ratio $\frac{I_p}{|-G|}$ is minimized. Once again this will not result in an improvement relative to the performance of a conventional negative-resistance amplifier.

It was expected that it will be possible to cascade regenerative amplifier stages to obtain higher gains. Some practical results have been given on the performance of cascaded amplifiers. The gain of the amplifier stages in cascade progressively reduces from stage to stage

and more than three stages in cascade produce very little extra amplification to that for three stages. Even the third stage in a three-stage amplifier does not have high enough gain to justify its use and therefore, for useful performance number of stages in cascade is restricted to two.

The form of output from one stage to another is such that the analysis of a multistage amplifier seems inordinately complicated and has not been attempted.

Unless first and subsequent stages in a cascaded amplifier have high enough gain figures, noise figure of the amplifier is expected to be considerably worsened by cascading.

Although as proposed at the outset, a unilateral multistage regenerative amplifier can be constructed, in practice gain figures achieved were disappointing and noise performance is expected to be even more so.

In this thesis, the author has proposed and shown the feasibility of a new type of regenerative amplifier. Using available components a wide band amplifier with useful gains is shown to be possible. It is disappointing in that the inherent advantages of tunnel diode are not exploited to their utmost. It is not inconceivable though that tunnel diode with smaller band gap materials (this will result in lower $\frac{I_p}{G}$ ratios) will be fabricated and an amplifier with wider bandwidth, higher gain figures, and lower noise may eventually be made possible.

This type of regenerative amplifier can be used as broad band amplifier or can be used for applications where it is required to sample a signal at high frequencies and amplify it at the same time.

Some parts of this thesis have more general applications. The tunnel diode switching analysis in general, and the approximate techniques developed for the sine wave pump (section 5.3) in particular should find use in tunnel diode logic circuit design.

Suggestions for Further Study.

It has been shown that gain and frequency response of the proposed regenerative amplifier can be optimized with respect to circuit parameters and amplifiers using practical and well known waveforms of square and sine waves have been studied. But no explicit study, to determine an optimum pump waveform, has been attempted.

An ideal pump waveform which will produce higher gains and wider frequency band of amplification may be that of Fig. C.1. This pump waveform has a fast leading edge and rises to very high magnitude such that the period t_1 is reduced to a minimum (consistent with the condition 3.20). As the circuit approaches the time t_1 , (when circuit conductance changes from positive to negative) the pump is reduced in magnitude so that just enough excess pump current is present to keep the circuit tolerances within reasonable limits. After this the excess pump current throughout the negative-conductance region is kept nearly at the value of excess pump current at $t=t_1$ (i.e. it is equal to i_{ego}). As the circuit current is reducing while tunnel diode voltage goes through the negative conductance area so is the pump current to obtain nearly constant value of i_{ego} and hence a large negative conductance area. At the end of negative-conductance area the amplified signal is damped back to the input level in the minimum period necessary to satisfy condition 3.38 and the next cycle then commences. This pump waveform will result in a maximum negative-conductance area and just sufficient positive conductance area. In this way high gain and high frequency operation could both be achieved.

Further investigation in the determination and generation of optimum pump waveform for regenerative amplifiers is recommended.

It has been shown at different stages through this work that gain of regenerative amplifier may be very sensitive under some conditions to small changes in circuit parameters. A full study of the gain-bandwidth capabilities of regenerative amplifier in relation to the allowable circuit tolerances is suggested as another field for further useful investigation.

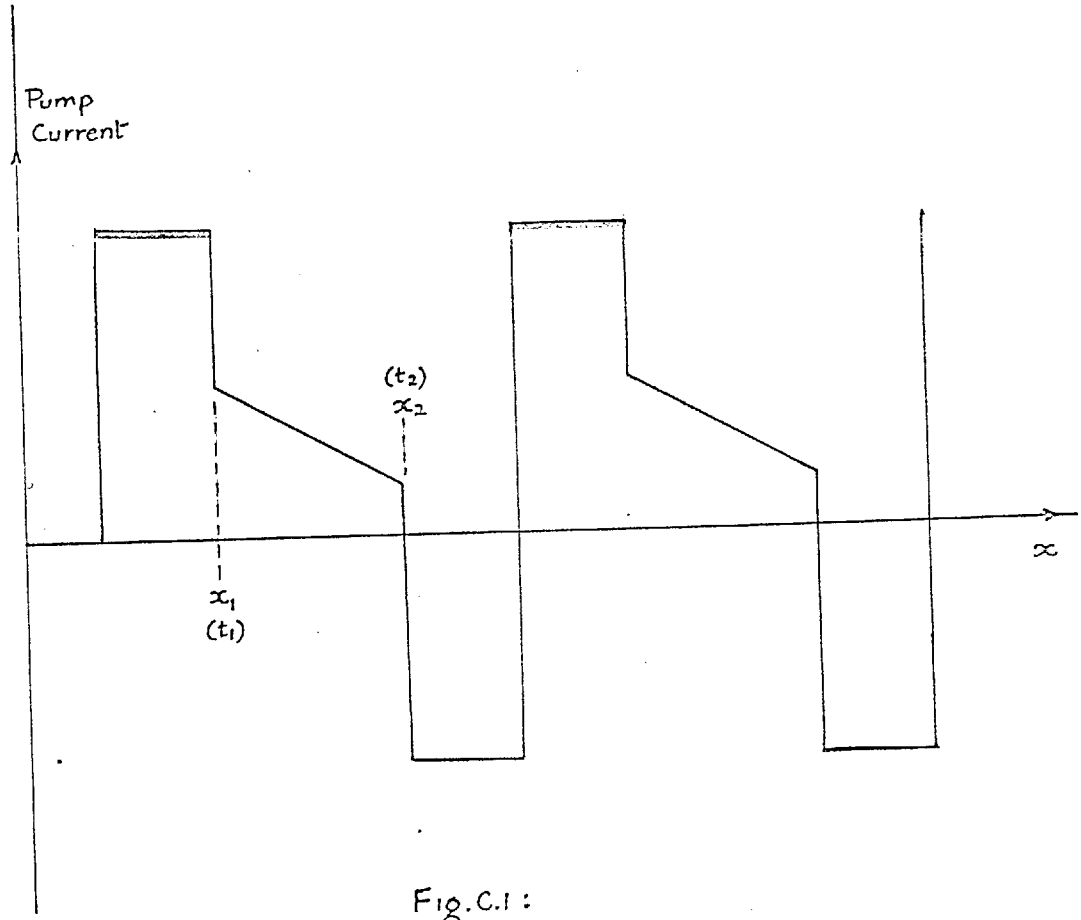


Fig.C.1 :

This thesis presents a very simple expression for noise figure of regenerative amplifiers. This expression has been demonstrated to predict the results to be obtained in practice to within 10 to 15 per cent. However, no rigour or precision is claimed for the expression obtained. An accurate study of noise in regenerative amplifier is suggested.

In the study of noise in regenerative amplifier only the noise contribution from tunnel diode and the associated circuit conductances was considered. The noise that may be injected into the amplifier by the pump source along with the pump current has been completely excluded from our discussion. It should be of great benefit to evaluate the effect of noise contributed by the pump source.

Some practical results have been presented in Chapter 6 on the performance to be obtained from regenerative amplifiers in cascade. Some conclusions on the performance of cascaded amplifiers have also been given. These conclusions are qualitative and have been based on our knowledge of the regenerative processes in a single stage amplifier. An analysis of cascaded amplifiers was considered outside the scope of this work. A considerable improvement in the performance of cascaded amplifiers may be achieved if optimization of such amplifiers is considered in detail.

The regenerative amplifier proposed in this thesis is a sampling amplifier. The maximum frequency of amplification is, therefore, restricted to half the pump frequency. Any frequency above this maximum frequency of amplification can, therefore, be converted down to a corresponding frequency in the frequency band of amplification. Some measurements on such a frequency converter were performed by the author. The conversion gain of the converter was found, up to fairly high frequencies, to be the same as the gain experienced by a signal in the frequency band of amplification. Noise figure of the converter was again found to be similar to that of the amplifier. It is expected that useful performance may be obtained from such converters and this is, therefore, suggested as a very promising field for further exploration.

REFERENCES

1. Appleton, R.V. and Van Der Pol, B. Phil. Mag. 42, p 201 (1921).
2. Armstrong, E.H., "Some recent developments in regenerative circuits", Proc. I.R.E., N.Y., Vol. 10, p 244 (Aug. 1922).
3. Becker, S., and Leeds, L.M., "A modern two-way radio system", Proc. I.R.E., N.Y., Vol.24, p 1183 (Sept. 1936).
4. Macfarlane, G.G. and Whitehead, J.R., "The super-regenerative receiver in a linear mode". Journal I.E.E., Vol. 93, Part III A, p 284 (March-May 1946).
5. Macfarlane, G.G. and Whitehead, J.R., "The theory of the super-regenerative receiver operated in the linear mode", Journal I.E.E., Vol. 95, Part III, p 143, (May 1948).
6. Hazeltine, A., Richman, D., and Loughlin, B.D., "Super-regenerative design", Electronics, p 99, Sept. 1948.
7. Gluckman, H.A., "Super-regeneration - an analysis of the linear mode", Proc. I.R.E., N.Y., Vol. 37, p 500 (May 1949).
8. Page, D.F., "The transistor as a super-regenerative detector", Imperial College Diploma Dissertation, 1955.
9. Page, D.F., "Transistor super-regenerative circuits", Wireless World, Dec. 1956, pp 606-609.
10. Chow, W.F., "Transistor super-regenerative detection", I.R.E. Transactions on cct. Theory, March 1956, pp 58.
11. Esaki, L., "New phenomenon in narrow germanium p-n junctions", Phys. Rev., Vol. 109, pp 603-604, January 1958.
12. Whitehead, J.R., "Super-regenerative receivers", Cambridge University Press, 1950.
13. Page, D.F., "Instability in transistor circuits with passive feedback with special reference to tuned oscillators and super-regenerative applications", Ph.D. Thesis, London University, 1959.

14. Chang, K.K.N., "Low noise tunnel diode amplifiers", Proc.I.R.E., Vol.47, p.1268, July 1959.
15. Hines, M.E., "High-frequency negative-resistance circuit principles for Esaki diode applications", B.S.T.J., Vol. 39, pp 477-514, May 1960.
16. Yarvin, A., Cook, J.S., and Butzien, P.E., "Operation of an Esaki diode microwave amplifier", Proc.I.R.E., Vol. 48, No. 6, p 1155, June 1960.
17. Trambarulo, R.F., "Esaki diode amplifiers at 7, 11 and 26 Kmc/s", Proc.I.R.E., Vol. 48, No. 12, p 2022, December 1960.
18. Skalski, C.A., and Kabaservice, T.P., "Results obtained with tunnel-diode super-regenerative receivers", Proc.I.R.E., Vol. 50, No. 2, p 215, February 1962.
19. Sommers, H.S., "Tunnel diodes as high frequency devices", Proc.I.R.E., Vol. 47, No. 7, p 120-1206, July 1959.
20. Pucel, R.A., "The equivalent noise current of Esaki diodes", Proc.I.R.E., Vol. 49, No. 6, pp 1080-81, June 1961.
21. Fukui, H., "The characteristics of an Esaki diode at microwave frequencies", Journal of Inst. of Electrical Comm. Engg. of Japan, Vol. 43, No. 11, Abstracts. Nov. 1960.
22. General Electric Tunnel Diode Manual, 1961.
23. The General Radio Experimenter, Vol. 34, Nos. 7 and 8, July-August 1960.
24. Yajima, T., and Esaki, L., "Excess noise in narrow germanium p-n junctions", Journal of the Phys.Soc. Japan, Vol. 13, No. 11, pp 1281-1287, November 1958.
25. Nielson, E.G., "Noise performance of tunnel diodes", Proc.I.R.E. (N.Y.), Vol. 48, No. 11, p 1903, November 1960.
26. Tietmann, J.J., "Shot noise in tunnel diode amplifiers", Proc.I.R.E. (N.Y.), Vol. 48, No. 8, pp 1418-1423, August 1960.

27. Friss, H.T., "Noise figure of radio receivers", Proc. I.R.E., Vol. 32, No. 7, pp 419-422, July 1944.
28. Wylie, C.R., "Advanced engineering mathematics", (McGraw Hill Book Co. 1951).
29. Ralston, A., and Wilf, H.S., "Mathematical methods for digital computers", (J. Wiley and Sons 1962).
30. Buckingham, R.A., "Numerical methods", (Pitman 1962).
31. Hamming, R.W., "Numerical methods for scientists and engineers", (McGraw Hill 1962).

APPENDIX A.1.

It series lead inductance L is included in the equivalent circuit of the regenerative amplifier, the input admittance of the amplifier (Fig.A.1) as seen by the signal is

$$Y_{in} = G_t + Y_d \quad A.1.$$

$$= G_{in} + jB_{in} \quad A.2.$$

where Y_d is the admittance of the diode and G_{in} and B_{in} are the conductance and the susceptance parts of Y_{in} .

The diode impedance Z_d at the signal frequency at the point where diode conductance $G(v) = -G$ is

$$\begin{aligned} Z_d &= j\omega L + \frac{1}{j\omega C - G} \\ &= \frac{(1 - \omega^2 LC) - j\omega LG}{j\omega C - G} \end{aligned}$$

$$\text{therefore } Y_d = \frac{j\omega C - G}{(1 - \omega^2 LC) - j\omega LG}$$

Rationalizing

$$Y_d = \frac{-G}{(1 - \omega^2 LC)^2 + (\omega LG)^2} + jB_e \quad A.3.$$

where jB_e is the susceptance of the tunnel diode.

From A.3., A.2. and A.1.

$$G_{in} = G_t - \frac{G}{(1 - \omega^2 LC)^2 + (\omega LG)^2} \quad A.4.$$

If $L = 0$

$$G_{in} = G_t - G$$

For $L > 0$ the input conductance reduces as the inductance L is increased. The conductance part of Y_d as given by the second term in the

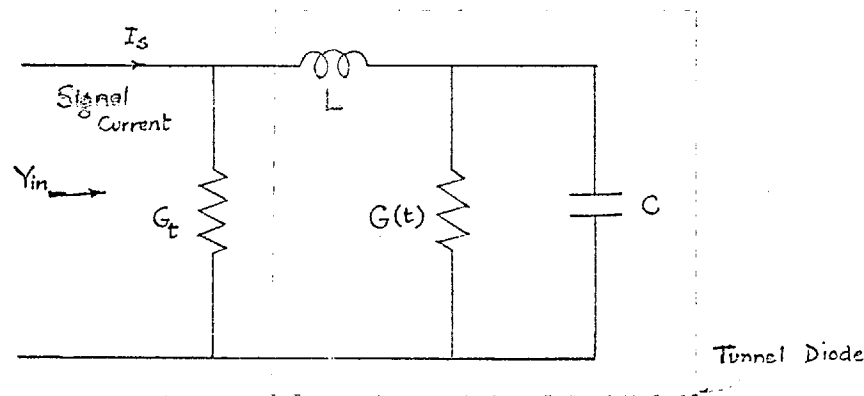
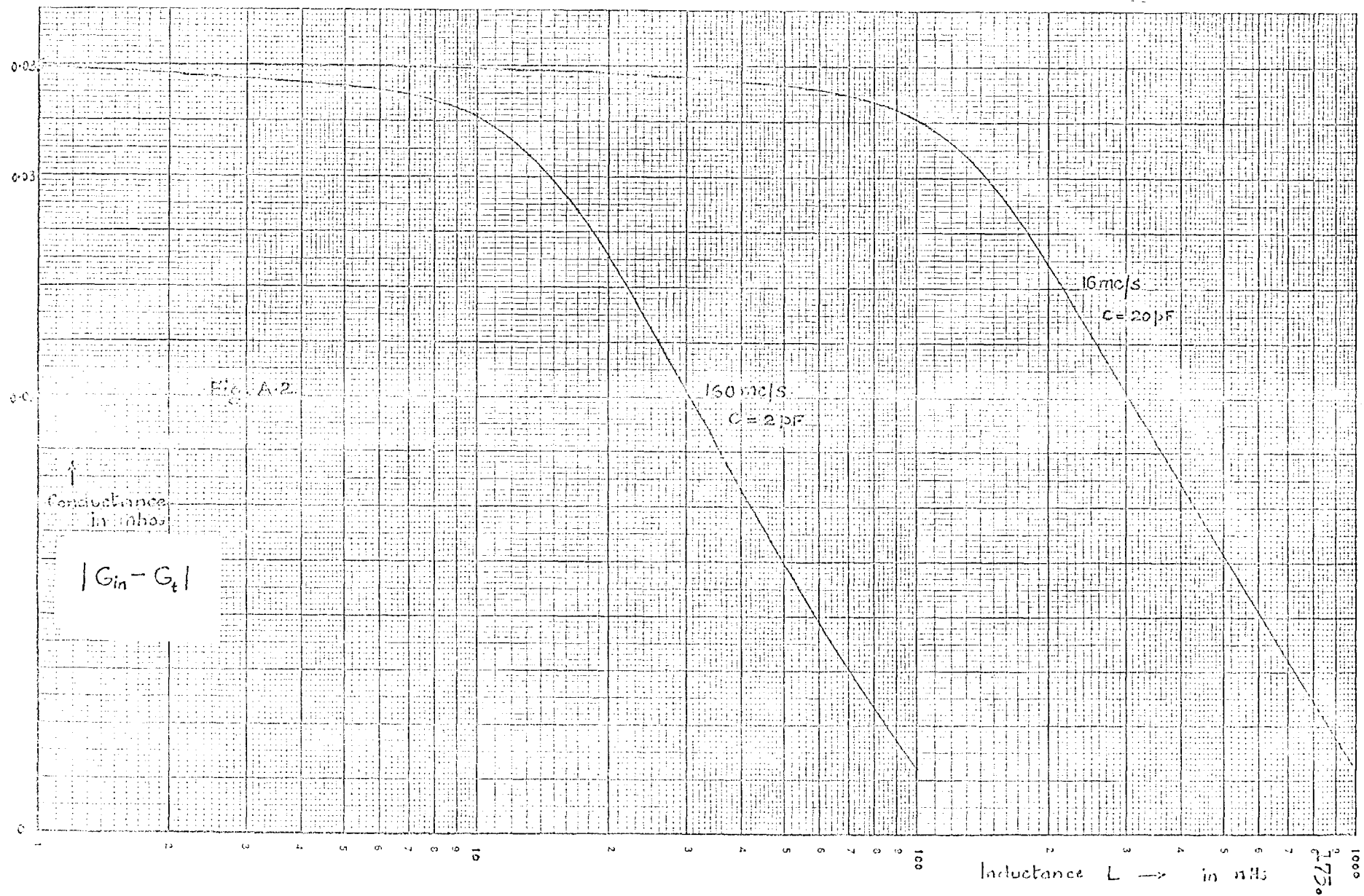


Fig. A.1. Circuit of the regenerative amplifier including L . (as seen by the signal).



expression A.4. is plotted for different values of L in Fig. A.2.

We note further that for regenerative amplification to take place

$$G_t < |-G| \quad \text{or} \quad R_t > \frac{1}{G}.$$

APPENDIX A.2.

The differential equation 4.16. can be rewritten as

$$x = \int_0^v \frac{dv}{I_b - f(v) - G_t v} \quad \text{A.5.}$$

$$\text{or } x = \int_0^v \frac{dv}{i_e(v)} \quad \text{A.6.}$$

where $i_e(v)$ is the excess pump current as a function of diode voltage v .

$$\text{or once again } x = \int_0^v \phi(v) dv \quad \text{A.7.}$$

where $\phi(v) = \frac{1}{i_e(v)}$

$\phi(v)$ can be tabulated for different values of v .

It is necessary to compute the running integral of this tabulated function $\phi(v)$ where v takes successive values for which $\phi(v)$ is tabulated. For such a calculation, the trapezoidal rule is especially well adapted. To the given table of $\phi(v)$ against v , we adjoint a column of the averages

$$\frac{\phi_0 + \phi_1}{2} \quad , \quad \frac{\phi_1 + \phi_2}{2} \quad , \quad \dots$$

The required integrals are precisely the entries in this column from the top down to each entry in turn, multiplied by $h = \delta_v$. Moreover, each sum can be found from the preceding one by adding to it the corresponding average. The following table shows the computation pattern in detail.

v	$\phi(v)$	Average	Sums	$\int_0^v \phi(v) dv$
$v_0=0$	ϕ_0	$S_0 = 0$	
v_1	ϕ_1	$\frac{1}{2}(\phi_0 + \phi_1)$	$S_1 = \frac{1}{2}(\phi_0 + \phi_1)$	hS_1
v_2	ϕ_2	$\frac{1}{2}(\phi_1 + \phi_2)$	$S_2 = S_1 + \frac{1}{2}(\phi_1 + \phi_2)$	hS_2
v_3	ϕ_3	$\frac{1}{2}(\phi_2 + \phi_3)$	$S_3 = S_2 + \frac{1}{2}(\phi_2 + \phi_3)$	hS_3
.

The accuracy of the results obtained depend upon the interval h . For the evaluation of the integral A.5, $h = 10$ mV was assumed. The results obtained from these calculations were later compared with more accurate calculations by the digital computer programme of the Appendix A.3. and found to be within better than 2% of each other.

APPENDIX A.3.

The calculation of voltage against time for the circuit of Fig. 4.6. can be carried out by the method of Appendix A.2. This method is quite simple but tedious. Further in the method of Appendix A.2., the diode characteristics is tabulated at an interval of 10 mV and characteristics between any two adjacent tabulated points are assumed to be straight lines (implied in the calculations). The time taken to traverse each 10 mV interval is then calculated.

To check the accuracy of the calculations carried out by the method of Appendix A.2. and to assist in further work a digital computer programme was written for the London University Computer 'Mercury'. This programme with very slight modifications can as well be used on the Atlas Computer of London University.

Essential characteristics of the programme are the following. The diode characteristic were once again tabulated for the computer at an interval of 10 mV. The computer was given a routine instruction by which it interpolated the diode current values by using the Backward Gregory-Newton formula²⁸ upto its third term i.e. the interpolation was carried out by fitting a parabola to three relevant adjacent points of the table of diode static characteristics. This is a better approximation to the points on the diode characteristics than the straight line approximation.

The form of equation more suitable for the computer is the equation 4.16. as compared with the equation A.5. for the hand calculations.

The method of integration employed is that due to Runge and Kutta. This method is self starting, i.e. only the initial conditions are required to start the integration. As is well known³¹ the procedure consists of five stages; the first four are the calculation of four approximate values of the increment in the value of the dependent variable, given a small fixed increment in the independent variable. The fifth and the final step is the addition, of the weighted values of the four approximate values obtained by the first four calculations, to the initial value to obtain the final value. This is a fourth order integration procedure and corresponds to taking the

first four terms of the Taylor series solution.

The solution starts from $x = 0$ and $v = 0$ and then the solution is obtained for a fixed increment in x of $h = \delta x = 10$ in contrast with a fixed increment of 10 mV for calculation of Appendix A.2. The computer solution is carried out for a time increment and most of the range of the solutions $v(t)$, the increment of voltage for the fixed step increment of time is much smaller than 10 mV. This implies that the accuracy of the computer calculations should be a considerable improvement on the calculations of Appendix A.2., where time required to traverse 10 mV is calculated for each step. But a comparison of the results obtained from the two methods shows that the results obtained are better than within two percent of each other.

For the sake of completeness the programme used for computer solutions is given under. Briefly, the first part following the title gives the interpolation routine. Chapter 1 orders the computer operation on the differential equation and Chapter 0 orders the read in operations for the data i.e. tunnel diode voltage-current characteristic the conductance G_t and the frequency or time limits for the integration steps.

```
title
operai u834 tunnel diode response 14 11 62
routine 1:
jn=0intpt(dy1)
n3=0frpt(dy1)
n3=n3+1
jump2, jn#0
jn=1
n3=n3-1
2) jn=jn+nai-nn
n1=cjn-c(jn-1)
n2=c(jn+1)-2cjn+c(jn-1)
a3=c(jn-1)+n3n1+0.5n3n3n2-c.5n3n2
return
psa
*****
chapter:
f>5
g>5
h>5
y>5
o>5
n>5
c>300
a>10
z>10
v>3
1)x=0
is=i(1)n
yin=bin
repeat
>>integrate500 steps until x=xn
k=i(1)500
intstep(10)
newline
yo=x
ix=o(1)n
print(yin)0,5
repeat
jump3, x>xn
repeat
halt

3)newline
newline
caption
time exeeded x0
across2/0
ic)yo=0
```

```

i=i(i)n
jumpdown(ni)
fi=ai+z(i-1)y(i-1)-dn-ziyi
repeat
end aux seq
close

```

```

chaptero
variables i
i)n=10
n=3
nn=50
b1=0
b2=0
b3=0
d=0.1
xn=1000
in=i(i)3
jn=i(i)nn
i=innn-nn+jn-1
read(ci)
repeat
repeat
read(w)
in=i(i)3
read(ain)
read(zin)
zin=1/zin
repeat
zo=0
across i/i
2)in=i(i)3
read(ain)
repeat
across i/i
psa
close
>
*****

```

APPENDIX A.4.

A programme to solve equation 5.1. is given under. This programme is very similar to that of Appendix A.3. The method of integration is exactly the same and therefore the discussion of Appendix A.3. applies directly to the programme given in this Appendix.

```

      title      Computer Programme (sine wave pump)
oberai  u834 tunnel diode response i  4  64

routine i
jn=pi*ntpt(dy1)
n3=pi*nrpt(dy1)
n3=n3+1
jump2, jn#0
jn=1
n3=n3-1
2) jn=jn+n*ni-nn
n1=c*jn-c*(jn-1)
n2=c*(jn+1)-2*c*jn+c*(jn-1)
n3=c*(jn-1)+n3*n1+0.5*n3*n3*n2-0.5*n3*n2
return
psa
*****

chapter i
T>5
S>5
H>5
Y>5
B>5
K>5
C>500
a>10
Z>10
W>5
1) X=0
in=1(i)n
yin=bin
repeat
>>integrate500 steps until x=xn
k=1(i)500
intstep(10)
newline
y0=x
in=0(i)n
print(yin)0,3
repeat
jump3, x>xn
repeat
halt

```

```

3)newline
newline
caption
time exceeded xn
across2/o
10)f=psin(wx)
yo=0
i=i(1)n
jumpdown(n1)
fi=ai*f+z(i-1)y(i-1)-dn-ziyi
repeat
end aux seq
psin
close

```

```

chapter0
variables1
1)h=10
n=1
m=50
b1=0
b2=0
b3=0
c=0.1
i0=i(1)n
jn=i(1)m
i=i0m-nn+jn-1
read(ci)
repeat
repeat
read(ai)
read(zi)
zi=1/zi
read(w)
xn=w
w=1/w
w=πw
across1/i
2)read(ai)
read(w)
xn=w
w=1/w
w=πw
across1/i
psa
close
*
XXXXXXXXXX

```


(Typical Data Input)

0	1.71	2.98	3.87	4.42	4.68	4.7	4.6	4.4	4
3.6	3.26	2.9	2.55	2.18	1.85	1.6	1.38	1.22	1.12
1.03	.96	.9	.83	.78	.74	.71	.68	.66	.65
.65	.64	.66	.68	.7	.73	.77	.8	.85	.95
1.05	1.18	1.28	1.46	1.72	2.08	2.48	3.2	4.14	4.85

6 100 340

6 400

6 500

6 600

6 700

6.8 160

6.8 208

6.8 340

APPENDIX A.5.

The following procedure was used to measure i_{eq} of the tunnel diode. (The circuit of Fig. A.3. was employed).

1. With tunnel diode removed out of the circuit and R (Fig. A.3.) set to some convenient value, the noise power from the receiver was measured.
2. The noise diode current was increased until this power is doubled. The noise diode current required to do this is the equivalent saturated diode current for the pre-amplifier stage and the Johnson noise of the resistance R.
3. The Signal Generator was then switched into the circuit. The output of the signal generator was increased to a convenient value large compared to the noise.
4. The tunnel diode was then inserted into the circuit, R replaced by a different convenient value and the bias on the diode was adjusted until the signal produced the same reading as before. At this point the combined conductance of the new R plus the tunnel diode conductance is equal to conductance of the original resistor.
5. Under this condition, the i_{eq} for pre-amplifier will be as before and the additional noise current required to double the noise power is due to the tunnel diode and the added conductance. By subtracting the contribution by the conductance and the pre-amplifier from the final reading we obtain the value for the tunnel diode alone.

Noise factor F for a temperature limited diode is given by the expression

$$F = 20 I_a R$$

where I_a is the saturated diode current of the noise diode
and R is the source resistance of the noise generator.

For R = 50

$$I_a = \frac{F}{20 \times 50}$$

$$\therefore F = I_a \text{ in milliamperes}$$

Thus noise factor of the noise source gives i_{eq} directly.

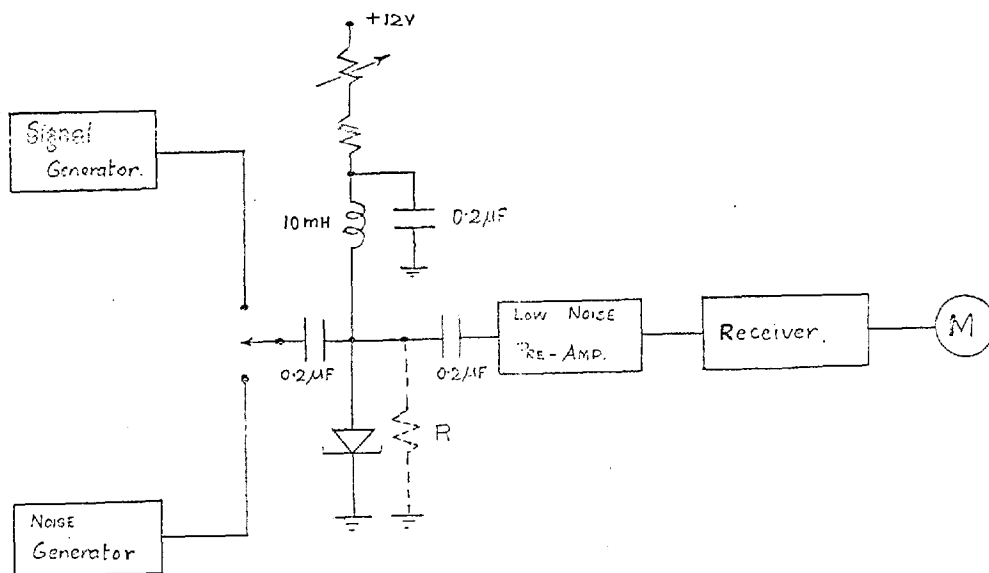


Figure A.3.